The Dissertation Committee for Joseph Quan Anh Pham Certifies that this is the approved version of the following dissertation:

Effects of Confinement on the Glass Transition of Polymer-Based Systems

Committee:

Peter F. Green, Supervisor

Keith P. Johnston

Donald Paul

Arumugam Manthiram

Desiderio Kovar

Effects of Confinement on the Glass Transition of Polymer-Based Systems

by

Joseph Quan Anh Pham, B.S. ChE, M.S.E

Dissertation

Presented to the Faculty of the Graduate School of

The University of Texas at Austin

in Partial Fulfillment

of the Requirements

for the Degree of

Doctor of Philosophy

The University of Texas at Austin

May, 2004

Dedication

To my parents, my brothers and sister for their endless love, generosity, encouragement, sacrifice, and understanding throughout my life.

Acknowledgements

I would like to express my sincerest thanks to all the people who have helped me in my life and in my studies. First, I thank my parents for their endless love, generosity, and understanding throughout all these years. Their sacrifice and support have been instrumental to all that I have accomplished. I thank my brothers and sisters, anh Tam, anh/chi Phuc/Lan, anh An, Quoc and Thu for their friendship and encouragement.

I am grateful to my advisor, Professor Peter F. Green for giving me an opportunity to work in his research group and inspiring me to love research. I thank him for his invaluable insights, guidance, and patience during the course of my graduate studies. I am also grateful to my co-advisor, Professor Keith P. Johnston. I thank him for providing me with valuable insights and direction.

I would like to thank various people that have aided my research. I am indebted to several of my colleagues and the past and present members of Professor Green's group, particularly Dr. Jean-Loup Masson, Dr. Ratchana Limary, Dr. Stephen Sirard, Dr. Steve Scheer, Karl Putz, Brian Besancon, Luciana Meli, Abraham Arceo, Yuan Li, Jamie Kropka, and Dr. Xiaogang Zhang.

I thank the following professors, Desiderio Kovar, Arumugam Manthiram, Donald Paul, and Keith P. Johnston for graciously serving as members of my dissertation

committee. I thank Lydia Griffith and Eddie Ebarra for their administrative and the procurement help. I also acknowledge the University of Texas for giving me the Continuing Fellowship. I also thank all of my friends at World Relief Refugee Ministry for their help and encouragement, particularly Jonathan Bao Thang.

Finally, I also would like to thank my friends in the Don Bosco Eucharistic Youth Society at the Holy Vietnamese Martyrs Catholic Church in Austin, particularly Loan, Loc, Binh, Bien, TLam, Huu, Dung, chi Lien, Thay Minh, Thay Thong, anh/chi Thang/Tien, anh Hoa, anh Giao, Sister Anne, and Cha Van. I appreciate and thankful for their encouragement and support throughout my college years. In addition, I thank them for showing me how to love, trust, and serve God.

Effects of Confinement on the Glass Transition of Polymer-Based Systems

Publication No._____

Joseph Quan Anh Pham, Ph.D.

The University of Texas at Austin, 2004

Supervisor: Peter F. Green

In recent years, considerable effort has been invested toward developing polymers for applications in which they serve as the active material component for devices such as transistors, light emitting diodes, and various sensors. Many of these applications require polymer thin films. Unfortunately, many of the properties of the thin films that impact device processing and performance are not well understood. Polymer films in this thickness range exhibit properties that are very different from the bulk. Properties such as the viscosity, the glass transition temperature, T_g, and phase transitions exhibit film thickness dependencies. This thesis examines three problems generally in the area of the glass transition temperature of polymer thin films. (1) *The T_g of polymer-polymer mixtures*: We examined the T_g of thin films of the miscible blend tetramethyl Bisphenyl-A polycarbonate (TMPC)/polystyrene (PS). Our results indicate that entropic, "chain packing," effects and enthalpic effects associated with interactions between the dissimilar chain segments and the external interfaces (free surface and substrate) determine the T_g of these mixtures. *(2) The glass transition of polymer-based nanocomposite films*: We

examined the film thickness dependencies of the glass transition temperatures of polystyrene based nanocomposite thin films containing small concentrations, 1-5 wt.%, of layered silicate clays and C_{60} fullerenes supported by silicon substrates, *PS-LSi/Si* and *PS-C_{60}/Si*, respectively. Our results show that at these small concentrations the nanoscale particles can change T_g appreciably, particularly in films with thicknesses less than 45 nm. Shifts in T_g of up to 20 degrees were observed, regardless of the chemistry of the nanoparticles. *(3) Polymer (polystyrene and polymethylmethacrylate) thin films in supercritical CO_2*: The effect of CO_2 on the glass transition plays a central role in the processing of thin films for microelectronic applications. Our most significant finding is the phenomenon of retrograde vitrification, where the polymer in a CO_2 environment exhibits a rubbery-to-glass transition as the temperature is decreased and surprisingly a glassy-to-rubbery transition with a further decrease in temperature. These findings have important implications on the processing of thin polymer films in CO_2 environments.

Table of Contents

List of Figures

Chapter 1: Introduction

1.1 MOTIVATION

Polymers play an important role in many aspects of our daily lives, with applications ranging from packaging of food to automobile parts. In recent years, considerable effort has been invested in developing polymers for new applications such as sensors and electronic device applications **[1-6]**. Polymer thin films are attractive materials for patterning applications associated with building microelectronic circuits. They are also used as materials in low dielectric constant interlayers in electronic devices **[1-3]**. Polymer thin films have also been used as liquid crystal display (LCD) and as antireflective coating **[1,4]**.

Many of these applications require polymer thin films in the thickness range of nanometers or tens of nanometers. The fabrication and performance of these technologies is critically dependent on the wetting, structural stability, viscosity, glass transition temperature (T_g), mechanical, optical and electrical properties of the polymer. Unfortunately, many properties of polymer thin films are still not well understood. Polymer thin films in this thickness range exhibit properties that are very different from the bulk. Properties such as viscosity, diffusion, glass transition temperature, phase transition in mixtures and crystallization have been shown to depend on film thickness **[6,13-18]**.

The glass transition temperature, T_g, of polymer thin films continues to be an active area of research. Simulations and experiments reveal that in polymers T_g may

increase or decrease with decreasing film thickness for films with thicknesses below 45 nm. These issues are not well understood. The research in this dissertation examines three problems in the area of the glass transition temperature of polymer thin films: (1) the glass transition temperature of thin film mixtures of compatible polymers; (2) the glass transition temperature of thin polymer based nanocomposites, where a polymer serves as the host for small concentrations of nano-scaled entities (carbon nanotubes, C_{60} fullerenes, layered silicate clays), and (3) polymer thin films in supercritical CO_2 environments.

The following sections in this chapter are intended to provide a background and context for the three problems examined in this thesis.

1.2 GLASS TRANSITION TEMPERATURE

Many liquids, if cooled at a sufficiently rapid rate, will solidify to form a solid in which the arrangement of its constituents (atom or molecules) lacks long-range order, a glass **[19-25]**. The temperature at which this occurs is the glass transition temperature. The glass transition temperature is accompanied by a gradual transition of the temperature dependence of the specific volume of the liquid from a larger to smaller temperature dependence in the solid state, as illustrated in Figure 1.1. Large changes in the thermal expansion and the heat capacity accompany the glass transition. The melting point, T_m, is also identified in Figure 1.1 and would generally occur if the material is cooled at a sufficiently slow rate to allow the molecules sufficient time to arrange into a structure that possesses long-range order. Melting is a first order phase transition,

accompanied by a discontinuity in the specific volume-temperature relation, as shown in the figure. One further difference between T_m and T_g is that T_g depends on the rate of cooling. In systems that form glasses, slightly larger values of T_g are exhibited by systems that are cooled at a slower rate. With this in mind, it should be noted that some liquids, by virtue of their structure, would always form glassy structures upon solidification. Amorphous polymers are excellent examples because their structural units (monomers) prohibit the formation of solids that possess long-range order.

The viscosity of glass-forming liquids increases rapidly with decreasing temperature and is often described in terms of the Vogel-Fulcher relation **[20-23]**

$$\ln t \propto \ln h \propto \frac{A}{(T - T_\infty)} \qquad (1.1)$$

In this equation, η is the viscosity; A, B and T_o are constants. Equivalently, the temperature dependence is also described using the Williams-Landel-Ferry equation,

$$\log \frac{h(T)}{h(T_g)} = \frac{-c_1^g (T - T_g)}{c_2^g + (T - T_g)} \qquad (1.2)$$

where c_1^g and c_2^g are constants that are associated with the polymer. The most popular method used to measure the glass transition temperature of bulk polymers is differential scanning calorimetry.

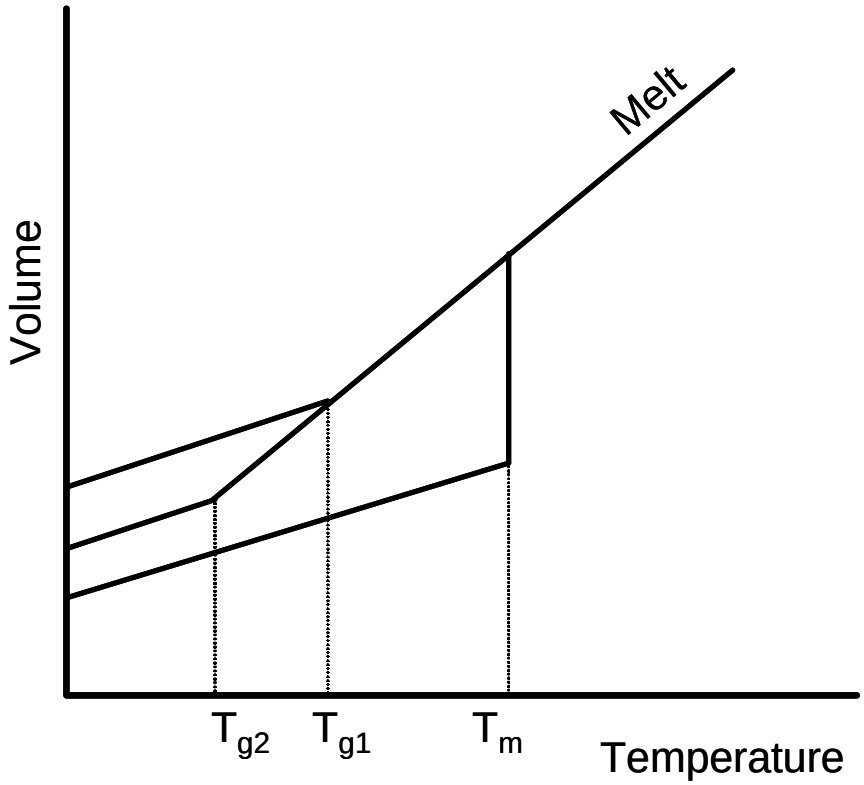

Figure 1-1: Schematic of volume-temperature relationship for a glass-forming liquid. T_m is the melting temperature; T_{g1} and T_{g2} are the glass transition temperatures of the rapidly cooled and slowly cooled liquids, respectively.

1.3 THE GLASS TRANSITION TEMPERATURE IN POLYMERS

The T_g of polymer is influenced by several factors that include chain stiffness, ease of rotation of bonds, interactions between molecules and chain length. In this regard, at least in bulk polymers T_g reflects specifics of the structure of the polymer. Recently, it has been shown that T_g depends on the thickness of the film. As the thickness of the film is reduced to length scales comparable to the radius of gyration of the chain, the T_g of the polymer may increase or decrease, depending on the nature of its interactions with its environments (free surface or substrate) **[7-12, 26, 27]**. Therefore, the glass transition of a polymer thin film is not intrinsically associated with the polymer but reflects its interactions with its environment. The following section provides a review of thickness influence on T_g in polymer thin films.

1.4 THE GLASS TRANSITION TEMPERATURE IN POLYMER THIN FILMS

Many research groups have utilized different techniques including ellipsometry, x-ray reflectivity, dielectric spectroscopy, and positron annihilation lifetime spectroscopy to investigate the effective T_g of the polymer thin films. These investigations show that the T_g of polymer thin films exhibit thickness dependence when the film is sufficiently thin, typically less than 45 nm **[7-9,11,12,26,27]**. The T_gs of polystyrene (PS) and poly(α-methylstyrene) films supported by SiO_x/Si substrates and the T_gs of poly(methylmethacrylate) (PMMA) on gold decrease with decreasing film thickness for films thinner than approximately 45 nm **[7-9]**. These depressions can be significant. For example, the T_g of h=10 nm thick PS films supported by SiO_x/Si substrates is

approximately 20°C lower than the bulk value as shown in Figure 1-2. In the examples just mentioned above the polymer chains have a weak interaction (typically ~van der Waals) with the supporting substrates.

In contrast, investigations of the T_g of polymer thin films where the polymer molecules have strong interactions with the substrates (i.e. hydrogen bonds) indicate that T_g increases with decreasing film thickness. Studies of PMMA and poly(vinyl pyridine) PVP supported by SiO_x/Si substrates indicate that the T_g increases with decreasing film thickness when the film is thinner than ~50 nm. The T_gs of freely standing films have also been examined. Forrest et al. showed that T_g of freely standing film PS decreased by approximately 2 times more than the same PS film on SiO_x/Si substrates **[12]**.

The issue is further complicated by the fact that the tacticity of the polymer also has a significant effect on the T_g film and in some cases the effect may be comparable to the effect of the substrate as shown by Grohen et al. **[10]**. They observed that while the T_g of isotactic PMMA on SiO_x/Si increased with decreasing film thickness, the T_g of syndiotactic PMMA on similar substrate showed an opposite trend.

Molecular simulations by Torres et al. and Jain et al. reported similar trends with the above experimental observations of freely standing polymer thin films as well as polymer thin films on weakly interacting and strongly interacting substrates **[8,13]**. These results indicate that interactions between chain segments and the free surface and the substrate dictate the T_g of polymer thin films.

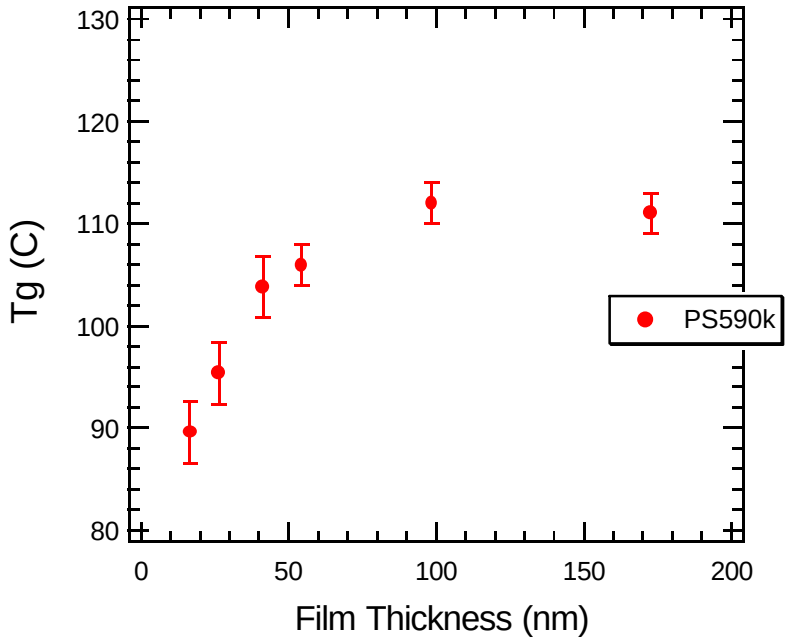

Figure 1-2: The glass transition temperature of PS versus film thickness.

While much is understood about the T_g of homopolymer thin films, very little is known about the T_g of polymer-polymer miscible blend thin films. In addition, miscible thin film blends are ideal for examining the effects of both free surface and substrate on T_g of polymer thin film. In miscible blend thin films, except in the case of a neutral interface, components of the blend preferentially interacts with the interfaces, leading to preferential segregation. If the surface energies of the two components differ, then the lower the surface energy component will preferentially enrich the free surface. In chapter 2 and chapter 3 of this thesis, the T_g of miscible blend thin films on SiO_x/Si substrates are discussed in detail.

1.5 SUPERCRITICAL FLUIDS

The supercritical state of a substance is defined by the temperature, T, and pressure, P, range above the critical T_c and P_c of the substance. In this state, there is no distinction between the liquid and vapor phase. Once in the supercritical state, if the pressure is increased, only the density of the fluid increases and no vapor to liquid transition occurs; hence, the density of the fluid can be tuned drastically by small changes in the temperature or pressure. In addition, supercritical fluids possess densities comparable to organic solvents while maintaining gas-like transport properties. Figure 1-3 shows a typical temperature-pressure phase diagram for a compound **[28]**.

1.6 LIQUID AND SUPERCRITICAL CARBON DIOXIDE

Liquid and supercritical carbon dioxide (CO_2) have been shown to be attractive alternatives to organic solvents in many polymer processes such as foaming, impregnation, separations, coating and synthesis as well as in the formation, development, cleaning, and drying of photoresist films **[28-36]**. CO_2 is an attractive option because it is non-toxic, non-flammable, in-expensive and leaves essentially no solvent residue due to its high volatility. In addition, the critical conditions of CO_2 can easily be accessible (T_c = 31°C and P_c= 73.8 bar). Moreover, the solvent strength of CO_2 can be tuned markedly with pressure and temperature. Figure 1-4 displays the CO_2 density as a function of temperature and pressure **[29]**. Because of its low surface tension, gas-like transport properties, and density comparable to that of organic solvents, supercritical CO_2 has been successfully used to dry aqueous based photoresist films without collapsing the high-aspect ratio features **[34,36,37]**. In addition, supercritical CO_2 with small amounts of surfactant and water has been successfully used to remove residues from patterned low k dielectric porous methylsilsesquioxane (MSQ) without damaging the features **[38]**. Supercritical CO_2 with hydrocarbon surfactants has also been used to dry water from small, high aspect ratio photoresist patterns without collapsing the features **[39]**. In consumer products, supercritical CO_2 has been used extensively in pharmaceutical, neutraceutical and food processing. For example, supercritical CO_2 was used to produce drug nanoparticles for drug delivery systems and to extraction of caffeine from coffee and tea **[40]**.

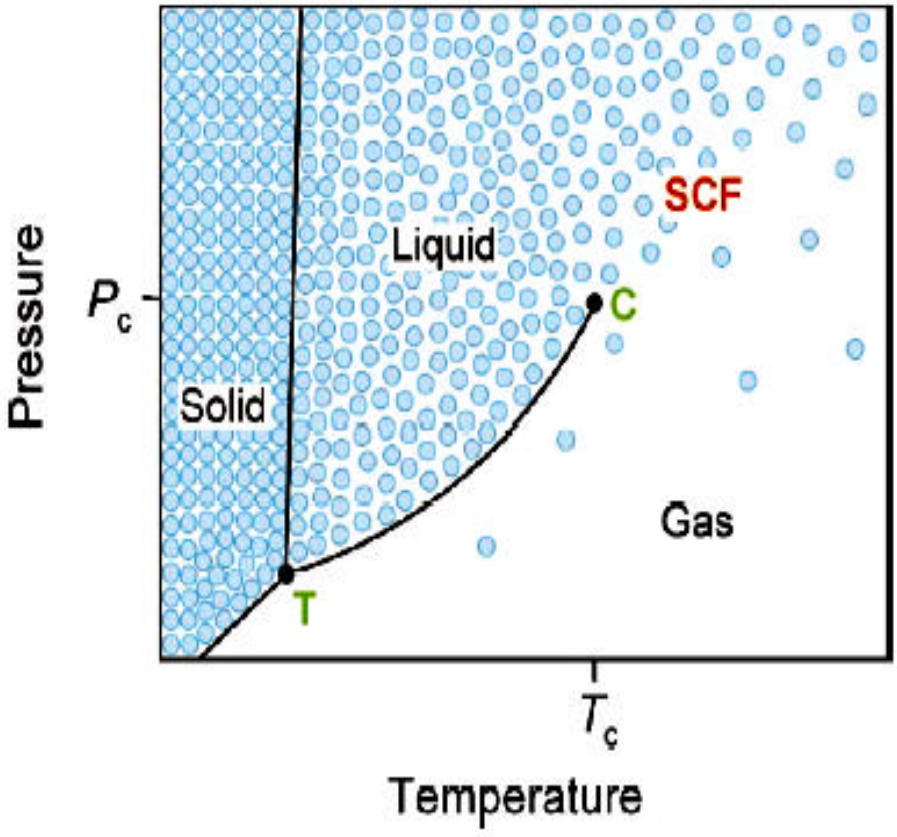

Figure 1-3: Typical temperature-pressure phase diagram of a compound – Reproduced by permission of The Royal Society of Chemistry **[29]**

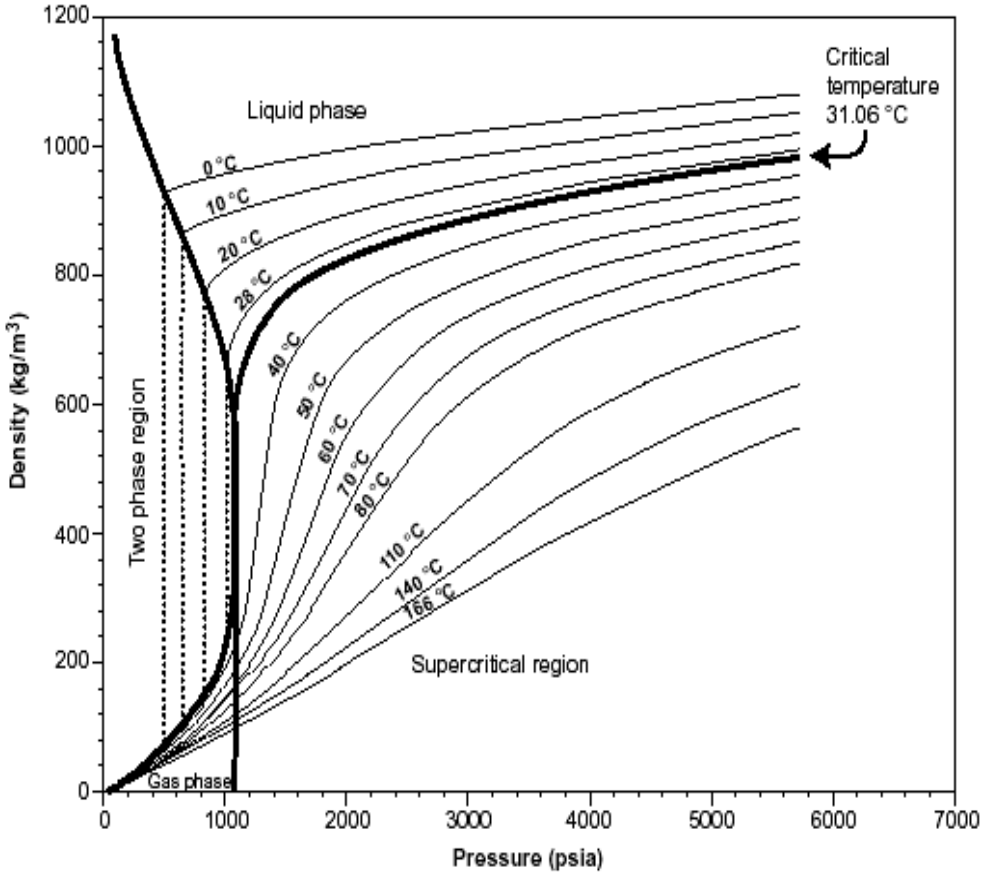

Figure 1-4: Density of CO_2 as a function of temperature and pressure **[28]**

Supercritical CO_2 has also been utilized to produce nanoparticles as well as to deposit various metal layers, such as Pt, Pd, Au, and Rh on inorganic and polymer substrates **[41,42]**.

1.7 POLYMER-LIQUID AND SUPERCRITICAL CARBON DIOXIDE INTERACTIONS

The solubility of CO_2 in the polymer is influenced by temperature, pressure, and polymer-CO_2 interactions **[33,43]**. For example, at the same pressure and temperature, CO_2 solubility in PMMA is approximately twice as much as that of PS **[43]**. This is due to the stronger interaction between CO_2 and carbonyl groups of PMMA comparing to a weaker interaction between CO_2 and phenyl groups of PS. Sorption of CO_2 into polymers can cause significant swelling and drastically lower the T_g of the polymers (plasticization).

The swelling and plasticization of polymer by compressed CO_2 reduces the viscosity and increases the diffusion coefficient of chains. The self-diffusion coefficient of polymer chains in CO_2 swollen polymer samples has been shown to increase several orders of magnitude over that of the same polymer in air/vacuum environments **[44]**. The increase of the diffusion coefficient was attributed to the increase of configurational freedom of chains in the swollen polymer sample. Supercritical CO_2 is also known to reduce the crystallization temperature and melting temperature of polymers **[45,46]**. The experimental results of Meli et al. indicated that the dewetting dynamics of polymer thin films is greatly suppressed in compressed CO_2 environment compared to that in air **[47]**. In addition, experimental results by Watkins et al. showed that the sorption of CO_2

lowered the LCST of polymer blends by as much as 100°C **[48]**. Vogt et al. demonstrated that the order-disorder transition temperature and kinetics of ordering of diblock copolymers can also be manipulated by changing the sorption of CO_2 into the polymer **[49]**.

In bulk polymer samples, previous studies have found peculiar CO_2-induced devitrification (plasticization). Condo et al. discovered that PMMA and PEMA undergo retrograde vitrification whereby upon decreasing temperature isobarically, the polymers exhibit a rubbery-to-glassy (vitrification) transition at high temperatures, and at lower temperatures exhibit a glassy-to-rubbery, devitrification, transition **[50,51]**. The CO_2 pressure where the devitrification of the polymer occurs is usually referred to as plasticization pressure (P_g). At constant pressure, devitrification is associated with the increasing solubility of CO_2 with decreasing temperature in the polymer. CO_2-induced plasticization is also different from one polymer system to another. For example, in PS/CO_2 system, only the vitrification transition occurs when decreasing temperature isobarically, and no devitrification happens at lower temperature **[50-54]**. On the other hand, the CO_2-induced plasticization of PMMA-co-PS exhibited the intermediate behaviors of PMMA and PS. Therefore, the complex plasticization phenomena observed in different polymer systems are due to the complex effects of temperature and pressure on the solubility of CO_2 in the polymers.

In polymer thin films, the sorption, swelling and CO_2-induced devitrification of T_g are not only influenced by temperature, pressure and polymer-CO_2 interactions but also by the excess adsorption of CO_2 onto the external interfaces (substrate and free surface). Experimental results by Sirard et al. and Koga et al. showed that in the presence

of high pressure CO_2, PMMA and PS thin films exhibited anomalous swelling in the region where CO_2 is most compressible, and this phenomenon was not observed in bulk samples **[55-57]**. In addition, experimental results of Sirard et al. have shown that swelling and CO_2 sorption into poly(dimethylsiloxane) (PDMS) thin film are higher than that of the bulk value **[55]**. The excess swelling was attributed to the adsorption of CO_2 at the free surface and the substrate.

Since the sorption of CO_2 into polymer thin films is different from the bulk, it is expected that CO_2-induced plasticization of polymer thin film is also different from that of the bulk. Chapter 6 and chapter 7 in this dissertation will address the CO_2-induced glass transition temperature in PMMA and PS thin films.

1.8 OBJECTIVES

In chapter 2 and chapter 3, the effects of confinement and interfacial interactions on the glass transition temperature (T_g) of thin film mixtures are investigated using spectroscopic ellipsometry. It is well known that PS/TMPC mixtures are miscible in the bulk and exhibit a lower critical solution temperature (LCST). On SiO_x/Si substrates, due to surface energies different and polymer-substrate interaction, PS preferentially segregates to the free surface and TMPC enriches to the substrate. Since the T_g difference between TMPC and PS is approximately 100°C, this blend system allows one to control the effects (T_g, mobility) in the vicinity of the substrate and free surface. In addition, depending on the interactions between mixture components, the T_g variation with composition of the mixtures could exhibit positive or negative deviations from linear additivity. The objectives of this chapter are to: (1) examine the T_g dependence on film

thickness of pure TMPC thin films on SiO_x/Si substrate, (2) investigate the effects of film thickness, composition and molecular weight on the T_g of PS/TMPC thin film mixtures on SiO_x/Si substrates, (3) study the dependence of T_g on composition for thin film mixtures, (4) compare the film thickness dependence of T_g with theory.

In chapter 4 and chapter 5, the influence of confinement and polymer-surface interactions on the mobility of chains and T_g are investigated by exploring the T_g of polymer-inorganic nanocomposite thin films using spectroscopic ellipsometry and differential scanning calorimetry (DSC). The confinement effects and interfacial interactions of polymer-inorganic nanocomposite thin films are expected to exaggerate due to large surface area to volume ratio posses by the nanoparticles. The objectives in this study are to: (1) investigate T_g dependence on film thickness of pure PS thin films, (2) measure the glass transitions of composites of PS/single walled carbon nanotubes (SWNT) and PS/functionalized SWNT both in the bulk and in thin films, (3) examine the film thickness dependence on T_g of PS/C_{60} fullerene and PS/layered silicate clay nanocomposite thin films.

In chapter 6 and chapter 7, in-situ spectroscopic ellipsometry is utilized to study the pressure, temperature, and film thickness dependence of CO_2-induced devitrification (plasticization) of polymer thin films. In the presence of high pressure CO_2, sorption of CO_2 into polymer leads to significant swelling and hence, increases the free volume, decrease the viscosity, and reduce T_g (plasticization). The objectives of this study are to: (1) demonstrate that ellipsometry can be utilized to measure the CO_2-induced T_g (plasticization) of polymer thin films on SiO_x/Si substrate, (2) examine the effect of film

thickness on the CO_2-induced devitrification of PMMA and PS thin films, (3) compare the retrograde vitrification phenomenon between bulk values and thin films.

1.9 APPENDIX: SPECTROSCOPIC ELLIPSOMETRY

Ellipsometry is a powerful optical technique that has been used extensively in the semiconductor industry **[58]**. However, it has been utilized extensively in the last 10 years by the polymer community to investigate a variety properties of polymer thin films such as the glass transition temperature, swelling of polymer films in the presence of solvents, interfacial thickness of phase separated blend, surface roughness, and monolayer formation **[7,10,55,56,59-61]**. Ellipsometry has many advantages over other thin film techniques because it is non-invasive and non-destructive and data may be rapidly acquired. Contrary to popular perception, the ellipsometry does not measure the film thickness and index of refraction directly; rather it measures the change in polarization state of the polarized incidence light upon reflection from a planar surface **[62-64]**. The polarized incident light is characterized by the amplitude and phase of the two components, in the plane of the incidence (p) and perpendicular to the plane of incidence (s). Therefore, the incidence light is usually quantified by an amplitude ratio A_p/A_s and the phase difference ($d_p - d_s$), where A_p, A_s, d_p, d_s are the amplitude and phase in the s and p planes. Upon reflection from a planar surface both the amplitude and phase of the incidence light change. The two parameters that the ellipsometry measured are the ellipsometric angles, ψ and Δ **[62-64]**. The ellipsometric angles, ψ and Δ, are related to the amplitude and phase change through the following equations 1.2 and 1.3.

$$\Delta = \left(d_p^r - d_s^r\right) - \left(d_p^i - d_s^i\right) \qquad (1.2)$$

$$\tan y = \frac{A_p^r / A_s^r}{A_p^i / A_s^i} \qquad (1.3)$$

In these equations, the superscripts r and i represent the reflected and the incident light; p and s denote in the plane of incidence and perpendicular to this plane, respectively. The schematic of light reflected from a surface is displayed in Figure 1-5.

The measured ψ and Δ can be related to the optical constant of the film by using the Fresnel reflection coefficients in the p and s planes, R_p and R_s, through the following equation:

$$\frac{R_p}{R_s} = \tan\o e^{i\Ä} \qquad (1.4)$$

Because of optical dispersion, the index of refraction of a material is dependent on the wavelength of light (λ). Since ψ and Δ are related to the index of refraction, they are also dependent of the refractive index of the material. For a single interface, the ellipsometric angles ψ and Δ are function of the incident angle and the index of refraction of the two mediums as shown in Figure 1-6. The Fresnel reflection coefficients for this system are described by the following equations **[63]**:

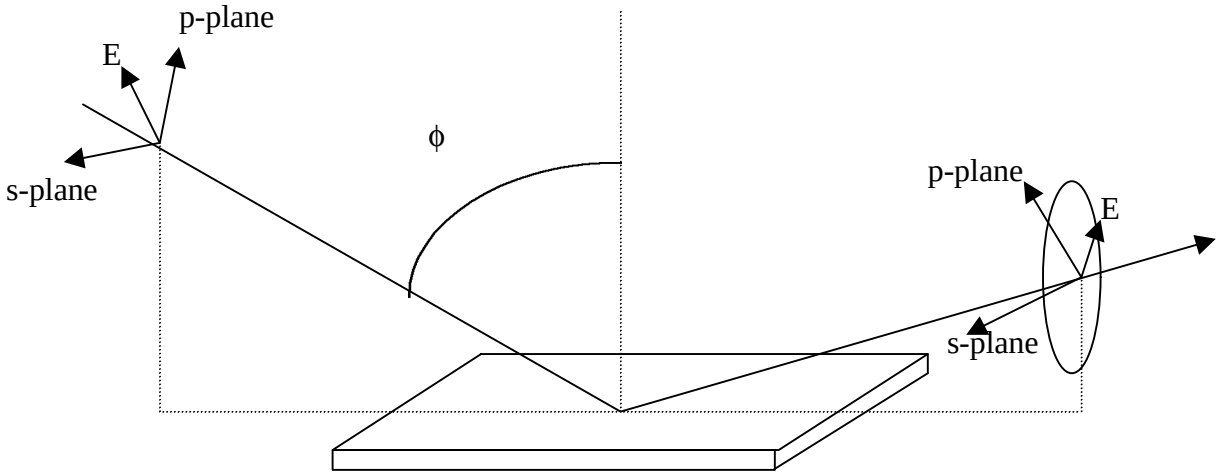

Figure 1-5: Schematic of reflection of polarized light from a planar surface where p is in the plane of reflection and s is perpendicular to this plane.

$$R_p = \frac{N_1 \cos f_0 - N_0 \cos f_1}{N_1 \cos f_0 + N_0 \cos f_1} \qquad (1.5)$$

$$R_s = \frac{N_0 \cos f_0 - N_1 \cos f_1}{N_0 \cos f_0 + N_1 \cos f_1} \qquad (1.6)$$

Where N_0 and N_1 are the index of refraction of medium 0 and 1; ϕ_0 and ϕ_1 are incident and refracted angles from vertical, respectively. However, in many applications, the incident light is reflected from many interfaces. The reflected light is composed of light reflected directly from the first interface as well as the transmitted light reflected from subsequent interfaces making back to the surface. A sketch of the multiple surfaces reflections systems is illustrated in Figure 1-6. The Fresnel reflection coefficients of the multiple interfaces are defined as the following **[63]**:

$$R_p = \frac{R_{01}^p + R_{12}^p \exp(-i2b)}{1 + R_{01}^p R_{12}^p \exp(-i2b)} \qquad (1.7)$$

$$R_s = \frac{R_{01}^s + R_{12}^s \exp(-i2b)}{1 + R_{01}^s R_{12}^s \exp(-i2b)} \qquad (1.8)$$

In these equations, the subscripts 01 and 12 refer to Fresnel reflection coefficients for the interfaces between medium 0 and 1, 1 and 2, respectively. β relates to the film thickness and defined as**[63]**:

$$b = 2p\left(\frac{h}{l}\right)N_1 \cos f_2 \qquad (1.9)$$

where h is film thickness as shown in Figure 1-7.

In a given experiment, depending on the type of ellipsometer, one or more set of ellipsometric angles (ψ and Δ) are collected. These ellipsometric angles are then modeled to obtain the film thickness, the optical constants or the combination of both. The data generated from the model are then compared to the experimental results and the model is adjusted to minimize the difference **[64]**.

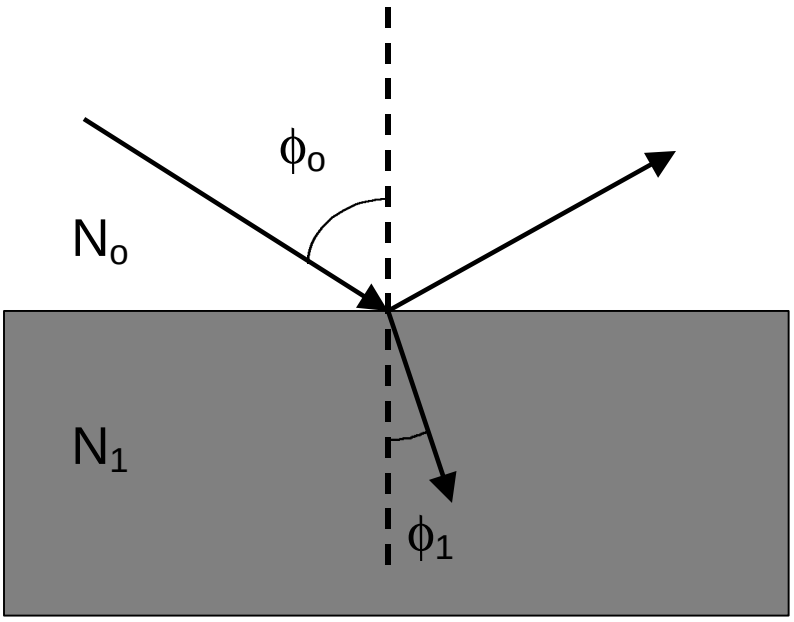

Figure 1-6: Schematic of reflection and transmission of the incident light from a planar single interface. N_0 and N_1 are the index of refraction of medium 0 and 1. ϕ_0 and ϕ_1 are incident angle from vertical and refracted angle from vertical, respectively.

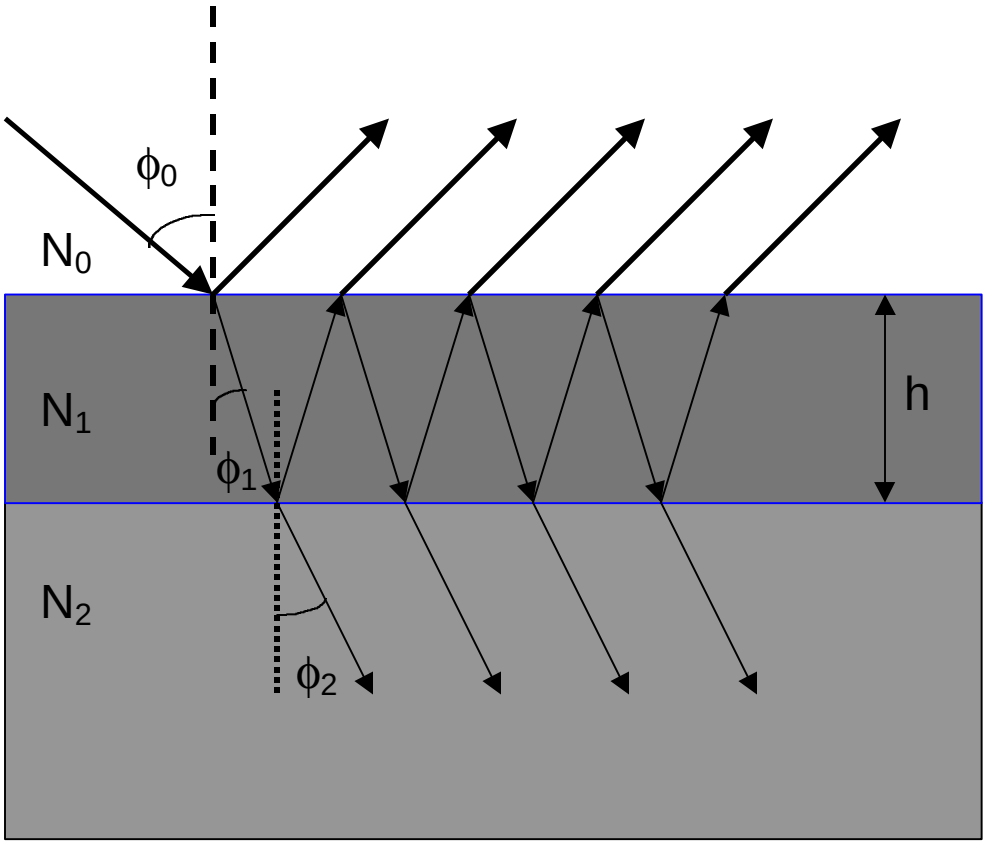

Figure 1-7: Schematic of reflections and transmissions of the incident light from a planar with multiple interfaces.

1.10 REFERENCES

(1) Frank, C. W.; Rao, V.; Despotopoulou, M. M.; Pease, R. F.; Hinsberg, W. D.; Miller, R. D.; Rabolt, J. F. *Science* **1996**, 273, 912.

(2) Dimitrakopoulos, C. D.; Mascaro, D. J. *IBM Journal of Research and Development* **2001**, 45, 11.

(3) Ziemelis, K. *Nature* **1998**, 393, 619.

(4) Ibn-Elhaj, M.; Schadt, M. *Nature* **2001**, 410, 796.

(5) Ashok, B.; Muthukumar, M.; Russell, T. P. *J. Chem. Phys.* **2001**, 115, 1559.

(6) Black, C. T.; Guarini, W.; Milkove, R.; Baker, S. M.; Russell, T. P.; Tuominen, M. T. *Applied Phys. Lett.* **2001**, 79, 409.

(7) Keddie, J. L.; Jones, R. A.; Cory, R. A. *Europhys. Lett.* **1994**, 27. 59.

(8) Torres, J. A.; Nealy, P. F.; de Pablo, J. J. *Phys. Rev. Lett.* **2000**, 85, 3221.

(9) Kawana, S.; Jones, R. A. *Phys. Rev. E* **2001**, 63, 21501.

(10) Grohen, Y.; Brogly, M.; Labbe, C.; Schultz, J. *Langmuir* **1998**, 14, 2929.

(11) van Zanten, J. H.; Wallace, W. E.; Wu, W. *Phys. Rev. E* **1996**, 53, R 2053.

(12) Forrest, J. A.; Dalnoki-Veress, K.; Stevens, J. R.; Dutcher, J. R. *Phys. Rev. Lett.* **1996**, 77, 2002.

(13) Jain, T. S.; de Pablo, J. J. *Macromolecules* **2002**, 35, 2167.

(14) Binder, K. *Adv. Poly. Sci.* **1999**, 138, 1.

(15) Green, P. F.; Limary, R. *Adv. Colloid and Interfacial Science* **2001**, 94, 53.

(16) Lin, E. K.; Kolb, R.; Satija, S.; Wu, W. *Macromolecules* **1999**, 32, 3753.

(17) Zheng, X.; Rafailovich, M. H.; Sokolov, J.; Strzhemecheny, Y.; Schwarz, S. A.; Sauer, B. B.; Rubinstein, M. *Phys. Rev. Lett.* **1997**, 79, 241.

(18) Reiter, G. *Phys. Rev. Lett.* **1992**, 68, 75.

(19) Rudin, A. "*The Elements of Polymer Science and Engineering*" Academic Press, San Diego, **1998**.

(20) Richards, R. W.; Jones, R. A. L. "*Polymers at Surfaces and Interfaces*" Cambridge University Press, Cambridge U.K. **1999**.

(21) Gibbs, J. H.; DiMazio, E. A. *J. Chem. Phys.* **1958**, 28, 373.

(22) Adam, G.; Gibbs, J. H. *J. Chem. Phys.* **1965**, 43, 139.

(23) Angell, C. A. *J. Phys. Chem. Solid* **1988**, 49, 863.

(24) Forrest, J. A.; Dalnoki-Veress, K. *Adv. In Colloid and Interface Science* **2001**, 94, 167.

(25) Cohen, M. H.; Turnbull, D. J. *J. Chem. Phys.* **1959**, 31, 1164.

(26) Fukao, K.; Miyamoto, Y. *Europhys. Lett.* **1999**, 46, 649.

(27) Kim, J. H.; Jang, J.; Zin, W. *Langmuir* **2001**, 17, 2703.

(28) Desimone, J. M. *Science* **2002**, 297, 799.

(29) Cooper, A. I. *J. Mater. Chem.* **2000**, 1, 207.

(30) DeSimone, J. M.; Maury, E. E.; Menceloglu, Y. Z.; McClain, J. B.; Romack, T. J.; Combes, J. R. *Science* **1994**, 265, 356. Stafford, C. M.; Russell, T. P.; McCarthy, T. J. *Macromolecules* **1999**, 32, 7610.

(31) Teja, A. S.; Eckert, C. A. *Ind. Eng. Chem. Res.* **2000**, 39, 4442.

(32) Perrut, M. *Ind. Eng. Chem. Res.* **2000**, 39, 4531.

(33) Kazarian, S. G. *Polymer Science, Ser. C* **2000**, 42, 78.

(34) Weibel, G. L.; Ober, C. K. *Microelectronic Eng.* **2003**, 65, 145.

(35) Wells, S. L.; DeSimone, J. *Angewandte Chemie* **2001**, 40, 518.

(36) Namatsu, H. J. Vac. Sci. Technol. B 2000, 18, 3308.

(37) Goldfarb, D. L.; de Pablo, J. J.; Nealy, P. F.; Simons, J. P.; Moreau, W. M.; Angelopoulos M. *J. Vac. Sci. Technol. B* **2000**, 18, 3313.

(38) Zhang, X.; Pham, J. Q.; Martinez, H. J.; Wolf, J.; Green, P. F.; Johnston, K. P. *J. Vac. Sci. Technol. B* **2003**, 21, 2590.

(39) Zhang, X.; Pham, J. Q.; Ryza, N.; Green, P. F.; Johnston, K. P. *J. Vac. Sci. Technol. B* **2004**, 22, 818.

(40) Sihvonen, M.; Jarvenpaa, E.; Hietaniemi, V.; Huopalahti, R. *Trends in Food Science & Technology* **1999**, 10, 217.

(41) Long, D. P.; Blackburn, J. M.; Watkins, J. J. *Advanced Materials* **2000**, 12, 913.

(42) Ye, X.; Wai, C. M. *J. Chem. Edu.* **2003**, 80, 198.

(43) Zhang, Y.; Gangwani, K. K.; Lemert, R. M. J. *Supercritical Fluids* **1997**, 11, 115.

(44) Gupta, R. R.; Lavery, K. A.; Francis, T. J.; Webster, J. R.; Smith, G. S.; Russell, T. P.; Watkins, J. J. *Macromolecules* **2003**, 36, 346.

(45) Liao, X.; Wang, J.; Li, G.; He, J. *J. Poly. Sci. Part B: Poly. Phys.* **2004**, 42, 280.

(46) Kato, S.; Tsujita, Y.; Yoshimizu, H.; Kinoshita, T.; Higgins, J. S. *Polymer* **1997**, 38, 2807.

(47) Meli, L.; Pham, J. Q.; Johnston, K. P.; Green, P. F. *Accepted to Physical Review E.*

(48) Watkins, J. J.; Brown, G. D.; RamachandraRao, V. S.; Pollard, M. A.; Russell, T. P. *Macromolecules* **1999**, 32, 7737.

(49) Vogt, B. D.; Brown, G. D.; RamachandraRao, V. S.; Watkins, J. J. *Macromolecules*, **1999**, 32, 7907.

(50) Condo, P. D.; Paul, D. R.; Johnston, K. P. *Macromolecules* **1994**, 27, 365

(51) Condo, P. D.; Johnston, K. P. *J. Polym. Sci. Part B: Polym. Phys.* **1994**, 32, 523.

(52) Wissinger, R. G.; Paulaitis, M. E. *J. Polym. Sci. Part B: Polym. Phys.* **1987**, 25, 2497.

(53) Wang, W-C. W.; Kramer, E. J.; Sachse, W. H. *J. Polym. Sci., Polym. Phys. Ed.* **1982**, 20, 1371.

(54) Chiou, J. S.; Barlow, J. W.; Paul, D. R. *J. Appl. Polym. Sci.* **1985**, 30, 2633.

(55) Sirard, S. M.; Green, P. F.; Johnston, K. P. *J. Phys. Chem. B* **2001**, 105, 766.

(56) Sirard, S. M.; Zeigler, K. J.; Sanchez, I. C.; Green, P. F.; Johnston, K. P. *Macromolecules* **2002**, 35, 1928.

(57) Koga, T.; Seo, Y-S.; Zhang, Y.; Shin, K.; Kusano, K.; Nishikawa, K.; Rafailovich, M. H.; Sokolov, J. C.; Chu, B.; Peiffer, D.; Occhiogrosso, R.; Satija, S. K. *Phys. Rev. Lett.* **2002**, 89, 125506.

(58) Vedam, K. *Thin Solid Films* **1998**, 313.

(59) Kressler,J.; Higashida, N.; Inoue, T.; Heckmann, W.; Seitz, F. *Macromolecules* **1993**, 26, 2090.

(60) Malmsten, M. *J. Colloid Interface Sci.* **1994**, 166, 333.

(61) Nee, S.-M. F. *Appl. Opt.* **1988**, 27, 2819.

(62) Azzam, R. M.; Bashara, N. M. *Ellipsometry and Polarized Light*; North-Holland Publishing Co.: Elsevier, **1997**.

(63) Tompkins, H. G.; McGahan, W. A. *Spectroscopic Ellipsometry and Reflectometry*; John Wiley & Sons, Inc.: New York, **1999**.

(64) Styrkas, D.; Doran, S. J.; Gilchrist, V.; Keddie, J. L.; Lu, J. R.; Murphy, E.; Sackin, R.; Su, T-J.; Tzitzinou, A. *Polymer Surfaces and Interfaces III*, edited by Richards, R. W.; Peace, S. K. John Wiley & Sons Ltd. **1999**.

Chapter 2: The Glass Transition of Thin Film Polymer/Polymer Blends: Interfacial Interactions and Confinement

Preprint with permission from:

Pham, J. Q.; Green, P. F. *J. Chem. Phys.* **2002**, 116, 5801-5806.

We examined the influence of film thickness and composition on the effective T_g of compatible thin film mixtures of polystyrene (PS) and tetramethylbisphenol-A polycarbonate (TMPC) on SiO_x/Si substrates using spectroscopic ellipsometry. Our measurements reveal that while the T_g of TMPC films increased with decreasing film thickness, h, the effective T_g of thin film mixtures of PS and TMPC decreased with decreasing film thickness. In these mixtures, T_g was independent of film thickness at large h. We also found that while the T_g of bulk mixtures of TMPC/PS exhibited large negative deviations from additivity with composition, such deviations were negligible in the thin film mixtures. The thickness dependence of T_g is compared with theory.

2.1 INTRODUCTION

Properties of thin polymer films are influenced by entropic effects, associated with chain "packing" and confinement, and by interfacial interactions **[1]**. In recent years, it has become apparent that in thin films, glass transition temperatures, viscosities and translational chain diffusion coefficients are influenced by confinement and by interfacial interactions **[2-20]**. Consequently a film thickness dependence of these properties is measured in different systems, provided the film is below a critical thickness. Additionally, in thin film A/B mixtures, the combined entropic and enthalpic effects (polymer segment/segment and segment/interface interactions) influence phase separation temperatures and the symmetry of the phase diagrams **[21-23]**. These effects also alter the ordering temperature of block copolymers **[24]**. The nature of these finite size effects and their fundamental origins are of current interest to researchers for scientific reasons and, more importantly, for the fact that polymer thin films are used in many applications, including membranes, adhesion, lithography, coatings and various device technologies.

Of particular interest in this chapter of the dissertation is the nature of interfacial interactions and confinement on the glass transition of polymers. Many studies have shown that the glass transition temperature of polystyrene thin films in the polystyrene/SiO_x/Si system decreases below its bulk value with decreasing film thickness when the film thickness $h < 40$ nm **[2,14,18]**. This effect is independent of molecular weight, M, for chains of $M > 10^5$g/mole. Computer simulations, theory and experiments reveal chain segments at surfaces have a higher mobility than the remainder of the sample due to a larger configurational freedom **[9,11,13,19,20,25,26]**. As argued by de Gennes,

the effect can extend a finite distance beneath the surface due to dynamic cooperative effects that propagate along segments of chains that extend from the surface **[11]**. Experimental data from Kawana and Jones indicate that the length scale of the high mobility region is independent of both temperature and of film thickness **[14]**. In the vicinity of the substrate, on the other hand, the chain segment/substrate interactions are such that the mobility of the chains is appreciably lower in the vicinity of the substrate **[19,20]**. Therefore one can in principle associate average relaxation times with chains in the vicinity of the surface, τ_s, chains in the interior of the film, τ_b, and chains in the vicinity of the substrate, τ_{sub}, where $\tau_s > \tau_b > \tau_{sub}$. With this in mind, one can envision a situation such that the glass transition occurs at the free surface at a lower temperature than it would near a strongly interacting substrate. It is argued that the decrease in the average glass transition temperature of the PS/SiO_x/Si system, as measured by ellipsometry, for example, is a manifestation of the fact that the dynamics of the surface layer exert a dominant influence on the average glass transition temperature of the film. Brillouin scattering experiments on freely standing PS films reveal that the decrease of T_g with film thickness is more significant than the decrease measured for supported PS films **[8,10]**. These data on freely standing films are consistent with the influence of two high mobility surface layers.

In cases where the polymer segment-substrate interaction is particularly strong, the relatively immobile layer of polymer in the vicinity of the substrate may exert the dominant influence on the average glass transition temperature of the film. For example, the effective T_g's of poly (methylmethacrylate) and poly (vinyl pyridine) thin films on

SiO_x/Si substrates are shown to increase with decreasing film thickness **[2,6]**. This is consistent with the fact that the more polar interactions of the PMMA and PVP chain segments with the oxide layer (hydrogen bonds) have a sufficiently strong influence on the dynamics of the segments in the vicinity of the substrate. Computer simulations of polymer chains on highly interacting substrates corroborate these findings, T_g increases with increasing film thickness **[13]**.

Having summarized the behavior of homopolymers, we move more specifically to our studies. We are interested in the manner in which confinement effects and interfacial interactions affect the average glass transition temperature of thin film polymer/polymer mixture that is known to be compatible in the bulk. Two important issues must be considered in order to provide a context for the studies described in this chapter of the dissertation. The first issue is that the glass transition temperature of bulk miscible blends varies with composition. Depending on the nature of the interactions between the blend components, the glass transition temperature could exhibit positive or negative deviations from linear additivity, as shown by extensive experimental and theoretical work **[28-38]**. The second issue is associated with the fact that, except in the case of a neutral interface, one component of the blend preferentially interacts with the interface, leading to preferential segregation. If the surface energies of the two components differ, then the lower surface energy component, provided the entropic effects are negligible, will preferentially reside at the free surface. Consequently, variations of composition of the film away from the interfaces may reflect local variations (heterogeneities) in mobility as well as in the glass transition.

Thin film mixtures of tetramethyl bisphenol-A polycarbonate (TMPC) and PS were investigated. This is a miscible blend whose bulk properties have been studied extensively **[30,32-38]**. In the bulk, TMPC/PS exhibits a lower critical solution temperature (LCST) between 513 K to 543 K, depending on molecular weight. The glass transition temperature of bulk PS is 373 K, just over 100 degrees lower than that of TMPC. In the sections that follow we examine the effects of film thickness and composition on the effective T_g of the PS/TMPC miscible blend.

2.2 EXPERIMENTAL SECTION

Samples of varying thickness and composition were prepared for ellipsometric measurements. Different weight percentage mixtures of polystyrenes of molecular weight Mw = 49, 000 g/mole (dispersity index of 1.06) and TMPC, of Mw = 37,900 g/mole (dispersity index 2.75), were dissolved in toluene and spin cast onto silicon substrates. There was a native SiO_x layer of thickness 2 nm on the Si substrate, determined using spectroscopic ellipsometry. By adjusting the spin rates and the solution concentrations, thin films ranging from ~ 20 nm to ~ 200 nm were prepared. The TMPC films were then annealed at 220°C under vacuum for a few hours to remove residual solvent and thermal history prior to ellipsometric measurements. The blends were annealed just above T_g for a few hours under vacuum to remove residual solvent and thermal history before the ellipsometric measurements were performed.

After the samples were annealed, thermal measurements were performed using the variable angle multi-wavelength ellipsometer (J.A. Woollam Co.) equipped with a home made heating stage. Ellipsometric angles, ψ and Δ, were measured at different

temperatures. The sample was held at a given temperature for approximately 2 minutes for each measurement. Three measurements were taken at each temperature. During our experiments, we increased the temperature at a constant heating rate of 1°C /min. The temperatures were controlled with an accuracy of ± 0.5°C. Film thicknesses were determined by fitting the ellipsometric angles with a Cauchy model (using software provided by the manufacturer). Since the measurements and analysis are standard we will not repeat the details here **[1,14,15,17]**. Figures 2-1a and 2-1b show typical thermal scans of two samples where the thicknesses differ by a factor of approximately five.. Each plot clearly exhibits distinct glassy and rubbery regions. T_g was determined by fitting straight lines through the data obtained from the glassy and rubber regions. The temperature at which these lines intersect is identified as the T_g of the film. The margin of error in our determination of T_g was less than ±3°. We note that based on our film thickness versus temperature measurements, all thin film mixtures exhibited a single transition temperature, typical of that shown in Figures 2-1a and 2-1b that resided between that of the PS and TMPC components.

2.3 RESULTS AND DISCUSSION

We begin with a discussion of the thickness dependence of the glass transition temperature of TMPC on the SiO_x/Si substrates. The data in Figure 2-2 clearly indicate that T_g increases with decreasing film thickness. This behavior is not surprising since TMPC interacts strongly with the substrate.

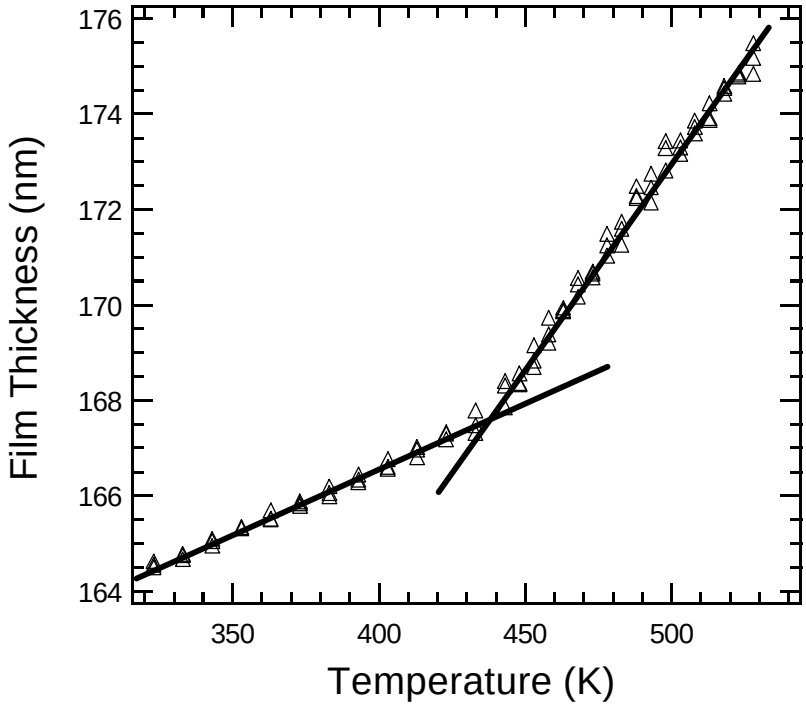

Figure 2-1a: Typical temperature versus film thickness data for films of two different thicknesses for a 50/50 weight percent blend of TMPC and PS are shown here. The glass transition is identified as the temperature at which the two lines drawn through the data intersect.

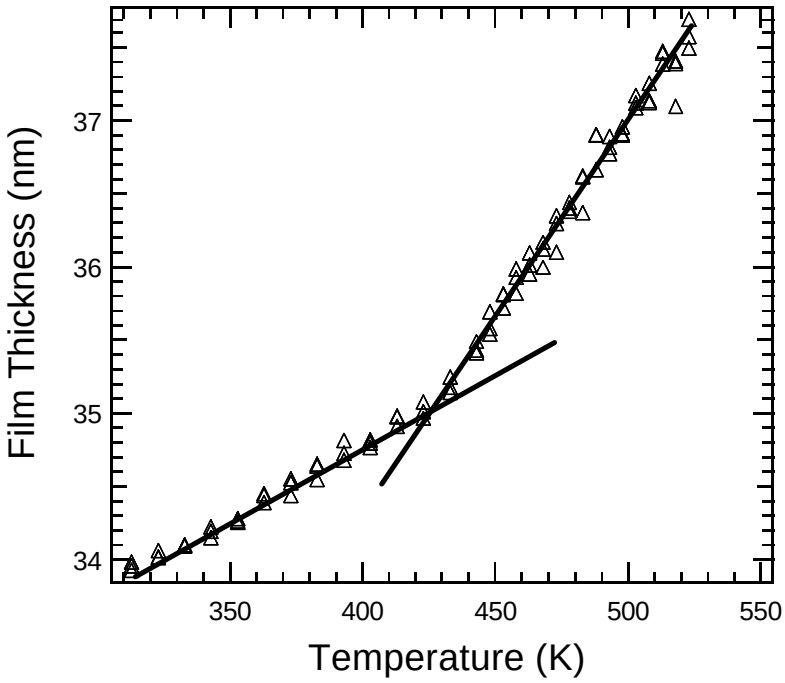

Figure 2-1b: Typical temperature versus film thickness data for films of two different thicknesses for a 50/50 weight percent blend of TMPC and PS are shown here. The glass transition is identified as the temperature at which the two lines drawn through the data intersect.

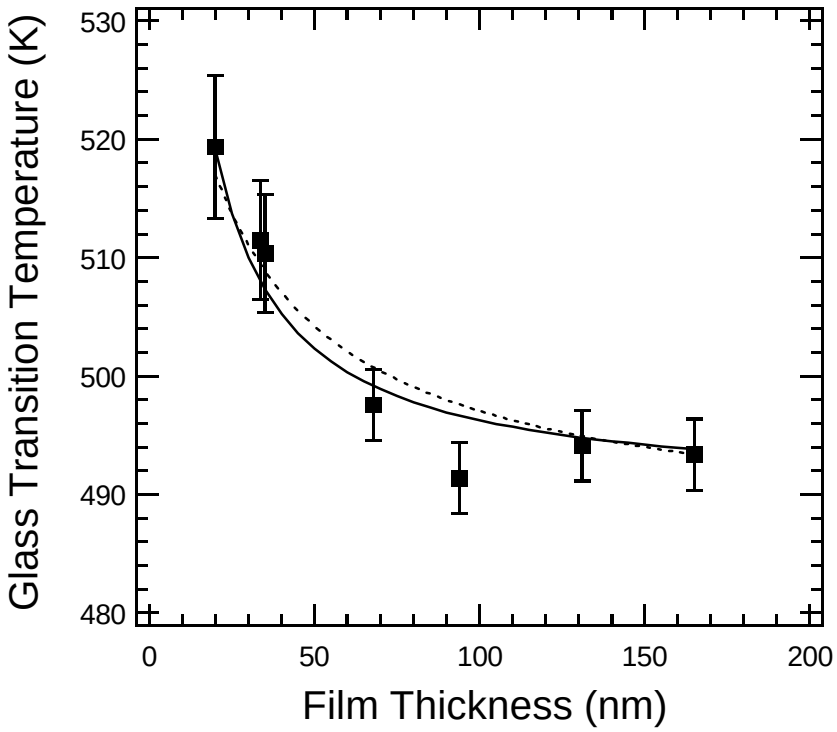

Figure 2-2: The glass transition temperatures, as determined from the break in the film thickness versus temperature data, versus film thickness are plotted for TMPC films of varying thickness. The solid line drawn through the data was computed using equation 2.1 (Kim at al.) whereas the broken line was computed using equation 2.2 (Long and Lequeux).

Specifically, the oxygen groups in TMPC have unshared electrons, which can form hydrogen bonds with the hydroxyl groups at the surface of the substrate. These interactions hinder the mobility of TMPC chain segments and create a region of low mobility in the vicinity of the polymer-substrate interface. This region in the vicinity of the substrate evidently exhibits a dominant effect on the average glass transition temperature of TMPC, leading to the increase in the effective T_g when the film is sufficiently thin. This behavior is similar to that observed in the poly (vinyl pyridine)/SiO_x and PMMA/SiO_x systems mentioned earlier **[2,6]**.

Kim et al. proposed the following equation to describe the average T_g of a polymer film **[15]**,

$$T_g(h) = T_{g,bulk}\frac{h(2k+h)}{(s+h)^2} \qquad (2.1)$$

In the model used to predict this equation, the film is imagined to be composed of a series of layers. Each layer has a different T_g, and the T_g increases gradually from the free surface to the polymer substrate interface where it is largest. In this equation, σ is believed to be the polymer segmental length, $T_{g,bulk}$ is the bulk glass transition temperature and k is a measure of the influence of the substrate on the average T_g of the film. We find that σ = 0.72±0.02 nm and k = 1.37±0.02 nm provide a good description of our data. Values of k = 1.5 nm and 0.8 nm were found to describe the data for PVP and PMMA on SiO_x/Si substrates, respectively. A smaller value of k for PMMA indicates

that it is not as strongly attracted to the substrate as PVP or TMPC, as suggested by Kim et al.

There has recently been an alternate prediction for the film thickness dependence of T_g for thin films by Long and Lequeux **[39]**. This phenomenological model is based on the notion that the dynamics in the vicinity of the glass transition is heterogeneous, characterized by domains of fast and slow dynamics. In their model they introduce a critical density above which the dynamics in the domain are slow, and below which the dynamics are fast. The existence of these domains is due to density fluctuations. The size of these high density domains in which the dynamics are slow is on the order of ξ~1-2 nanometers. Each such domain is, on average, composed of N_c monomers and the average relaxation time of the dynamics is assumed to be long, comparable to the relaxation time at the glass transition. At high temperatures the probability of existence of these domains is low and the average dynamics of the system are determined by the highly mobile fluid regions which these high density regions exist. At lower temperatures the number of such domains increases. The glass transition occurs when these domains percolate to form a three dimensional network. It is argued that since the percolation threshold is lower in three dimensional than in two dimensions, the thin films should not experience a glass transition at the same temperature as bulk films. Since the thin films are assumed to be quasi two dimensional in this model, the transition should occur at a lower temperature A strongly interacting substrate has the effect of inducing percolation into the film because its effect is to increase the number of slow domains in the system. Consequently, the T_g of a thin film on a strongly interacting substrate should increase with decreasing film thickness. This model, clearly, views T_g in a dynamical

sense. To this end, the following equation was proposed to describe the average T_g of a film of thickness h on a strongly interacting substrate:

$$\frac{T_g(h) - T_{g,bulk}}{T_{g,bulk}} \approx \frac{5}{N_c^{(1/2-1/(3n))}} \frac{a}{h} \log\left(\frac{h}{2x}\right) \qquad (2.2)$$

In this equation, ν is a universal exponent, the parameter a is a segmental length and $x = aN_c^{1/3}$. Using values of a = 0.5 nm and ν = 0.88, as suggested by the authors, we determined that N_c = 32 and ξ = 1.6 nm best described our data for TMPC. These values are not unreasonable in view of the fact that the equation is an approximate analytical solution. Recall that the size of the heterogeneous domains is expected to be on the order of 2 nm.

We now discuss the results for the TMPC/PS mixtures by first comparing the glass transition temperatures of the mixtures with that of pure TMPC in the plateau regions of the curves in Figures 2-3. The glass transition temperatures of the blend containing 70% TMPC and 50 wt % TMPC are $T_g(0.7)$ = 452 K and $T_g(0.5)$ = 435 K, respectively. In contrast, that the T_g of TMPC is approximately T_g(TMPC) = 494 K. The reduction in the average T_g with increasing PS content is expected since PS has a lower T_g, 100 K lower, than that of TMPC. We saw no evidence of a change in slope in the h versus T data of the blends to indicate evidence of a T_g in the vicinity of TMPC nor of PS. We can therefore safely conclude that the reduction in T_g with increasing PS content is consistent with a well established fact that the blend is miscible.

It is interesting that in spite of the fact that TMPC is preferentially attracted to the substrate and interacts strongly with it, the glass transition temperatures of the mixtures decreased with decreasing film thickness when h < 50 nm. This is illustrated in Figure 2-3 for two PS/TMPC blend compositions, containing 70 wt % TMPC and 50 wt % TMPC. It is known that in binary thin film PS/TMPC mixtures, TMPC preferentially resides at the substrates **[35-37]**. This is not surprising because of the more polar interactions of TMPC with the substrate than PS. The bulk and the free surface of thin film TMPC/PS blends are phase mixed with PS having a higher surface concentration than the bulk **[35-37]**. In fact, we performed X-ray photoelectron spectroscopy measurements on our samples of thickness h = 30 nm and h = 130 nm thick and found that within the first 10 nm, the composition of PS as 72 wt %, consistent with the data in references 35 and 37. With this in mind, it follows that the surface should have a lower glass transition than the remainder of the sample. More importantly, the chains at the free surface have a much higher mobility than the higher T_g TMPC chains that interact strongly with the SiO_x/Si substrate, $\tau_s >> \tau_{sub}$. Indeed the higher mobility of the chain segments at the surface is due not only to the inherent features of the free surface dynamics, but also because the excess PS chains with their intrinsically higher mobility than TMPC **[35-37]**. The reduction in T_g is consistent the fact that the high mobility surface layer exerts a dominant influence on the average T_g of the film.

In an effort to quantify the film thickness dependence of T_g, two equations have been used. Below we compare our results with these predictions. An empirical equation was proposed by Keddie et al. **[2]**

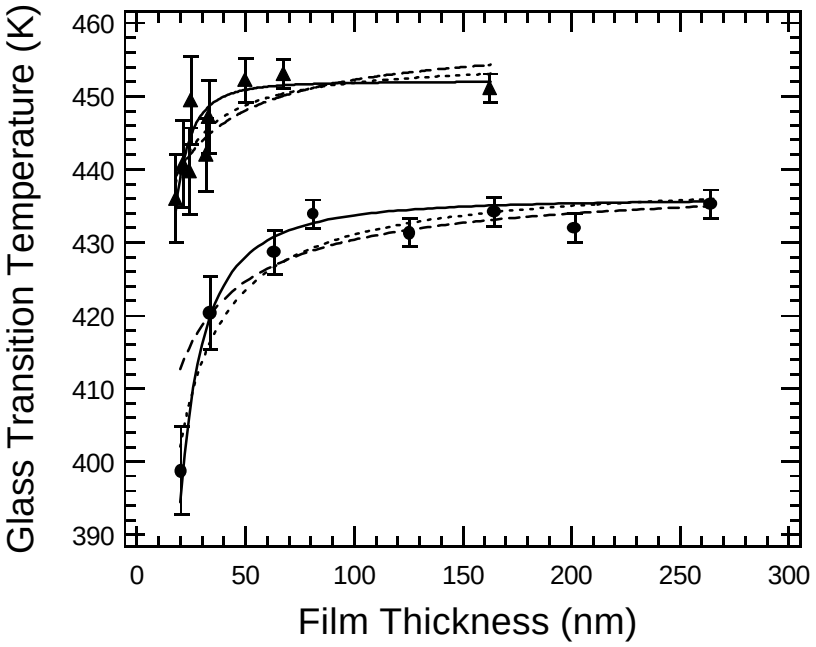

Figure 2-3: The glass transition temperatures versus film thickness are plotted for two compositions, 50 wt % (triangles) and 70 wt % (squares) TMPC. The solid lines were computed using equation 2.3; the broken line (----) was computed using equation 2.4 and the dotted line (…..) was computed using equation 2.5. The fitting parameters are identified in the text.

$$T_g = T_{g,bulk}[1-(A/h)^{\delta}] \qquad (2.3)$$

This equation has two adjustable parameters; A which has units of length and δ. δ is an indication of the degree to which T_g decreases with decreasing film thickness. This equation accurately described the T_g versus film thickness data for polystyrene on SiO_x/Si substrates, where it was determined that A = 3.2 nm and δ = 1.8. Based on equation 2.3, the values for the 70 wt % TMPC blend were $T_{g,bulk}$ = 452K, A = 5.4 nm and δ = 2.7. For the 50 wt % blend, on the other hand, $T_{g,bulk}$ = 436K, A = 5.4 nm and δ = 1.8. The values of A determined from this fit are comparable to the value found by Keddie et al. to describe PS on SiO_x/Si **[2]**. Note that in the blend containing 70 wt % TMPC, δ = 2.7 whereas it has a value of 1.8 in the blend containing 50 wt % TMPC, comparable for the value that described the PS data. The relative magnitudes of δ reflect the relative influence of the regions of fastest dynamics (free surface) versus regions of slowest dynamics (at the substrate) on the average T_g of the film. Clearly, larger values of δ suggest a weaker thickness dependence of the decrease of glass transition temperature.

An alternate equation was proposed by Kim et al. to describe the same data **[15]**,

$$T_g(h) = T_{g,bulk}\frac{h}{s+h} \qquad (2.4)$$

Here σ is a measure of the rate at which the glass transition temperature decreases with decreasing h. A value of σ = 0.67 nm was found to do a very good job describing the T_g versus h data for polystyrene. Kim et al. proposed that σ should be independent of chain length and in fact they found it to be approximately 0.7 nm, regardless of the system. They concluded that it might be a statistical segmental length **[15]**. Using equation 2.4 to fit our data (Figure 2-3), we determined that σ = 0.695 nm and 1.84 nm for the 70 wt % TMPC and 50 wt % TMPC samples, respectively. Clearly, the value for the 50 wt % mixture is more than twice as large as the other two so σ may not be a statistical segment length. Based on the sample compositions and the values of σ, one might conclude that the value of σ reflects the influence of the relative difference between the fastest and slowest dynamical regions on the T_g of the film.

Long and Lequeux, also had a prediction for the decrease in glass transition temperature with film thickness **[39]**,

$$\frac{T_g(h) - T_{g,bulk}}{T_{g,bulk}} \approx \frac{-2.6}{N_c^{(1/2-1/(3n))}} \frac{a}{h} \log\left(\frac{h}{2x}\right) \qquad (2.5)$$

Using the values they suggested for a and ν as 0.5 nm and 0.88 respectively, we determined that ξ = 0.8 nm for the 50 wt % mixture and 1.3 nm for the 70 wt % TMPC sample. These values of ξ, particularly the latter value of 0.8 nm, are unrealistically small. In view of the unrealistically small parameters, it is possible that the theory may have to be revisited. We nevertheless interpret the trends in the values of î as follows.

The model treats the system such that percolation, and hence the glass transition, occurs when the sample is cooled from high to low temperatures. The number and size of these regions determine the temperature at which percolation occurs. When the system is cooled, the number of regions of slow dynamics increases with decreasing temperature. If the size of the slow domains is small, then the temperature at which the glass transition occurs is low. The smaller value of î for the 50 wt % mixture is associated with a lower T_g. In conclusion, we note that we do not know, a priori, whether this would be true to the 50 wt % blend. This would have to await further theory and experiments.

We now examine the dependence of T_g on composition for the thin film blend. The values of T_g plotted in Figure 2-4 were obtained from thicker films for which T_g was independent of film thickness. It is clear from these data that the T_g's of the thin film blends exhibit relatively small deviations from linearity. The bulk analogs exhibit relatively larger negative deviations from linear additivity. The implications regarding the deviations of the compositional dependencies of T_g for the bulk and the thin film mixtures from linearity can be understood from the following. The glass transition of a large number of bulk mixtures has been examined extensively, experimentally and theoretically **[28-38]**. Depending on the nature of the thermodynamic interactions between the components, the glass transition of the blend could exhibit positive or negative deviation from linear additivity. Different models have had varying levels of success at describing the compositional dependence of T_g in *miscible* blends. Gordon and Taylor argued that when a compatible mixture is created, the free volume of the blend is determined by the sum of the fractional free volumes of the constituents, leading to **[29]**

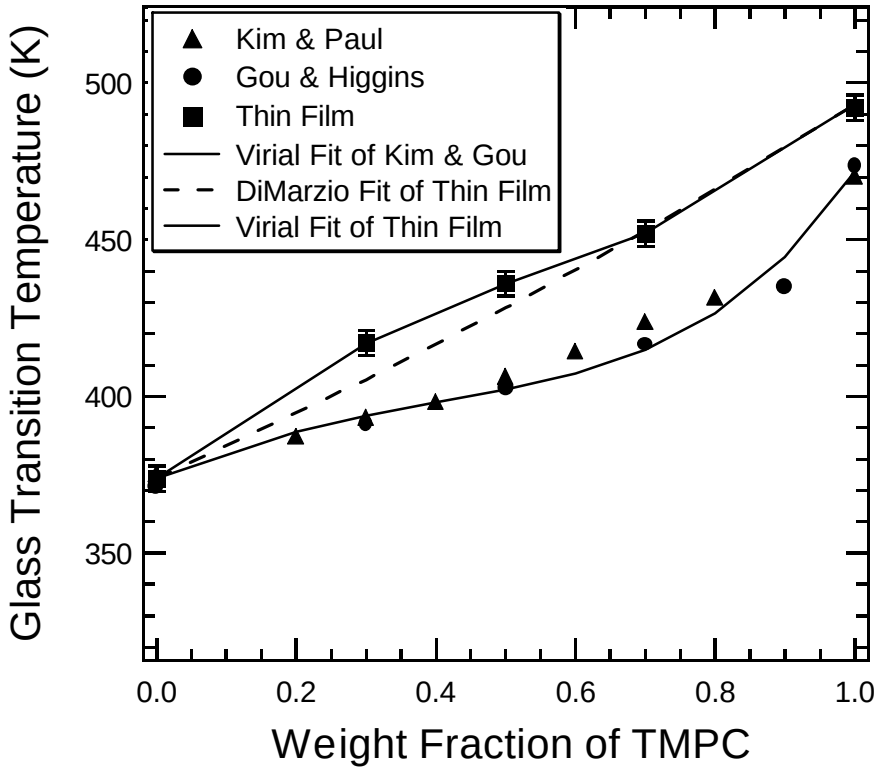

Figure 2-4: Glass transition temperature of the TMPC/PS blend is plotted as a function of weight fraction of TMPC. The filed squares represent our data, the data for the thin film mixtures whereas the other symbols represent the bulk data, determined by other authors.

$$T_g = \frac{w_1 T_{g1} + K w_2 T_{g2}}{w_1 + K w_2} \qquad (2.6)$$

Here free volume is interpreted in terms of an "open" or "unoccupied" volume, associated with packing irregularities. The parameter K is a function of the densities of the constituents and of the differences in the thermal expansion coefficients of the melt and glassy states of the constituents. DiMarzio proposed an equation that is virtually identical to equation 2.6, except that K has a different meaning **[28].** In the DiMarzio model, the onset of the glass transition occurs when the number of configurations available to the system reaches a very small value. Since the number of states available to a system undergoing flow is small, flow is impeded; flow is envisioned as transitions from one state to another. It is assumed that the number of flexible bonds on the monomer plays a critical role in that it is responsible for accommodating conformational changes that the chains experience upon mixing. Polymer units with a large number of flexible bonds should experience the largest configurational changes. For the DiMarzio model, K depends on the number of flexible bonds on each repeat unit and on the molecular masses of the constituents. There are no adjustable parameters in equation 2.6. This equation, however, fails to describe the compositional dependence of T_g in the presence of strong segmental interactions (e.g. electron/donor interaction) between the components. An alternate "virial-like" equation, proposed by Brekner, Schneider, and Cantow **[30,31]**, is capable of describing the positive and negative deviations of T_g from additivity in a large number of mixtures,

$$\frac{T_g - T_{g1}}{T_{g2} - T_{g1}} = (1 - K_1)w_{2c} - (K_1 + K_2)w_{2c}^2 + K_2 w_{2c}^3 \qquad (2.7)$$

where $w_{2c} = \frac{Kw_2}{w_1 + Kw_2}$ and $K=T_{g1}/T_{g2}$. K_1 is determined largely by the difference between interaction energies associated with like and unlike contacts and K_2 is determined exclusively by changes in conformational entropy of the chains between the homogeneous and heterogeneous environments. When $K_1 = K_2 = 0$, equation 2.7 becomes identical to equation 2.6, except that now $K = T_{g1}/T_{g2}$. This incidentally, is known as the Flory-Fox equation **[27]**. When $K_1 > 0$ and $(K_1-K_2) > 0$, the glass transition temperatures of the mixtures is enhanced relative to predications based on a rule of mixtures and the curve is concave down. This means that the energetic interactions are strong, resulting in larger conformational transitions upon mixing, accompanied by lower free volume than linear additivity would predict. The free volume of course refers to the static packing of chains. For $K_1 < 0$ and $(K_1-K_2) < 0$, T_g is reduced relative to predictions based on the rule of mixtures for all compositions and the curve is concave up. This situation arises when the energetic A-B interactions are comparatively weaker, hence the chains do not experience large conformational changes upon mixing and the overall free volume is *increased* relative to that predicted by a rule of mixtures. This leads to the reduction in T_g. While one drawback of equation 2.7 is that it has three fitting parameters, its utility is that it successfully describes the relevant trends in the T_g observed in a large number of blends where there exists relatively strong and weak

specific enthalpic interactions. We introduce it here so that we can make a comparison between the bulk and thin film results.

We now address the behavior of the TMPC/PS thin film more specifically. In the bulk, the negative deviations from linear dependence is related to the fact that the chains undergo large changes in conformational entropy upon mixing that results in a larger fractional free volume; $K_1 > 0$ and $(K_1-K_2) < 0$. We note, incidentally, that changes in specific volume with composition in this blend follow a similar pattern with trends in T_g shown here for the bulk blends **[32]**.

The reason that the T_g's of the thin film mixtures exhibit much smaller deviations from linearity than they do for the bulk mixtures is now discussed. Generally in miscible blends, when the energetic interactions are comparable to effects due to entropy (free volume), the deviations of T_g from additivity are negligible **[30,31]**. One might be tempted to argue that this small deviation in the thin film mixtures may be due to an increase in the influence of energetic interactions between the components. However, this is not possible, and in fact, quite the opposite might be expected, particularly in light of the preferential interfacial interactions. Alternatively, one might argue that this trend is due to a significant amount of interfacial segregation by the TMPC. This is not the case for two reasons. There is no evidence of two glass transition temperatures and secondly the TMPC/PS is phase mixed in thin films **[35-37]**. The small deviation is most probably due to a confinement effect that reduces the influence of the entropic effects, described above, on T_g. Further experiments involving low molecular weight, unentangled, PS chains are being considered in order to further investigate the entropy effects on the behavior of the system.

2.4 CONCLUSIONS

We examined the effects of film thickness and composition on the effective T_g of TMPC/PS miscible blend on SiO_x/Si substrates using spectroscopic ellipsometry. This is a miscible asymmetrically adsorbing system, where TMPC interacts preferentially with the substrate and PS with the free surface. We made three important observations.

(1) We showed that the glass transition temperature of TMPC increased with decreasing film thickness. This is due to the fact that TMPC interacts strongly with the substrate, forming hydrogen bonds. This leads to a relatively immobile layer, with a lower free volume, in the vicinity of the substrate. If the average T_g of the film is dominated by this interaction then the measured increase in T_g with decreasing h is expected.

(2) We also examined mixtures containing 70 wt % TMPC and 50 wt % TMPC and found that T_g decreased with decreasing film thickness. The effect was more significant in the 50 wt % blend, as expected. The thickness dependences in both the TMPC and the mixtures were compared with theory.

(3) Finally, we examined the variation of T_g with blend composition and determined it was much smaller in thin films than in the bulk, reflecting the influence of confinement on the entropic (free volume) contribution to the T_g of the thin film system.

2.5 REFERENCES

(1) Binder, K. *Adv. Polymer Sci.* **1999**, 138, 1.

(2) Keddie, J. L.; Jones, R. A.; Cory, R. A. *Faraday Discuss.* **1994**, 98, 219; Keddie, J. L.; Jones, R. A.; Cory, R. A. *Europhys. Lett.* **1994**, 27, 59.

(3) Orts, W. J.; van Zanten, J. H.; Wu, W.; Satija, S. K. *Phys. Rev. Lett.* **1993**, 71, 867; Wu, W.; van Zanten, J. H.; Orts, W. J. *Macromolecules* **1995**, 28, 771.

(4) Tseng, K.C., Turro, N.J. and Durning, C.J. *Phys. Rev. E.* **2000**, E61, 1800.

(5) Wallace, W.E.; van Zanten, J. H.; Wu, W. *Phys. Rev. E* **1995**, 52, R3329.

(6) van Zanten, J. H.; Wallace, W. E.; Wu, W. *Phys. Rev. E* **1996**, 53, R 2053.

(7) Frank, B.; Gast, A. P.; Russell, T. P.; Brown, H. R.; Hawker, C. *Macromolecules* **1996**, 29, 6531.

(8) Forrest, J. A.; Dalnoki-Veress, K.; Stevens, J. R.; Dutcher, J. R. *Phys. Rev. Lett.* **1996**, 77, 2002.

(9) Wallace, W.E., Fischer, D.A., Efimenko, K., Wu, Wen-Li and Genzer, J., *Macromolecules* **2001**, 34, 5081.

(10) Forrest, J. A.; Mattsson, J. *Phys. Rev. E* **2000**, 61, R53; Mattsson, J.; Forrest, J. A.; Borjesson, L. *Phys. Rev. E* **2000**, 62, 5187.

(11) de Gennes, P. G. *Euro. Phys. J. E* **2000**, 2, 201.

(12) Xie, L.; DeMaggio, G. B.; Frieze, W. E.; DeVries, J.; Gidley, D. W.; Hristov, H. A.; Yee, A. F. *Phys. Rev. Lett.* **1995**, 74, 4947.

(13) Torres, J. A.; Nealy, P. F.; de Pablo, J. J. *Phys. Rev. Lett.* **2000**, 85, 3221.

(14) Kawana, S.; Jones, R. A. *Phys. Rev. E* **2001**, 63, 21501.

(15) Kim, J. H.; Jang, J.; Zin, W. *Langmuir* **2001**, 17, 2703.

(16) DeMaggio, G. B.; Frieze, W. E.; Gidley, D. W.; Hristov, H. A.; Yee, A. F. *Phys. Rev. Lett.* **1997**, 78, 1524.

(17) Grohens, Y.; Brogly, M.; Labbe, C.; David, M. –O.; Schultz, J. *Langmuir* **1998**, 14, 2929.

(18) Fukao, K.; Miyamoto, Y. *Europhys. Lett.* **1999**, 46, 649.

(19) Lin, E. K.; Wu, W.; Satija, S. *Macromolecules* **1997**, 30, 7224.

(20) Lin, E. K.; Kolb, R.; Satija, S.; Wu, W. *Macromolecules* **1999**, 32, 3753.

(21) Kerle, T.; Klein, J.; Binder, K. *Phys. Rev. Lett.* **1996**, 77, 1318.

(22) Kerle, T.; Klein, J.; Binder, K. *Euro. Phys. J. E.* **1999**, 7, 401.

(23) Muller-Buschbaum, P.; Gutmann, J. S.; Stamm, M. *Macromolecules* **2000**, 33, 4886.

(24) Green, P.F. and Limary, R., *Advances in Colloid and Interfacial Science* **2001**, 94, 53.

(25) Mansfield, K. F.; Theodorou, D. N. *Macromolecules* **1991**, 24, 6283.

(26) Baschnagel, J.; Binder, K. *Macromolecules* **1995**, 28, 6808.

(27) Ferry, J. D. *Viscoelastic Properties of Polymers*, Academic Press, New York, **1980**.

(28) Di Marzio, E. A. *Polymer* **1990**, 31, 2954.

(29) Gordon, M.; Taylor, J. S. *J. Appl. Chem., USSR* **1952**, 2, 493.

(30) Schnieder, H. A.; DiMarzio, E. A. *Polymer* **1992**, 33, 3453.

(31) Brekner, M. –J.; Schneider, H. A.; Cantow, H. –J. *Polymer* **1988**, 78, 78.

(32) Fernandez, A. C.; Barlow, J. W.; Paul, D. R. *Polymer* **1986**, 27, 1788.

(33) Kim, C. K.; Paul, D. R. *Polymer* **1992**, 33, 1630.

(34) Gou, W.; Higgins, J. S. *Polymer* **1990**, 31, 699.

(35) Kim, E.; Krausch, G.; Kramer, E. J.; Osby, J. O. *Macromolecules* **1994**, 27, 5927.

(36) Kim, E.; Kramer, E. J.; Osby, J. O. *Macromolecules* **1995**, 28, 1979.

(37) Kim, E.; Kramer, E. J.; Osby, J. O.; Walsh, D. J. J. *Poly. Science part B: Poly. Phys.* **1995**, 33, 467.

(38) Lui, J.; Jean, Y. C.; Yang, H. *Macromolecules* **1995**, 28, 5774.

(39) Long, D., Lequeux, F. *Eur. Phys. J. E.* **2001**, 4, 371.

Chapter 3: The effective T_g of confined polymer-polymer mixtures: Influence of molecular size

Preprint with permission from:

Pham, J. Q.; Green, P. F. *Macromolecules* **2003**, 36, 1665-1669.

Polystyrene (PS) and poly(tetramethyl bisphenol polycarbonate) (TMPC) form thermodynamically compatible mixtures below a lower critical solution temperature. In this regime, the PS-component in thin PS-TMPC films, supported by SiO_x/Si substrates, preferentially enriches the free surface, forming a wetting layer, whereas the TMPC component enriches to the polymer-substrate interfacial region. We examined the dependence of the effective glass transition temperature, T_g, on film thickness, h, for 50/50 wt. % mixtures on SiO_x/Si substrates. In these experiments, the molecular weight, M_{PS}, of the PS component was varied by over two orders of magnitude (4 kg/mol < M_{PS} <900 kg/mol) while the TMPC molecular weight remained fixed. The glass transition temperature of the M_{PS} = 4 kg/mol sample is approximately 25^0C lower than that of the other PS samples. We show that the effective glass transition temperature decreases with decreasing film thickness, $\Delta T_g = T_g(\infty) - T_g(h) < 0$, where $T_g(\infty)$ is the glass transition temperature at large h. Moreover, despite the variation in the glass transition temperatures associated with the PS components in the mixtures, $\Delta T_g(h)$ was, within experimental error, independent of M_{PS}. $T_g(\infty)$, on other hand, was sensitive to the T_g of the PS component. Implications of these findings are discussed.

3.1 INTRODUCTION

The glass transition continues to be an active area of research, and interest has broadened in scope due to recent experiments which reveal evidence for a film thickness dependence of the effective glass transition temperature, T_g, of polymer films when the films are sufficiently thin [**1-26**]. In the polystyrene (PS)-SiO_x/Si system, the effective T_g decreases with decreasing film thickness when h is thinner than a threshold film thickness of $h_c \sim 50$ nm **[4,10,11,15]**. In freely standing PS films the same trends are apparent, except that the effect is more significant, wherein the decrease is approximately twice as much as that of the same polymer on SiO_x/Si **[10]**. The opposite trends, T_g increasing with decreasing h, have been observed in the poly vinylpyridine (PVP)-SiO_x/Si, poly(methyl methacrylate) (PMMA)-SiO_x/Si and tetramethyl bisphenol polycarbonate (TMPC)/SiO_x/Si systems **[1,5,8,16]**. In these systems, unlike the PS-SiO_x/Si system, the polymer segments have particularly strong interactions with the substrate (hydrogen bonding). Therefore, in thin polymer films, the effective glass transition is influenced by the nature of the polymer segment-segment interactions in relation to the segment-"wall" (free surface or substrate) interactions. Sufficiently strong segment-"wall" interactions contribute to an increase in the glass transition of the film, provided the film is sufficiently thin.

While to date there is no universally accepted explanation, a number of models have been proposed. Keddie et al. used an empirical equation to describe the decrease in T_g with decreasing film thickness for PS films in SiO_x/Si substrates **[4]**,

$$T_g = T_g(\infty)\,[1-(A/h)^{\delta}] \qquad (3.1)$$

In the above equation $T_g(\infty)$ is the glass transition temperature at large h, δ indicates of the degree to which T_g decreases with decreasing film thickness and A is a length scale. They argue that the decrease in T_g is due to the presence of a high mobility ("liquid-like") layer at the surface. The high mobility surface layer exerts an increasingly larger influence on the average T_g of the film, leading to the observed decrease in T_g. It suffices to mention that chain segments at the free surface exhibit higher segmental mobilities than those in the interior of the film **[28,29]**. This is consistent with the notion that the polymer-segment-segment density is lower at the free surface and that these segments possess larger configurational freedom. It has further been suggested that the size of the high mobility surface region is related to the average size of the chains in the melt **[27]**.

Kim et al. proposed an alternate model for the decrease of T_g with decreasing h **[16]**. They suggest that a series of layers, each possessing a different T_g, comprise the film. The layer at the free surface has the lowest T_g whereas the layer adjacent to the substrate possesses the largest. Of course, the fact that chain segments at the free surface possess larger configurational freedom and lower packing density is not inconsistent with the possibility of a lower surface T_g **[27,31,32]**. An excess concentration of chain ends and associated larger free volume at the free surface are among other reasons that have been suggested to account for the possibility of a surface T_g **[29,30]**. Kim et al. predicted that the effective $T_g(h)$ of the film would be

$$T_g = T(\infty)\frac{h}{s + h} \qquad (3.2)$$

Here, σ measures the extent to which T_g decreases with h, particularly at small h.

A percolation, free volume-based, model was proposed by Long and Lequeux **[3]**. In this model, they propose that domains of rapidly and of slowly relaxing clusters of particles comprise the sample (dynamic heterogeneity). Percolation of the slow domains denotes the onset of the glass transition temperature. Since the percolation threshold in three dimensions is lower than in two dimensions, the glass transition should in principle occur at a lower temperature in sufficiently thin films than in the bulk. The effect of the strong polymer-substrate interactions is to increase the effective number of slow domains in the sample; hence the effective temperature at which percolation occurs is much higher than that for bulk analogues.

Recently we used spectroscopic ellipsometry to examine the dependence of the effective T_g on film thickness in the miscible blend system of TMPC and PS **[1]**. While one might be initially inclined to argue that a study involving mixtures might complicate the issues further, there is a good reason to do this. Consider that in this miscible blend, the T_g of TMPC is much larger than that of PS, ~220ºC compared to 100ºC. Second, TMPC interacts strongly with the SiO_x substrate whereas PS preferentially enriches the free surface (lower surface energy) **[1,33-35]**. The friction coefficient, which controls the segmental mobilities, in TMPC is also much larger than PS. Hence this is a system in which a high-mobility, lower T_g, polymer-free surface region (layer) and a low mobility, and appreciably higher T_g, polymer-substrate "layer" are "tailored."

In our previous study, we examined the thin films (10 nm < h < 200 nm) of TMPC and of PS-TMPC mixtures (the PS molecular weight was 49 kg/mol). We showed that the T_g of TMPC increased with decreasing h ($\Delta T_g(h) > 0$) for $h < h_c$, where $h_c \sim 50$ nm. On the other hand, the effective T_g of mixtures containing 30 and 50 wt. % PS decreased with h for h < 50 nm ($\Delta T_g(h) < 0$). We also investigated the compositional dependence of mixtures of films with thicknesses h > 50 nm. While the compositional dependence of T_g for both bulk and thin films exhibited negative deviations from predictions based on a rule of mixtures, we learned that the deviation in the films was appreciably smaller. This difference was attributed to the fact that the increase in the specific volume that results from mixing PS and TMPC, leading to the negative deviation in the T_g vs. composition dependence, is suppressed in thin films (confinement).

In this chapter of the dissertation we examine the effect of changing the molecular weight of the PS component by two orders of magnitude, from M_{ps} = 4 to 900 kg/mol, while keeping that of the TMPC molecular weight fixed. Decreasing the PS molecular weight from 900 to 4 kg/mol results in a decrease in the PS bulk T_g from 100ºC to 75ºC and a decrease in the radius of gyration of the PS chains by just over an order of magnitude. Since the PS component preferentially resides at the free surface, varying the PS molecular weight and associated T_g will enable an understanding of how the size of the chains and the T_g of the PS component influences $T_g(\infty)$ and $\Delta T_g(h)$.

3.2 EXPERIMENTAL SECTION

Variable angle spectroscopic ellipsometry was used to determine the glass transition temperatures of thin PS-TMPC films on SiO_x/Si substrates. 50/50 wt %

mixtures of polystyrenes of different molecular weights, 4, 49, 290, and 900kg/mole (dispersity index of 1.06, 1.06, 1.06, and 1.10, respectively) with TMPC of molecular weight 37,900 g/mole (dispersity index 2.75) were dissolved in toluene and spin cast onto silicon substrates. The silicon substrate has a native SiO_x layer of thickness 2 nm. This thickness was determined by spectroscopic ellipsometry. By adjusting the spin rates and the solution concentrations, thin films ranging from ~ 20 nm to ~ 200 nm were prepared. All samples were then annealed above their bulk T_g for several hours before the spectroscopic ellipsometry measurements were performed.

After the samples were annealed, thermal measurements were performed using the variable angle multi-wavelength spectroscopic ellipsometer (J.A. Woollam Co.) equipped with a home made heating stage. Ellipsometric angles, ψ and Δ, were measured with a constant heating rate of 1°C /min. Increments of 10°C and 5°C were used for temperatures far away from and close to T_g, respectively. Each sample was held at a given temperature for approximately 2 minutes before increasing to the next temperature for subsequent measurements. Three data points were collected at each temperature. The temperatures were controlled with an accuracy of ± 0.5°C. Film thicknesses were measured by fitting the ellipsometric angles with a Cauchy model (using software provided by the manufacturer).

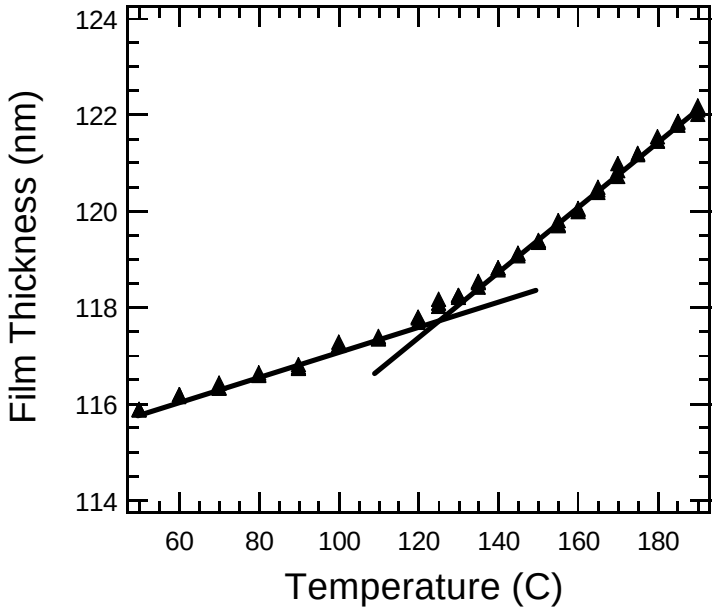

Figure 3-1a: Typical temperature versus film thickness data for films of two different thicknesses for a 50/50 wt% blend of TMPC and PS are shown here. The glass transition is identified as the temperature at which the two lines drawn through the data intersect.

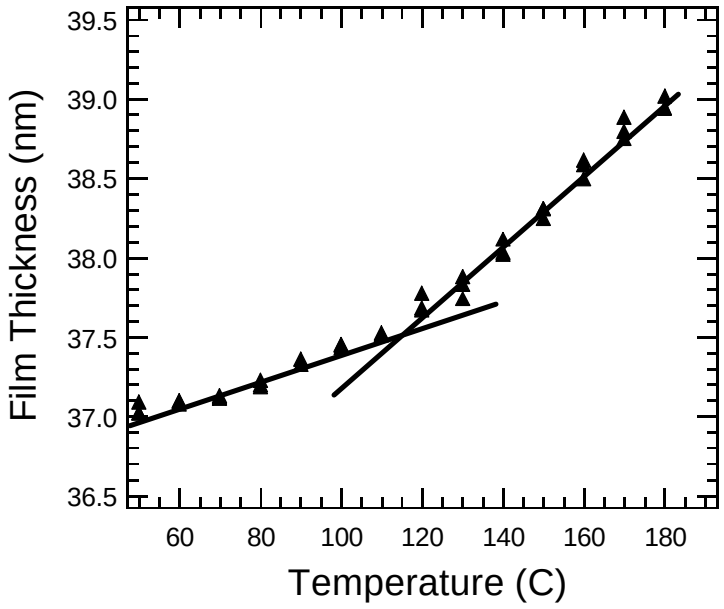

Figure 3-1b: Typical temperature versus film thickness data for films of two different thicknesses for a 50/50 wt% blend of TMPC and PS are shown here. The glass transition is identified as the temperature at which the two lines drawn through the data intersect.

Since the measurements and analysis are standard and will not repeated in this chapter of the dissertation **[1,4,16]**. Parts a and b of Figure 3-1 show typical thermal scans of the samples. The data in each graph clearly exhibits distinct glassy and rubbery regions. T_g was determined by fitting straight lines through the data in the glassy and rubber regions. The temperature at which the lines intersect is identified as the average T_g of the film.

This is a well characterized system, both in bulk and thin films. It is well known that in this mixture the free surface is enriched with PS and that TMPC resides at the substrate **[33-35]**. Since we are in the miscible regime, below the LCST, of the mixture, the layers of enrichment are essentially wetting layers and are therefore of order nanometers. We performed angle resolved X-ray photoelectron spectroscopy (XPS) on samples that were annealed above the T_gs of the samples (typically at 150^0C) and the mass fraction of PS in these 50/50 mixtures ranged between 71 and 75%, regardless of the PS molecular weight. Note that in the miscible regime, the surface enrichment is, at best, weakly dependent on temperature and molecular weight. Note that in the temperature range above 240^0C, thin film of these samples undergo surface directed spinodal decomposition **[34-35]**. Here macroscopic layers of PS and TMPC develop at the appropriate boundaries and the interfacial segregation would be molecular weight dependent. Our experiments were conducted below this temperature in the miscible regime.

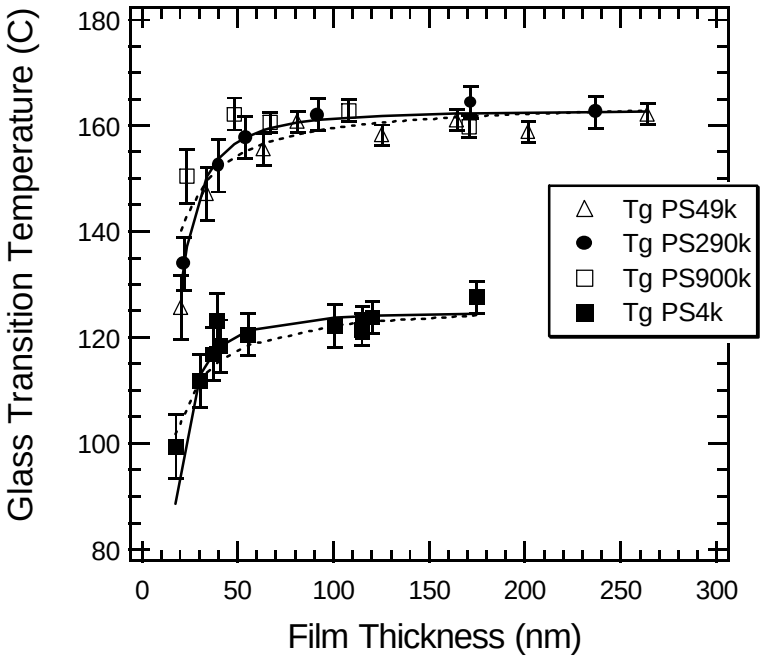

Figure 3-2: The glass transition temperatures are plotted as a function of film thickness for 50/50 weight percent mixtures of TMPC/PS4k, TMPC/PS49k, TMPC/PS290k, and TMPC/PS900k. The solid lines were computed using equation 3.1; the broken lines (----) were calculated using equation 3.2.

3.3 RESULTS AND DISCUSSION

The thickness dependencies of the glass transition temperatures for various 50:50 wt % mixtures containing PS of varying molecular weights, M_{ps}, are plotted in Figure 3-2. The glass transition temperatures of the samples with the M_{PS} = 4 kg/mol PS component are approximately 40ºC lower than those which include PS molecular weights of $M_{PS} \geq 49$ kg/mole. We first comment on the latter data set involving PS samples of M $\geq$ 49 kg/mol. T_g is constant (162°C) for $h > h_c \sim 50$ nm, whereas it decreases for $h < h_c$. Equation 3.1 was used to fit these data, using A = 5.4 nm and $\delta = 1.93 \pm 0.3$. These values of A and δ are, within experimental error, equal to those used by Kawana and Jones ($\delta = 1.1$, A = 8.6) to describe that PS/SiO_x/Si system **[4]**. Using equation 3.2, we found that $\sigma = 1.1 \pm 0.1$ nm, independent of M_{PS} **[16]**. Clearly, both predictions provide reasonable descriptions of our data.

The effective $T_g(\infty)$ of the mixture that includes the M_{PS} = 4 kg/mol PS component is approximately 40ºC lower than that of the higher molecular weight PS-component mixtures. This is not surprising since it is well known in miscible blends involving components with different T_gs, that the T_g of the mixture resides between the T_gs of the pure constituents. There are in fact two related reasons that low molecular weight polymers exhibit lower T_gs than their high molecular weight analogues. One explanation is that the lower T_g is due to the extra fractional free volume associated with the excess number of chain ends per unit volume in low molecular weight polymers compared to their high molecular weight analogues. This argument leads to the following prediction for the molecular weight dependence of the glass transition, $T_g(M_n)$ =

$T_g(M_n \rightarrow \infty)$ - constant/M_n, where M_n is the number average molecular weight **[36]**. DiMarzio and Gibbs, on the other hand, pointed out a long time ago that it is more useful to think about differences in configurational entropy of the chains **[37]**. Specifically, the low molecular weight species have lower T_g's than their high molecular weight analogues because of the larger configurational entropy associated with packing small chains compared to long chains. They predicted virtually the same dependence for T_g on M_n, avoiding ambiguities associated with specifying a reliable and consistent definition of free volume.

The depression in the effective glass transition, $\Delta T_g(h)$, of these 50:50 wt % samples is the same, regardless of M_{PS}. This is illustrated in Figure 3-3, which shows a plot of $T_g(h)/T_g(\infty)$ versus h. These data show that regardless of the PS molecular weight, ΔT_g remains the same, within experimental error. We now proceed by recalling that this mixture is below the lower critical solution temperature, in the miscible regime, where the surface is enriched with a thin PS wetting layer with mass fraction ~ 72%. A wetting layer of TMPC resides at the substrate. The interior of the film is of course a mixture of both components. The data in Figures 3-2 and 3-3 indicate that by changing M_{PS}, with the accompanying changes in T_g, mobility, chain size, and associated changes with fractional free volume, do not, at least to first order, affect h_c and $\Delta T_g(h)$. The primary effect of adding the 4 kg/mol PS-component to TMPC is to decrease $T_g(\infty)$, as anticipated. In addition, it is noteworthy that the depression in T_g is comparable to that observed in PS homopolymers. While equations 3.1 and 3.2 describe the trends in our data very well, there are obvious concerns.

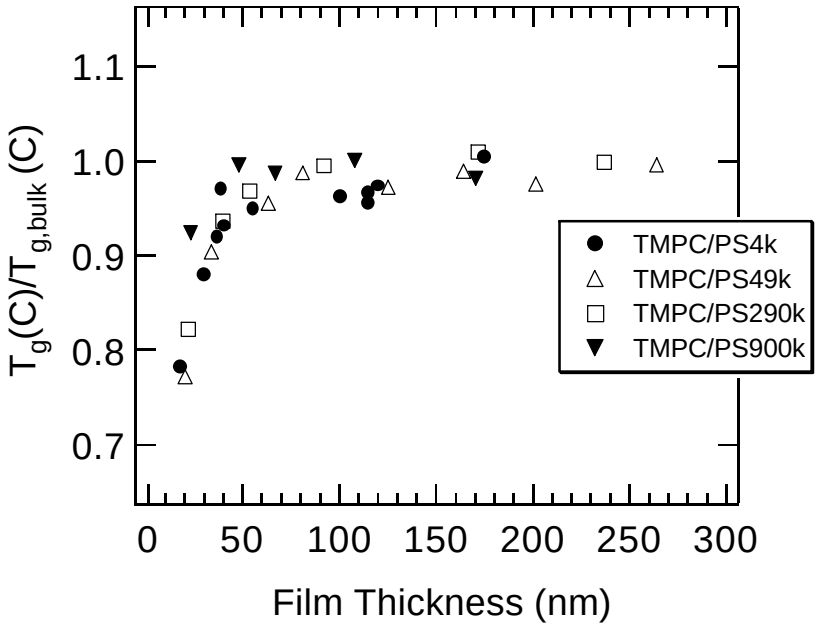

Figure 3-3: The glass transition temperatures, normalized by bulk glass transition temperature, $T_g(\infty)$, are plotted as a function of h for different PS molecular weights.

We begin by pointing out that variations in the composition of the film, from the free surface (enriched with the lower T_g PS component) and throughout the interior of the film, toward the substrate (enriched with the higher T_g TMPC-component) should, in principle, reflect local variations in T_g. It follows that if in fact a sample is composed of layers, with each layer possessing a different T_g, which increases from the free surface toward the substrate, then one would anticipate different values of ΔT_g between the high and low M_{PS} samples (recall that the T_g of the M_{PS} = 4 kg/mol sample is 25^0C smaller than the other). This was not observed. These observations therefore rule out the notion of such a heterogeneous layered structure. Our observations also rule out the existence of a "liquid-like" layer that would exert an increasing influence on the effective T_g of the film as the film thickness decreased. Had such been the case, then the ΔT_g in PS(4 kg/mol.)-TMPC sample should have been much larger than that observed in the others, and this too was not the case.

Studies of PS-poly(2,6dimethyl-p-phenylene oxide) (PPO) mixtures on SiO_x/Si substrates reveal that $\Delta T_g < 0$ over a range of compositions and that the magnitude of ΔT_g is comparable to that observed in the It is noteworthy that that what is particularly remarkable is that ΔT_g is comparable to that observed in the PS/SiO_x/Si system **[39]**. Clearly the results of the PS-PPO/SiO_x/Si and PS-TMPC/SiO_x/Si system suggest that ΔT_g is comparable for both the homopolymers and polymer-polymer mixtures.

We suggest that $\Delta T_g(h)$ is determined by the packing of chains over three basic length scales. The first is the distance from the free surface over which the polymer

segment-segment packing (configurational entropy) are modified, the second length-scale is the distance from the substrate over which the polymer segment-segment packing is modified, and the third is the interior of the film which we assume is bulk-like. There is, of course, ample precedence for such assignments **[13,31,32,38]**. The length scale of the free surface is not believe to be determined by the size of the chains. Near the free surface, the chains will have a larger configurational freedom. Near a hard interface, the configurational freedom is reduced. Tentatively, it appear that $T_g(\infty)$ is determined largely by the "bulk" properties (packing), whereas ΔT_g is influenced by the packing of chains at the interfaces. This is more apparent below.

Curro and McCoy proposed the following model to describe the depression in the glass transition in thin homopolymer films **[38]**. They initially consider the packing of segments in a bulk material. They then imagine segments in this material are confined within two impenetrable boundaries a distance H apart. The segment density near the boundaries changes in order to equalize the chemical potentials in the region. They suggested that the depression in the glass transition would be written as

$$\Delta T_g = \frac{1}{k}\frac{dT_g}{dP}\frac{2\Gamma(H)}{Hr_{bulk}} \qquad (3.3)$$

where κ is the bulk modulus, $\Gamma(H) = \frac{1}{2}\int_0^H [r(z) - r_{bulk}]dz$ and z is the direction normal to the sample surface. In this symmetrically confined system, $\Delta T_g < 0$ if there is a

depletion of segments at the boundaries and $\Delta T_g > 0$ if the segment-"wall" interactions are strong in relation to the segment-segment interactions. Using equation-of-state information about some specific homopolymers, they made reasonable estimates of ΔT_g. We argue, by extension, that if the system is asymmetric (bounded by a free surface and a substrate), then $\Delta T_g > 0$ if the monomer-"wall" interactions are sufficiently strong to dominate the depletion of chain segments near the free surface, otherwise $\Delta T_g < 0$. It would appear from the above equation that the bulk compressibility (κ^{-1}) largely determined the order of magnitude of the T_g depression.

While our sample is not a homopolymer, it is a miscible system in which the dissimilar chains pack intimately and define new free volume, or configurational entropy, characteristic of the system. The packing of chains in the interior plays an important role in determining the effective $T_g(\infty)$ of the mixture. The polymer chains at the boundaries and the nature of their interactions with the boundaries influence ΔT_g when the film becomes sufficiently thin.

Our results clearly indicate that the PS component has opposite effect on the effective T_g compared to the TMPC component. Since $\Delta T_g > 0$ for TMPC, and $\Delta T_g < 0$ for PS, there must exist a PS composition at which $\Delta T_g \sim 0$. This composition is approximately 10 wt % PS, as shown in Figure 3-4, for the 4 kg/mol. PS component samples. For larger PS weight fractions both $T_g(\infty)$ and ΔT_g increase, but the changes in $T_g(\infty)$ are larger than those of ΔT_g.

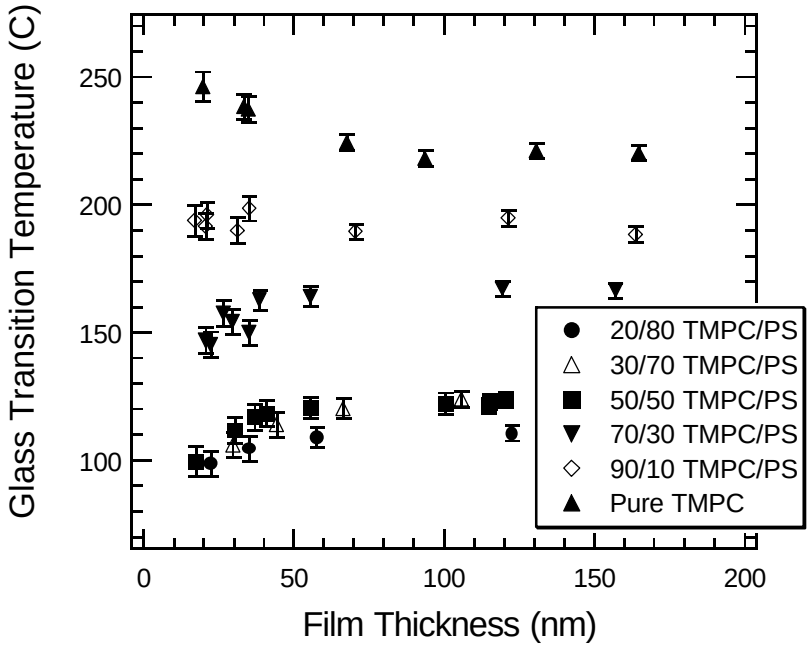

Figure 3-4: The film thickness dependencies of T_g for the TMPC-PS(4 kg/mol) mixtures are plotted here at different compositions, $\Delta T_g<0$ for all mixtures containing more that 10 wt.% PS.

When the PS composition increases beyond 50 wt %, ΔT_g becomes roughly independent of composition. These results confirm the fact that ΔT_g(PS-TMPC) ~ ΔT_g(PS) for PS weight fractions greater than 10%.

3.4 CONCLUSIONS

Effects associated with molecular weight and film thickness on the effective glass transition temperature of the TMPC/PS blend system on SiO_x/Si substrate were examined using spectroscopic ellipsometry. All experiments were conducted in the miscible range below the LCST, where the free surface is enriched with a PS layer and the substrate with a thin TMPC layer. The PS molecular weight varied by two orders of magnitude, with an accompanying change in the glass transition temperature of the polymer by 25^0C. For the studies conducted on the 50:50 wt. % mixtures, T_g decreased with decreasing h and the depression in the glass transition, ΔT_g(h), remained relatively constant regardless of the glass transition temperature of the PS component. The primary influence of the low molecular weight PS component is to decrease $T_g(\infty)$, which is expected for miscible blends. The packing of the dissimilar, yet compatible, blend constituents in the interior of the film determine $T_g(\infty)$ whereas the comparative nature of the relevant monomer-"wall" interactions determines ΔT_g.

3.5 REFERENCES

(1) Pham, J. Q. ; Green, P. F. *J. Chem. Phys.* **2002**, 16, 5801.

(2) Kim, J. H.; Jang, J.; Lee, D-Y.; Zin, W-C. *Macromolecules* **2002**, 35, 311.

(3) Long, D., Lequeux, F. *Eur. Phys. J. E.* **2001**, 4, 371.

(4) Keddie, J. L.; Jones, R. A.; Cory, R. A. *Faraday Discuss.* **1994**, 98, 219; Keddie, J. L.; Jones, R. A.; Cory, R. A. *Europhys. Lett.* **1994**, 27. 59.

(5) Orts, W. J.; van Zanten, J. H.; Wu, W.; Satija, S. K. *Phys. Rev. Lett.* **1993**, 71, 867. Wu, W.; van Zanten, J. H.; Orts, W. J. *Macromolecules* **1995**, 28, 771.

(6) Wallace, W.E.; van Zanten, J. H.; Wu, W. *Phys. Rev. E* **1995**, 52, R3329.

(7) van Zanten, J. H.; Wallace, W. E.; Wu, W. *Phys. Rev. E* **1996**, 53, R 2053.

(8) Efremow, M. Y.; Warren, J. T.; Olson, E. A.; Zhang, M.; Kwan, A. T.; Allen, L. H. *Macromolecules* **2002**, 35, 1481.

(9) Forrest, J. A.; Dalnoki-Veress, K.; Stevens, J. R.; Dutcher, J. R. *Phys. Rev. Lett.* **1996**, 77, 2002.

(10) Forrest, J. A.; Dalnoki-Veress, K. *Advances in Colloid and Interface Science* **2001**, 94, 167.

(11) Forrest, J. A.; Mattsson, J. *Phys. Rev. E* **2000**, 61, R53; Mattsson, J.; Forrest, J. A.; Borjesson, L. *Phys. Rev. E* **2000**, 62, 5187.

(12) Xie, L.; DeMaggio, G. B.; Frieze, W. E.; DeVries, J.; Gidley, D. W.; Hristov, H. A.; Yee, A. F. *Phys. Rev. Lett.* **1995**, 74, 4947.

(13) Torres, J. A.; Nealy, P. F.; de Pablo, J. J. *Phys. Rev. Lett.* **2000**, 85, 3221.

(14) Jain, T. S.; de Pablo, J. J. *Macromolecules* **2002**, 35, 2167.

(15) Kawana, S.; Jones, R. A. *Phys. Rev. E* **2001**, 63, 21501.

(16) Kim, J. H.; Jang, J.; Zin, W-C. *Langmuir* **2001**, 17, 2703; Kim, J. H.; Jang, J.; Zin, W-C. *Langmuir* **2000**, 16, 4064.

(17) DeMaggio, G. B.; Frieze, W. E.; Gidley, D. W.; Hristov, H. A.; Yee, A. F. *Phys. Rev. Lett.* **1997**, 78, 1524.

(18) Grohens, Y.; Brogly, M.; Labbe, C.; David, M. –O.; Schultz, J. *Langmuir* **1998**, 14, 2929.

(19) Fukao, K.; Miyamoto, Y. *Europhys. Lett.* **1999**, 46, 649.

(20) Kleidciter, G.; Prucker, O.; Bock, H.; Frank, C.; Lechner, M.; Knoll, W. *Macromol. Symp.* **1999**, 145, 95.

(21) Tsui, O. K. C.; Zhang, H. F. *Macromolecules* **2001**, 34, 9139.

(22) Fryer, S. D.; Nealey, F. P.; de Pablo, J. J. *Macromolecules* **2000**, 33, 6439.

(23) Fryer, S. D.; Peters, D. R.; Kim, J. E.; Tomaszewski, E. J.; de Pablo, J. J.; Nealey, F. P.; White, C. C.; Wu, W-L. *Macromolecules* **2001**, 34, 5627.

(24) Tate, S. R.; Fryer, S. D.; Pasqualini, S.; Montague, F. M.; de Pablo, J. J.; Nealey, F. P. *J. Chem. Phys.* **2001**, 115, 9982.

(25) Doruker, P.; Mattice, L. W.; *Macromolecules* **1999**, 32, 194.

(26) Soles, C. L.; Douglas, F. J.; Wu, W. –l.; Dimeo, R. M. *Phys. Rev. Lett.* **2002**, 88, 037401-1.

(27) de Gennes, P. G. *Euro. Phys. J. E* **2000**, 2, 201.

(28) Wallace, W.E., Fischer, D.A., Efimenko, K., Wu, Wen-Li and Genzer, J., *Macromolecules* **2001**, 34, 5081.

(29) Kajiyama, T.; Tanaka, K.; Takahara, A. *Macromolecules* **1995**, 28, 3482; Tanaka, K.; Taura, A.; Ge, S-R.; Takahara, A.; Kajiyama, T. *Macromolecules* **1996**, 29, 3040; Tanaka, K.; Takahara, A.; Kajiyama, T. *Macromolecules* **1997**, 30, 6626; Kajiyama, T.; Tanaka, K.; Takahara, A. *Macromolecules* **1997**, 30, 280; Kajiyama,

T.; Tanaka, K.; Satomi, N.; Takahara, A. *Macromolecules* **1998**, 31, 5150; Tanaka, K.; Jiang, X.; Nakamura, K.; Takahara, A.; Kajiyama, T.; Ishizone, T.; Hirao, A.; Nakaham; S. *Macromolecules* **1998**, 31, 5150; Tanaka, K.; Takahara; A.; Kajiyama, T. *Macromolecules* **1998**, 31, 863.

(30) Xie, F.; Zhang, H. F.; Lee, F. K.; Du, B.; Tsui, O. K.; Yokoe, Y.; Tanaka, K.; Takahara, A.; Kajiyama, T.; He, T. *Macromolecules* **2002**, 35, 1491.

(31) Mansfield, K. F.; Theodorou, D. N. *Macromolecules* **1991**, 24, 6283.

(32) Baschnagel, J.; Binder, K. *Macromolecules* **1995**, 28, 6808.

(33) Kim, E.; Krausch, G.; Kramer, E. J.; Osby, J. O. *Macromolecules* **1994**, 27, 5927.

(34) Kim, E.; Kramer, E. J.; Osby, J. O. *Macromolecules* **1995**, 28, 1979.

(35) Kim, E.; Kramer, E. J.; Osby, J. O.; Walsh, D. J. J. *Poly. Science part B: Poly. Phys.* **1995**, 33, 467.

(36) Ferry, J. D. *Viscoelastic Properties of Polymers*, Wiley, NY **1980**.

(37) Gibbs, J.H. and DiMarzio, E.A., *J. Chem. Phys.* **1958**, 28, 373; DiMarzio, E. A.; Gibbs, J.H. *J. Polym. Sci.* 1959, 40, 121; DiMarzio, E.A.; Gibbs, J. H. *J. Polym. Sci.* 1963, A1, 1417.

(38) McCoy, J. D.;Curro, J. D. *J. Chem. Phys.* **2002**, 116, 9154.

(39) Kim, J. H.; Jang, J.; Lee, D.-Y.; Zin, W.-C. *Macromolecules* **2002**, 35, 311.

Chapter 4: Glass Transition of Polymer/Single-Walled Carbon Nanotube Composite Films

Preprint with permission from:

Pham, J. Q.; Mitchell, C. A.; Bahr, J. L.; Tour, J. M.; Krishanamoorti, R.; Green, P. F. *J. Poly. Sci. Part B: Poly. Phys.* **2003**, 41, 3339-3345.

The glass transition temperatures (T_g's) of nanocomposites of polystyrene (PS) and single walled carbon nanotubes (SWNTs) were measured in the bulk and in thin films using differential scanning calorimetry and spectroscopic ellipsometry, respectively. The bulk T_g of the nanocomposites is increased by approximately 3 ^oC and became much broader than that of PS. For the nanocomposite films thinner than 45 nm, the T_g decreased with decreasing film thickness [i.e., $\Delta T_g(nano) < 0$]. This phenomenon also occurs in thin PS films, the magnitude of the depression in PS [$\Delta T_g(PS)$] being somewhat larger. The film thickness dependence and the differences in magnitude of ΔT_g in the two systems were examined in light of current theory and a quantitative comparison was made.

4.1 INTRODUCTION

Polymer thin films play an important role in many technologies, including lubricating layers and active material components in a range of microelectronic devices and sensors. Thin film composites of polymers with single-walled carbon nanotubes (SWNTs) offer even more interesting opportunities because of unusual properties that the nanotubes possess, such as exceptionally high Young's moduli and unusual electrical conductivity characteristics **[1]**. The properties of such composites could potentially be tailored for applications in which polymers may be desirable but lack the requisite properties.

The properties of polymer films in the thickness range of nanometers to tens of nanometers often differ substantially from the intrinsic bulk behavior **[2-7]**. Changes are generally due to the increasing influence of entropic effects (confinement and chain packing) and interfacial interactions on the properties of the films with decreasing thickness. Herewith, properties such as the glass transition temperature (T_g), viscosity, and translational chain diffusion exhibit film thickness (h) dependence **[8-44]**. Confinement and interfacial interactions also change the phase behavior of blends and block copolymers. In thin film A/B mixtures, for example, phase separation temperatures and the symmetry of phase diagrams often differ from bulk analogues **[2]**. In block copolymers, these effects are responsible for thickness dependent order-disorder transition temperatures in thin films **[2,4,8]**. This chapter of the dissertation discusses the influence of h constraints on the T_g of thin films nanocomposites of polystyrene (PS) and SWNTs.

In polymers, the variations of T_g with h are sensitive to the nature of the interactions of the polymer chains with the interfacial constraints (substrate or free surface) on the film and to the tacticity of the polymer **[9,10,27,31,32]**. The earliest measurements of the glass transition of thin films were performed by Keddie et al. **[13,14]** on thin PS films on silicon substrates on which a native oxide layer resided. Keddie et al. showed that T_g decreased with decreasing film thickness when the film was less than approximately 45 nm **[13]**. Subsequent studies of PS by other groups confirm the general observations of a decreasing T_g with decreasing film thickness h as long as the substrate remained nominally the same in each experiment. In freely standing PS films, the decrease in T_g is more significant, as shown by Brilluoin scattering measurements **[20-24]**. Studies were also performed on low molecular weight PS samples whose bulk T_gs were as much as 30 degrees lower than that of the high molecular weight bulk PS, with $T_g = 100\ ^oC$. These measurements reveal that the critical h at which the T_g decreases is virtually identical to that of the high molecular weight analogues, and this suggests that the depression ($\Delta T_g < 0$) is not strictly a confinement effect in which h/R_g (R_g is the radius of gyration of the polymer) is the relevant parameter. In the poly(vinyl pyridine) (PVP)-SiO_x/Si , poly(methyl methacrylate) (PMMA)-SiO_x/Si and tetramethyl bisphenol polycarbonate (TMPC)/SiO_x/Si systems, the opposite trends, T_g increasing with decreasing h (i.e. $\Delta T_g > 0$), has been documented **[9,13,14,17,18,27,34]**. Unlike the PS-SiO_x/Si system, the PVP, TMPC and PMMA segments exhibit particularly strong interactions with the substrate (hydrogen bonding). There is evidence that the tacticity of the polymer also influences the thickness

dependence of T_g. These results together suggest that the effective glass transition is influenced by an interplay between the polymer segment-segment interactions and the segment-"wall" (free surface or substrate) interactions.

However, in the case of organic – inorganic nanocomposites, the mobility of chains and T_g are significantly affected by the confinement and strength of polymer – surface interactions **[45,46]**. In particular, the effects of a confining surface on these effects and other polymer phase transitions are particularly exaggerated because of the extremely large surface to volume afforded by the nanoparticles (in some cases approaching 800 – 1000 m^2/g **[46,47]**.

We are interested in the glass transition of composites of PS and SWNTs both in the bulk and in thin films. Until recently a major impediment toward the development of such composites is availability of appropriately functionalized SWNTs to ensure increased compatibility with polymers. Without appropriate functionalization, the nanotubes aggregate to form bundles and ropes throughout a sample. Recently Mitchell et al. **[48]** succeeded in preparing nanocomposites of SWNTs with 4-(10-hydroxydecyl) benzoate moieties covalently linked to the nanotubes to ensure functionality. As little as 1% SWNT was found to form a percolated network in the polymer host, and this clearly revealed the strength of the polymer-SWNT(functionalized) interactions. In A-B, polymer-polymer, thin film mixtures in which there exists favorable A-B interactions, the effective T_g of the film varies with composition and with film thickness, as shown by Pham and Green **[9,10]**. In this chapter of the dissertation, we are specifically interested in the manner in which the polymer-SWNT interactions influence the effective glass transition in these composites.

4.2 EXPERIMENTAL SECTION

The polystyrene used in this study was obtained from Polymer Source and used as obtained. The molecular weight was determined by gel permeation chromatography; the weight average molecular weight (M_w) was 152,000 Da, and the polydispersity ratio (weight-average molecular weight/number-average molecular weight) was less than 1.05. 4-(10-Hydroxydecyl) benzoate modified SWNTs (with one functional group every 66 carbon units) were prepared by the in-situ generation and reaction of the 4-(10-hydroxydecyl) aminobenzoate as described in previous publications **[48-51]**. Composites were prepared by solution mixing appropriate quantities of pristine SWNTs or the organically modified SWNTs and the polymer in toluene at room temperature. The solutions were dried extensively at room temperature and subsequently annealed at 180 °C in a vacuum oven for approximately 24 h to remove any remaining solvent. Bulk differential scanning calorimetry (DSC) measurements were performed using a Perkin Elmer Pyris 1 DSC with subambient capability. The samples were treated at approximately 175^0C for 16 hours before the DSC measurements. Measurements were performed at three different heating rates and data from heats after a programmed heat to the melt state and controlled cooling to the vitrified state were used. Bulk DSC measurements were conducted at heating rates of 5, 10 and 20 ^{o}C/min and the data are plotted in Figure 4-1. All reported data were obtained from a second heating cycle. Cooling always leads to hysteresis and is therefore not as reliable as heating.

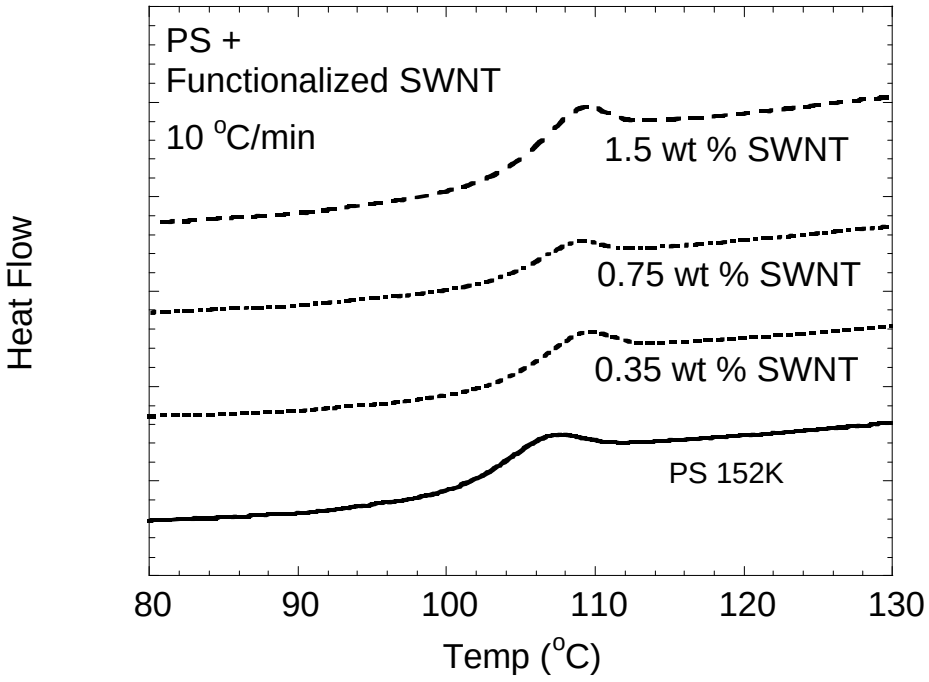

Figure 4-1: Plots of bulk DSC measurements conducted at heating rates of 5, 10 and 20 °C/min.

The T_g's were determined by locating the midpoint of the ΔC_p (the heat capacity change in the vicinity of T_g) function and the width assigned by the end-points of the ΔC_p function. The T_g's estimated by the mid-point of the jump in heat capacity for the three heating rates were linearly extrapolated to zero heating rates and those T_g values are plotted in Figure 4-2 for different weight percentages of SWNT.

The determination of the thin film T_g's is now examined. Samples of PS and of PS-SWNTs with varying thickness were prepared for ellipsometric measurements. A native SiO_x layer 2 nm thick, determined using spectroscopic ellipsometry, resided on the silicon substrate. By adjustment of the spin rates and the solution concentrations, thin films ranging from approximately 20 nm to approximately 200 nm were prepared. The films were annealed at 30^0C above T_g in vacuum for 2 h for the removal of the residual solvent and thermal history before the ellipsometric measurements.

After the samples were annealed, thermal measurements were performed with a variable angle multi-wavelength ellipsometer (J.A. Woollam Co.) equipped with a homemade heating stage. Ellipsometric angles (ψ and Δ) were measured at different temperatures. The sample was held at a given temperature for approximately 2 min for each measurement. Three measurements were taken at each temperature. During our experiments, we increased the temperature at a constant heating rate of 1°C /min. The temperatures were controlled with an accuracy of ± 0.5°C. In these films, within experimental error, comparable T_g's were observed for both cooling and heating. We chose to extract data from the heating cycle because those results were more consistently reliable.

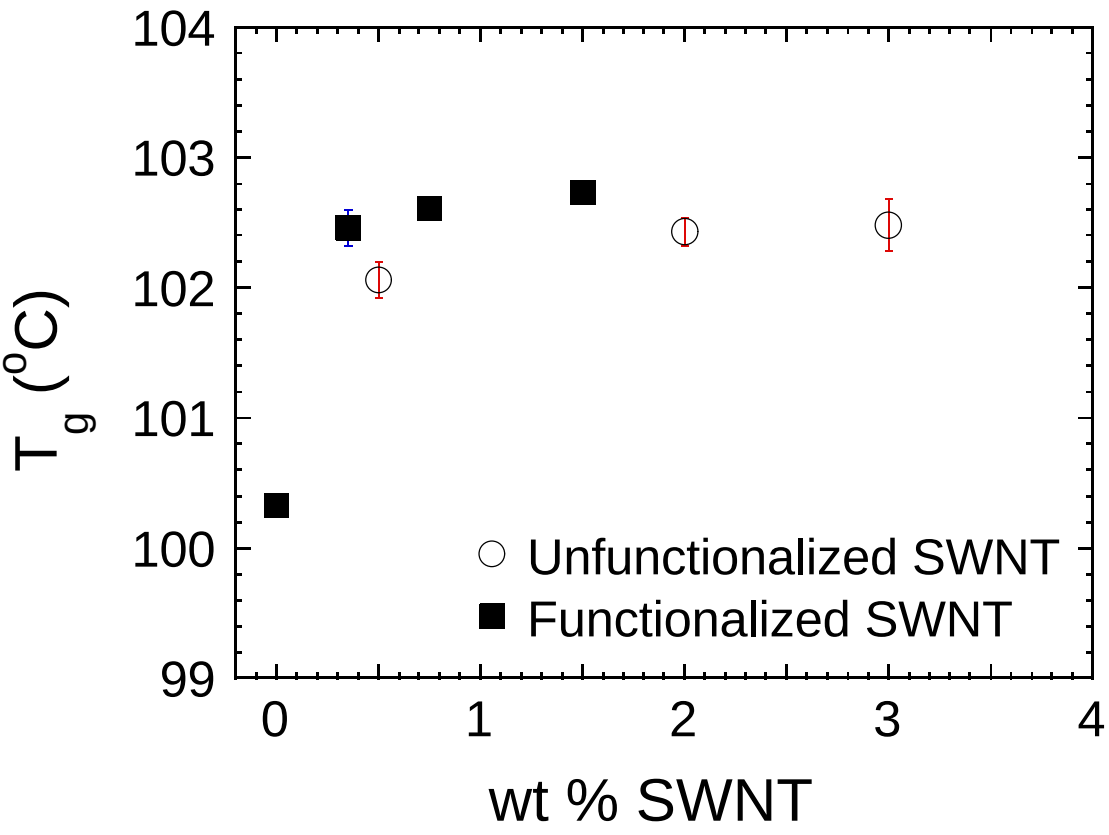

Figure 4-2: The T_g's estimated by the mid-point of the jump in heat capacity for the three heating rates were linearly extrapolated to zero heating rates. The error bars are smaller that the symbol when they are not indicated.

In fact, Dalnoki-Veress and coworkers **[20,21]** used ellipsometry to examine the effects of heating and cooling cycles and found, within experimental error, no difference in the values. The h values were determined by fitting the ellipsometric angles with a Cauchy model (using software provided by the manufacturer). Because the measurements and analysis were standard we will not repeat the details here. Figures 4-3a and 4-3b show typical thermal scans of two samples, PS and a nanocomposite thin film, of comparable thickness. Each plot clearly exhibits distinct glassy and rubbery regions. T_g was determined by fitting straight lines through the data obtained from the glassy and rubber regions. The temperature at which these lines intersect was identified as the T_g of the film. The margin of error in our determination of T_g was less than ± 3 °C.

4.3 RESULTS AND DISCUSSION

The nanocomposites in the bulk exhibit higher T_g's than the pure PS samples. Moreover, T_g's for the nanocomposites are virtually independent of the nanotube loading for both the functionalized and unfunctionalized nanotube composites, as illustrated in Figure 4-2. In fact, at the lower heating rates, the width of the glass transition, as measured from the calorimetric heat flow, is considerably broader for the SWNT nanocomposites than for the unfilled polymer. The onset of T_g was only slightly different from that of the PS (for the un-functionalized nanotubes the deviation was less than 0.5 °C and for the functionalized nanotubes the deviation was less than 1°C). The end point of the transition, on the other hand, increased appreciably (as much as 4 - 5°C higher than that of PS). This leads to the broadening.

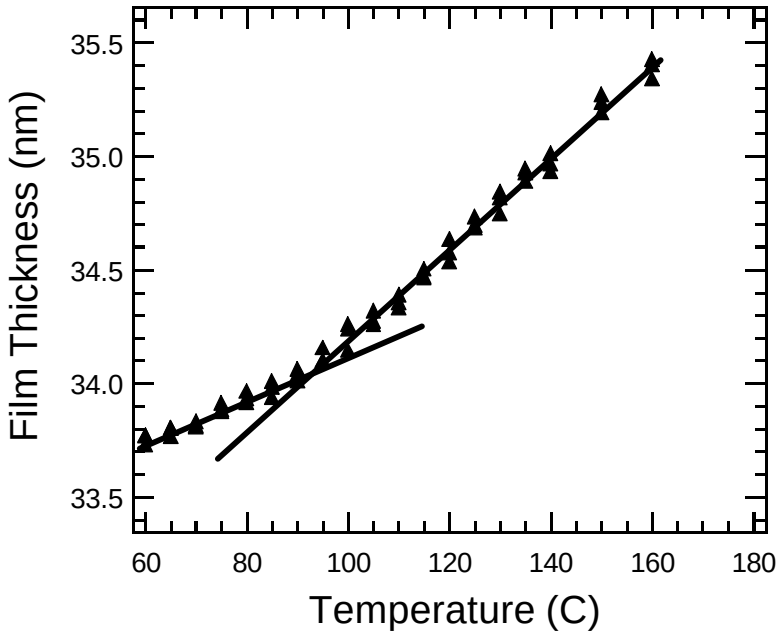

Figure 4-3a: h plotted as a function of temperature for a PS film. The glass transition is identified at the intersection of the two lines.

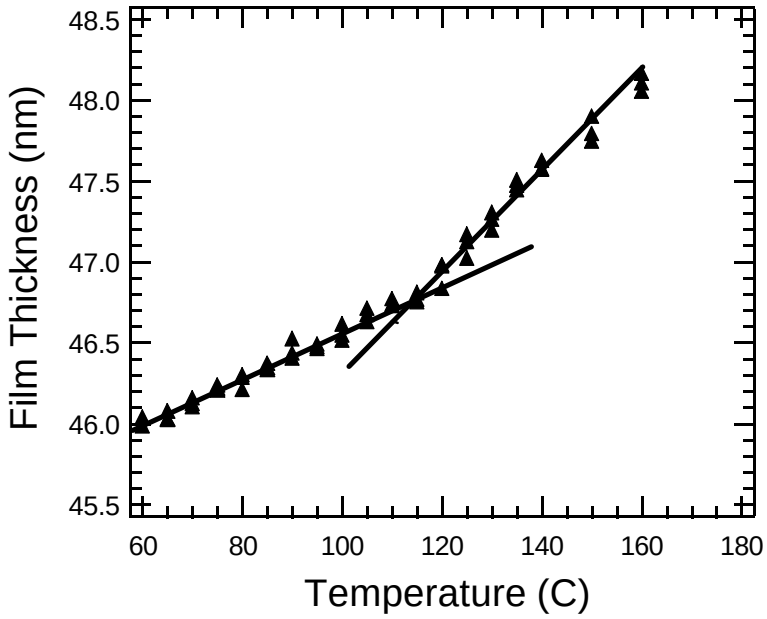

Figure 4-3b: h plotted as a function of temperature for PS-SWNT (functonalized 0.75%) film. The glass transition is identified at the intersection of the two lines.

The uncertainties are less than 0.1°C and the reproducibility is less than 0.2 °C. For the cooling rate of 10°C /min, the transition upon cooling is broader than that upon heating. Wei et al., **[52]** through molecular dynamics simulations, showed that the density of composites is larger than that of a pure polymer and that there is an associated increase in the glass transition. The increase in T_g, they argued, is due to the fact that the dynamics of the polymer chains are reduced in composites. One could argue further that a broader distribution of dynamical processes should characterize the behavior of the composites. The structure of the composites should be heterogeneous on a small scale comparable to the chain dimensions; chains locally in contact with the SWNTs would exhibit slower dynamics than chains in an environment rich with polymer chains. Lodge and McLeish **[53]** argued that variations in local composition do in fact lead to a broadening of the glass transition.

The T_g values are plotted as a function of film thickness for a series of samples [PS, PS-SWNT(0.75 wt.% functionalized), and PS-SWNT(3 wt.% unfunctionalized)] in Figure 4-4. In the PS-SWNT (functionalized) thin films, T_g exhibits a small decrease with h when h is smaller than approximately 45 nm. This decrease ($\Delta T_g < 0$), although similar to that exhibited by PS on the same SiO_x/Si substrates, is appreciably smaller [ΔT_g(PS) > ΔT_g(PS-nano)]. We discuss these findings later.

Glass-forming liquids exhibit increasingly slow dynamics with decreasing temperature. At T_g, the dynamics become effectively frozen on the time-scale of the experiment.

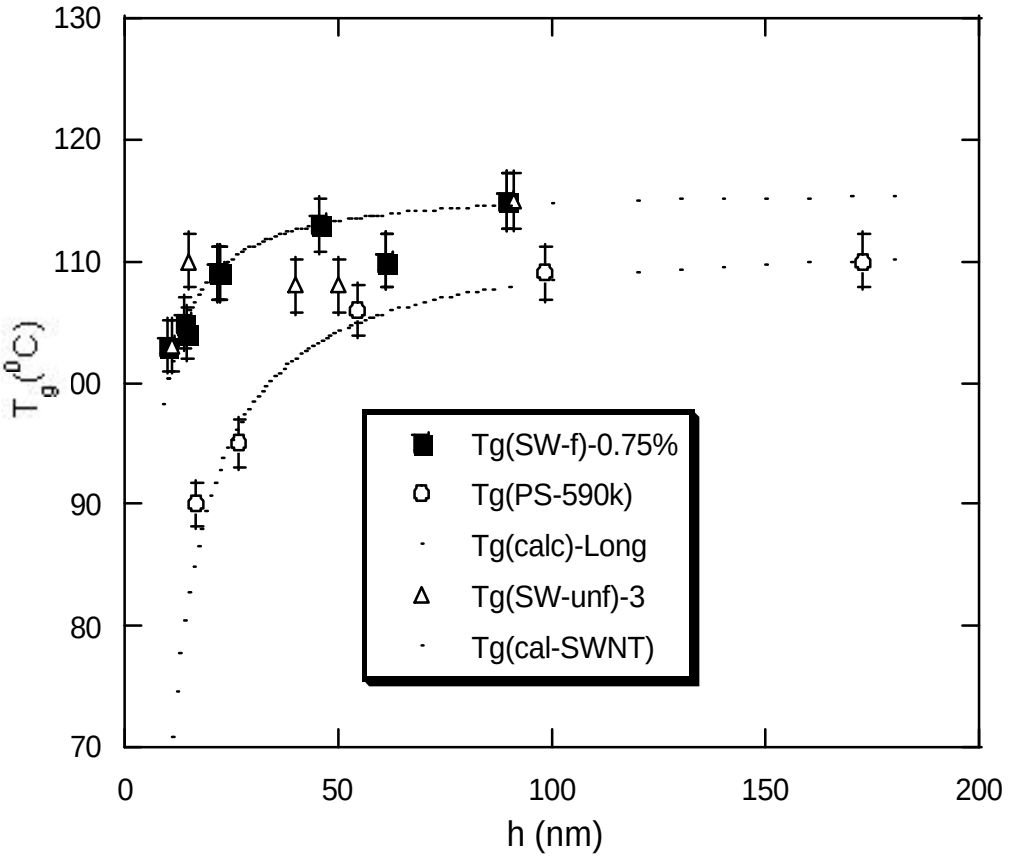

Figure 4-4: h dependence of T_g for different thin films: PS, PS-SWNT(functionalized) and PS-SWNT(unfunctionalized)

In glass forming systems, the timescale associated with the temperature, T, dependence of the dynamics is well described by the Vogel-Fulcher equation:

$$\ln t \propto \ln h \propto \frac{A}{(T - T_{\infty})} \qquad (4.1)$$

Where τ is the relaxation time and η is the viscosity; A and T_{∞} are constants.

The viscosity of 10^{13} P (corresponding to a time-scale of ca.100 s) is often taken as the definition of T_g in non-polymeric glass-forming systems. Other signatures of T_g are associated with the discontinuities in the heat capacity (DSC), the thermal expansion (ellipsometry) or dielectric properties.

Although currently there is no currently universally accepted explanation of change in T_g with decreasing h, a number of points are worth considering. An empirical equation first proposed by Keddie et al. **[13,14]**

$$T_g = T_g(\infty) [1-(A/h)^{\delta}] \qquad (4.2)$$

has been used to describe the data. In this equation, $T_g(\infty)$ is the glass transition temperature at large h, δ indicates of the degree to which T_g decreases with decreasing film thickness and A is a length scale. Values of δ=1.1 and A=8.3 nm were used by Kwawna and Jones **[30]** to describe the PS data.

The decrease in T_g, predicted by this empirical equation, is rationalized as follows. A high mobility (liquid-like) layer of polymer resides at the free surface. This high-mobility surface layer exerts an increasingly larger influence on the average T_g of the film, with increasing temperature, leading to the observed decrease in T_g. It is well documented that the packing density of chain segments near the free surface is lower than that of the interior of the film **[26, 39-41]**. The lower configurational freedom of chains at the free surface could be associated with the enhanced dynamics of chain segments at the free surface. We will return to this point later.

A very similar equation was derived by Long and Lequeux **[12]** with a percolation, free volume-based, model. They proposed that domains of fast and of slowly relaxing clusters of particles comprise the sample (dynamic heterogeneity) and that percolation of the slow domains denotes the onset of the T_g. Upon cooling, since the percolation threshold in three dimensions is lower than in two dimensions, the glass transition should in principle occur at a lower temperature in sufficiently thin films than in the bulk. The predicted dependence is

$$T_g(h) = T_g\left[1 - b\left(\frac{a}{h}\right)^{1/n_3}\right] \qquad (4.3)$$

where β is a function of size of the cluster of particles that constitute a slow domain and of the fraction of percolated domains in three dimensions. It is approximately unity, as suggested. a is a monomer size and ν_3 is the critical exponent for percolation in three dimensions ($1/\nu_3 \approx 1.1$). They pointed out that the parameters used in equation 4.3 are in

agreement with those used to describe the PS data. We note, in passing, that the theory also discusses the case in which ΔT_g is greater than 0. They showed that the effect of the strong polymer-substrate interactions is to increase the effective number of slow domains in the sample; hence the effective temperature at which percolation occurs is much higher than that for bulk analogues.

The importance of the polymer-polymer (and polymer – nanoparticle) interactions with respect to the polymer-interface (substrate and free surface) interactions is very clear from the following. Ellipsometric measurements were conducted on the miscible blend of PS and TMPC **[9,10]**. In TMPC, as mentioned previously, the glass transition increased with decreasing film thickness for h < 45 nm. The free surface region had an excess of PS (wetting layer), whereas an excess of TMPC (wetting layer) resided at the substrate. Bearing in mind that ΔT_g was greater than 0 in the TMPC/SiO_x/Si system, we note that as little as 10 wt % PS in the PS/TMPC mixture resulted in a decrease in T_g with decreasing h for h < 45 nm, and ΔT_g changed from positive to negative. The magnitude of ΔT_g increased toward that of pure PS with increasing PS content. When the PS molecular weight was varied by orders of magnitude, at a fixed composition, with an accompanying change in T_g by up to 30°, the turn over still occurred at h ~ 45 nm, and the magnitude of ΔT_g remained constant (within the experimental error). The primary effect of adding low molecular weight PS was to reduce $T_g(\infty)$. These results have two implications. We note in passing that they rule out the suggestion that implicates a liquid-like surface layer as responsible for the glass transition depression. More importantly, they show the influence of the TMPC-PS interactions on the film thickness dependence of the glass transition.

An alternative model that accounts for the T_g depression was developed by Curro and McCoy **[29]**. They suggested that the depression of the glass transition in thin homopolymer films could be explained by the difference between the average density of the film (ρ_{film}) and that of the bulk (ρ_{film}):

$$\Delta T_g = \frac{1}{k_T}\frac{dT_g}{dP}(r_{film} - r_{bulk}) \qquad (4.4)$$

where κ_T is the bulk modulus. In this symmetrically confined system, ΔT_g is less than 0 if there is a depletion of segments at the boundaries, and ΔT_g is greater than 0 if the segment-wall interactions are strong in comparison with the segment-segment interactions **[26,39-41]**. Scattering experiments and simulations indicate that segmental packing densities near substrates are higher than the bulk and packing densities near the free surface are lower. Using equation-of-state information about some specific homopolymers polymers, they made reasonable estimates of ΔT_g. We argue, by extension, that if the system is asymmetric (bounded by a free surface and a substrate), then ΔT_g is greater than 0 if the monomer-wall interactions are sufficiently strong to dominate the depletion of chain segments near the free surface; otherwise ΔT_g is less than 0.

We have shown that the changes of the glass transition can be rationalized in terms of the both static and dynamic pictures. We first consider the static picture. That

ΔT_g(PS) is greater than ΔT_g(PS-nano) suggests that the average density of the film is larger than that of the bulk PS film of identical thickness. This is not unreasonable because in the filled system the PS chains have a strong and favorable interaction with the nanotubes. In fact even in the absence of a particularly favorable interaction, their contact with a hard surface will tend to increase the local segment density profile. Bulk DSC measurements of the films were performed, and the T_g of the PS-nanotube systems were approximately 2-3^oC higher. If the effect of the interactions of the PS with the nanotubes is to increase the chain segmental density, with a resultant in an increase in configurational entropy, then an increase in T_g will be anticipated and observed. In thin films, the T_g's of the nanocomposite are higher than that of PS. (The fact that T_g is a few degrees different from the DSC data is not too surprising considering the differences in the techniques and the fact that the chain configurations might be slightly perturbed in the thin films in relation to the bulk). The suppression of the large drop in T_g at small values of h in the nanocomposite films is an indication of the influence of the PS-SWNT interactions with respect to the polymer-substrate and polymer-free surface interactions.

Further insights into this phenomenon can be derived by considering the percolation model. In this case, the suppression could be related to the fact that the fraction of slow domains is effectively higher in the PS-SWNT samples. The rheological measurements show that these composites exhibit somewhat higher elasticity, corresponding to a higher viscosity and hence longer relaxation times (slower dynamics) associated with chain dynamics **[48]**.

We now compare the predictions of equation 4.3 with our data. It is clear from Figure 4-4 that equation 4.3 provides an adequate description of our data. We use a = 0.6

nm, $\nu_3 = 1.1$ and $\beta = 9$ to describe the PS data. A value of $\beta = 3$ was used to describe the PS-SWNT data. A smaller value of β indicates the average cluster size of the slow domain is large in the PS-SWNT system, which is to be expected. Our experiments using the unfunctionalized nanotubes reveal that to get the same changes in T_g, we must use a quantity of unfunctionalized nanotubes four times as large. This illustrates the influence of functionalization on T_g. Future experiments should involve experiments using different concentrations of functionalized SWNTs with functionalization (as a fraction of nanotube carbon concentration) systematically varied.

4.4 CONCLUSIONS

We examined the T_g's of mixtures of polystyrene (PS) with functionalized SWNTs using spectroscopic ellipsometry. The bulk T_g, as determined by DSC, of the PS-SWNT composite is 3°C higher than that of PS. The T_g's of thin films of these nanocomposites have also been examined and shown to decrease with h when h is less than approximately 45 nm. This thickness dependence is similar to that of PS, except that in PS the depression is more pronounced, as indicated by the comparison of the theoretical fit to the data. This behavior has been rationalized in terms of two theories of the glass transition in thin films. Our results emphasize the influence on polymer-SWNT interactions versus polymer-interface (free surface and substrate) interactions on the T_g of the film.

4.5 REFERENCES

(1) Saito, R., Dresselhaus, G., Dresselhaus, M. S., "*Physical Properties of Nanotubes*", Imperial College Press, London **1998**.

(2) Binder, K. *Advances in Polymer Sci.* **1999**, 138, 1

(3) Green, P. F.; Limary, R. *Adv. Coll. Int. Sci.* **2001**, 94, 53.

(4) Binder, K. *Adv. Polymer Sci.* 1994, 112, 181.

(5) Russell, T. P. *Current Opinion in Colloid and Interface Science* **1996**, 1, 107.

(6) Fasolka, M. J.; Mayes, A. M. *Ann. Rev. Mater. Res.* **2001**, 31, 323.

(7) Masson, J.L.; Green, P. F. *Phys. Rev. E.* **2002**, 65, 031806

(8) Limary, R.; Green, P. F.; Shull, K. *Eur. Phys. J. E.* **2002**, 8, 103.

(9) Pham, J. Q.; Green, P. F. *J. Chem. Phys.* **2002**, 16, 5801.

(10) Pham, J.; Green, P. F. *Macromolecules* **2003**, 36, 1665.

(11) Kim, J. H.; Jang, J.; Lee, D-Y.; Zin, W-C. *Macromolecules* **2002**, 35, 311.

(12) Long, D., Lequeux, F. *Eur. Phys. J. E.* **2001**, 4, 371.

(13) Keddie, J. L.; Jones, R. A.; Cory, R. A. *Faraday Discuss.* **1994**, 98, 219.

(14) Keddie, J. L.; Jones, R. A.; Cory, R. A. *Europhys. Lett.* **1994**, 27. 59.

(15) Orts, W. J.; van Zanten, J. H.; Wu, W.; Satija, S. K. *Phys. Rev. Lett.* **1993**, 71, 867.

(16) Wu, W.; van Zanten, J. H.; Orts, W. J. *Macromolecules* **1995**, 28, 771.

(17) Wallace, W.E.; van Zanten, J. H.; Wu, W. *Phys. Rev. E* **1995**, 52, R3329.

(18) van Zanten, J. H.; Wallace, W. E.; Wu, W. *Phys. Rev. E* **1996**, 53, R 2053.

(19) Efremow, M. Y.; Warren, J. T.; Olson, E. A.; Zhang, M.; Kwan, A. T.; Allen, L. H. *Macromolecules* **2002**, 35, 1481.

(20) Forrest, J. A.; Dalnoki-Veress, K.; Stevens, J. R.; Dutcher, J. R. *Phys. Rev. Lett.* **1996**, 77, 2002.

(21) Forrest, J. A.; Dalnoki-Veress, K. *Advances in Colloid and Interface Science* **2001**, 94, 167.

(22) Forrest, J. A.; Dalnoki-Veress, K. *Advances in Colloid and Interface Science* **2001**, 94, 167.

(23) Forrest, J. A.; Mattsson, J. *Phys. Rev. E* **2000**, 61, R53.

(24) Mattsson, J.; Forrest, J. A.; Borjesson, L. *Phys. Rev. E* **2000**, 62, 5187.

(25) Xie, L.; DeMaggio, G. B.; Frieze, W. E.; DeVries, J.; Gidley, D. W.; Hristov, H. A.; Yee, A. F. *Phys. Rev. Lett.* **1995**, 74, 4947.

(26) Binder, K; Baschnagel, J.; Bennemann, C.; Paul, W. *J. Phys. Condens. Matter* **1999**, 11, A47

(27) Grohens, Y.; Hamon, L.; Soldera, A.; Holl, Y. *Eur. Phys. J. E.* **2002**, 8, 217.

(28) Torres, J. A.; Nealy, P. F.; de Pablo, J. J. *Phys. Rev. Lett.* **2000**, 85, 3221.

(29) McCoy, J. D.;Curro, J. G. *J. Chem. Phys.* **2002**, 116, 9154.

(30) Kawana, S.; Jones, R. A. *Phys. Rev. E* **2001**, 63, 21501.

(31) Kim, J. H.; Jang, J.; Zin, W-C. *Langmuir* **2001**, 17, 2703

(32) Kim, J. H.; Jang, J.; Zin, W-C. *Langmuir* **2000**, 16, 4064.

(33) DeMaggio, G. B.; Frieze, W. E.; Gidley, D. W.; Hristov, H. A.; Yee, A. F. *Phys. Rev. Lett.* **1997**, 78, 1524.

(34) Grohens, Y.; Brogly, M.; Labbe, C.; David, M. –O.; Schultz, J. *Langmuir* **1998**, 14, 2929.

(35) Tsui, O. K. C.; Zhang, H. F. *Macromolecules* **2001**, 34, 9139.

(36) Fryer, S. D.; Nealey, F. P.; de Pablo, J. J. *Macromolecules* **2000**, 33, 6439.

(37) Fryer, S. D.; Peters, D. R.; Kim, J. E.; Tomaszewski, E. J.; de Pablo, J. J.; Nealey, F. P.; White, C. C.; Wu, W-L. *Macromolecules* **2001**, 34, 5627.

(38) Tate, S. R.; Fryer, S. D.; Pasqualini, S.; Montague, F. M.; de Pablo, J. J.; Nealey, F. P. *J. Chem. Phys.* **2001**, 115, 9982.

(39) Doruker, P.; Mattice, L. W.; *Macromolecules* **1999**, 32, 194.

(40) Mansfield, K. F.; Theodorou, D. N. *Macromolecules* **1991**, 24, 6283.

(41) Baschnagel, J.; Binder, K. *Macromolecules* **1995**, 28, 6808.

(42) de Gennes, P. G. Euro. *Phys. J. E* **2000**, 2, 201.

(43) Wallace, W.E., Fischer, D.A., Efimenko, K., Wu, Wen-Li and Genzer, J., *Macromolecules* **2001**, 34, 5081.

(44) Tanaka, K.; Takahara; A.; Kajiyama, T. *Macromolecules* **1998**, 31, 863.

(45) Zax DB, Yang DK, Santos RA, Hegemann H, Giannelis EP, Manias E, *J. Chem. Phys.* **2000**, 112, 2945.

(46) Giannelis EP, Krishnamoorti R, Manias E, *Adv. Polym. Sci.* **1999**, 138, 107.

(47) Krishnamoorti R, Silva AS, Mitchell CA, *J. Chem. Phys.* **2001**, 108, 7175.

(48) Mitchell, C. A.; Bahr, J. L.; Arepalli, S.; Tour, J. M. Tour; Krishanamoorti, R. *Macromolecules* **2002**, 35, 8825.

(49) Bahr, J. L.; Tour, J. M. *Journal of Materials Chemistry* **2002**, 12, 1952-1958

(50) Bahr, J. L.; Tour, J. M. *Chemistry of Materials* **2001**, 13, 3823

(51) Bahr, J. L.; Yang, J. P.; Kosynkin, D. V.; Bronikowski, M. J.; Smalley, R. E.; Tour, J. M. *J Am. Chem. Soc.* **2001**, 123, 6536.

(52) Wei, C.; Shrivastava, D.; Choi, K. *Nano Letters* **2002**, 2, 647.

(53) Lodge, T. P.; McLeish, T. C. B. *Macromolecules* **2002**, 33, 5278.

Chapter 5: The Glass Transition Temperature of Polymer/Layered Silicate Clays and Polymer/C_{60} Fullerene Nanocomposite Thin Films

The film thickness dependencies of the glass transition temperatures of polystyrene based nanocomposite thin films containing small concentrations, 1-5 wt.%, of layered silicate clays and C_{60} fullerenes supported by silicon substrates, *PS-LSi/Si* and *PS-C_{60}/Si*, respectively, were examined. Spectroscopic ellipsometry studies show that the glass transition temperatures of the nanocomposite thin films of thickness h > 45 nm were constant and equal to the glass transition temperature of PS over the same thickness range. The T_gs of the nanocomposite films containing 1% C_{60} and 1% LSi decreased with film thickness for h < 45 nm. While the magnitude of the decrease is comparable for both systems (and in fact comparable to the decrease exhibited by thin film nanocomposites of polystyrenes with 0.75 wt.% functionalized single walled carbon nanotubes) the decrease exhibited by *polystyrene* thin films is more significant. For a film of thickness of h = 20nm, PS films exhibit a T_g that is 6 degrees lower. The film thickness dependencies of the nanocomposites containing 5 wt. % C_{60} and LSi exhibited the opposite trend for h < 45 nm. They increased with decreasing film thickness. These results point generally to the influence of particles of nano-scale dimensions on the T_g of thin films. The results are examined in light of current models on the T_g of thin films.

5.1 INTRODUCTION

Properties at the nanoscale are of broad interest, cross-cutting many disciplines, from physics and chemistry to engineering. The technical issues are diverse, ranging from electron transport and single-molecule transistors to mechanical properties and automobile bumpers **[1-2]**. Carbon nanotubes, inorganic layered silicates (clays), fullerenes (buckyballs, C_{60}) and various nanoparticles such as Au and CdSe are very interesting in their own right **[1-6]**. Polymer-based nanocomposites in which the polymer serves as a host for inorganic nanoparticles are technologically important. Polymer-inorganic layered silicates have been shown to exhibit superior thermal (heat of distortion) and mechanical properties to those of the pure polymer host and are now being used for a range of new structural and thermal applications **[1,4]**. The polymer-nanoparticles (e.g. CdSe) are important for device applications such as sensors and light emitting diodes **[1,3,5,6]**. The nano-scale particles offer new pathways to "tailor" properties of materials, achieving properties not possible with homopolymers. Current scientific questions evolve around the connection between the structure and properties at the nanoscale and the macroscopic characteristics of the system. Polymer thin films are used in many device applications.

The role of confinement and interfacial interactions on the properties of thin polymer films has been of particular interest to researchers. In polymer thin films, it is well documented that because of the influence of confinement and of polymer-segment/interfacial (free surface and substrate) interactions, properties such as the viscosity, diffusion and glass transition temperature (T_g) are very different from the bulk **[7-36]**. Confinement and interfacial interactions have been shown to change the phase

transition temperatures of polymer blends, melting temperatures of crystals and order-disorder temperatures of diblock thin films **[37-42]**.

In this chapter of the dissertation, we are interested in the glass transition temperature of thin film polymer-based nanocomposites wherein the polymer serves as a host for low concentrations of particles of nano-scale dimensions. In pure homopolymer thin films, the T_g is not intrinsically connected to the structure of the polymer to the extent that it is in the bulk. In thin films T_g is influenced by confinement (thickness) and by the nature of the segmental interactions with the external environment (typically free surface and substrate). While a universally accepted explanation of the thickness dependence of T_g of polymers remains elusive, some general observations may be made. For freely standing films, T_g always decreases with decreasing film thickness **[17-19]**. For asymmetric systems, where one interface is a free surface and the other is a substrate, T_g may increase or decrease, depending on the nature of the interactions between the polymer segments and the substrate. Systems in which the polymer segments hydrogen bond with the substrate exhibit an increase in T_g with decreasing film thickness for thicknesses $h < 45$ nm **[11-15,21,22,33]**. Examples of these systems include poly(methyl methacrylate) (PMMA) on SiO_x/Si substrates (PMMA/SiO_xSi), tetramethyl bisphenyl-A polycarbonate (TMPC)/SiO_x/Si and poly(vinyl pyridine) (PVP)/SiO_x/Si. For other systems, such as polystyrene (PS)/SiO_xSi and PMMA/Au, in which particularly strong cohesive interactions between the polymer segments and the substrate are absent, the T_g decreases with decreasing film thickness when $h < 45$ nm **[13,14,20, 25-27,29-32]**. There is evidence that the tacticity of the polymer may complicate this picture further **[21,29]**. In miscible thin film polymer/polymer mixtures, polymer-A segment/polymer-B segment

interactions and interactions between polymer segments and the interfaces collectively dictate the behavior of the glass transition of polymer thin films, as Pham and Green and Kim et al. have shown in TMPC/PS and PPO/PS mixtures, respectively **[11,12,28]**. Here the film thickness dependence depends on composition of the mixture.

In polymer-inorganic nanocomposites, due to confinement and to interactions between polymer segments and inorganic nanoparticles, it is well known that physical properties such as the viscosity and T_g are greatly influenced **[43-48]**. Simulations by Wei et al. reveal that the density of PS/SWNT nanocomposites is larger than that of pure PS **[43]**. Recently, Pham et al. showed that the T_g of thin film nanocomposites of polystyrene with 0.75 wt.% functionalized SWNT supported by SiO_x/Si substrates decreased with decreasing film thickness for $h < 50$ nm **[10]**. The depression of T_g is this system was appreciably smaller than the depression exhibited by the PS/SiO_x/Si system with decreasing film thickness. The difference was as much as 10 degrees for a film of thickness $h = 25$ nm. The difference between the thickness dependencies the T_gs of both systems was largely associated with the influence of PS/f-SWNT interactions in the former.

In light of the unexpected large influence of the small quantity of f-SWNTs on the T_g of PS thin films, it is worthwhile to examine the influence of similar concentrations of other additives of nano-scale dimensions, organo-modified layered silicate clay and C_{60} fullerenes, on the glass transition of thin PS films. We show that as little as 1 wt% of these additives has a comparable effect on the T_g of PS as did the f-SWNTs. Higher concentrations, 5 wt.%, of the fullerenes and clays were examined and the T_g of PS was observed exhibit the opposite trend, it increased with decreasing h. These results point to

a more general effect associated with the influence of the size of the nanoparticles on the T_g of thin films.

5.2 EXPERIMENTAL SECTION

The polystyrene used in our experiments, molecular weight 590,000 g/mole with polydispersity of 1.06, was purchased from Pressure Chemical. The montmorillonite layered silicate clays (LSi), modified with stochiometric quantities of alkylammonium surfactant (dimethyl-dioctadecylammonium bromide), were provided by Southern Clay Products and further purified for us by Ramanan Krishnamoorti. These clays contained silicate sheets with thickness of about 1 nm and the lateral dimensions of approximately 1 μm. The structures, physical and electrical properties of unmodified and organo-modified silicate clays are well documented in the literature **[2,4,49-54]**. The characteristics of these organo-modified clays are discussed in an earlier publication **[44,45]**. C_{60} fullerenes (99.9% purity) were purchased from Alfa Aesar Co. and used as obtained. The nanocomposite samples were prepared by mixing PS/clay and PS/ C_{60} of different clay and C_{60} concentrations in toluene and chloroform, respectively.

Films of varying thicknesses were prepared for ellipsometric measurements. The solution concentration and spin rates were adjusted to prepare films with thicknesses, ranging from approximately 20 nm to approximately 200 nm, supported by SiO_x/Si substrates. The substrates possessed a native SiO_x layer of approximately 1.5 nm thick, as measured by ellipsometry. All the samples were annealed at approximately 30°C above T_g in vacuum for 2 hrs to remove residual solvent, thereby establishing the same thermal history.

After the samples were annealed, optical measurements were performed with a variable-angle multiwavelength ellipsometer (J.A. Woollam Co.) equipped with a homemade heating stage. Ellipsometric angles (Psi and Delta) were measured over a range of temperatures in 5 to 10°C intervals. Three measurements were performed at each temperature. The heating rate was approximately 1°C/min. The temperatures were controlled within an accuracy of ± 0.5°C /min. Film thicknesses were obtained by analyzing the ellipsometric data (Cauchy/SiOx/Si model) using software provided by the manufacturer. Details of the model and fitting procedures can be founded elsewhere **[11-14,26-28]**.

Figures 5.1a and 5.1b show the thermal scans of two PS/5wt% layered silicate nanocomposite thin films of different thicknesses. The data in these figures exhibit two regions of distinct different slope, denoting glassy and rubbery regions. The temperatures at which they intersect are identified as the glass transition temperatures.

5.3 RESULTS AND DISCUSSION

The film thickness dependencies of the glass transition temperatures of PS and of PS-layered silicate nanocomposite are shown in Figure 5.2a. While the T_g's of the nanocomposites are comparable to those of pure PS at large h, they deviate at smaller values of h. The glass transition temperatures of the PS-nanocomposite containing 1 wt % layered silicate, PS-LSi(1%), exhibited a weaker decrease with decreasing h than does the T_g of PS. The decrease of T_g of the 1 wt% LSi for the thinnest film (h = 20 nm) is approximately 6°C whereas it is approximately 20°C for pure PS.

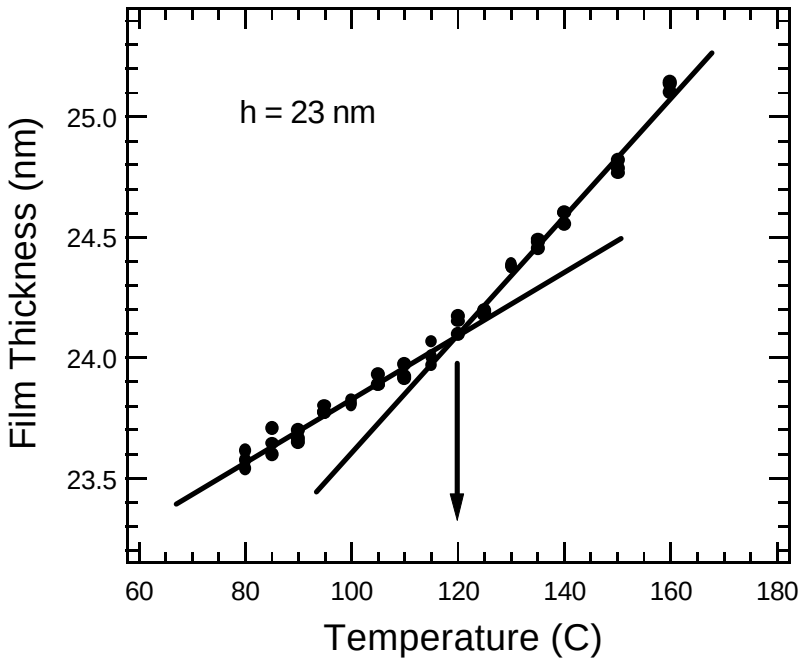

Figure 5-1a: Typical film thickness versus temperature for PS590k/5wt% layered silicate clay film thicknesses. The glass transition temperature (T_g) is identified as the temperature at which the two straight lines intersect.

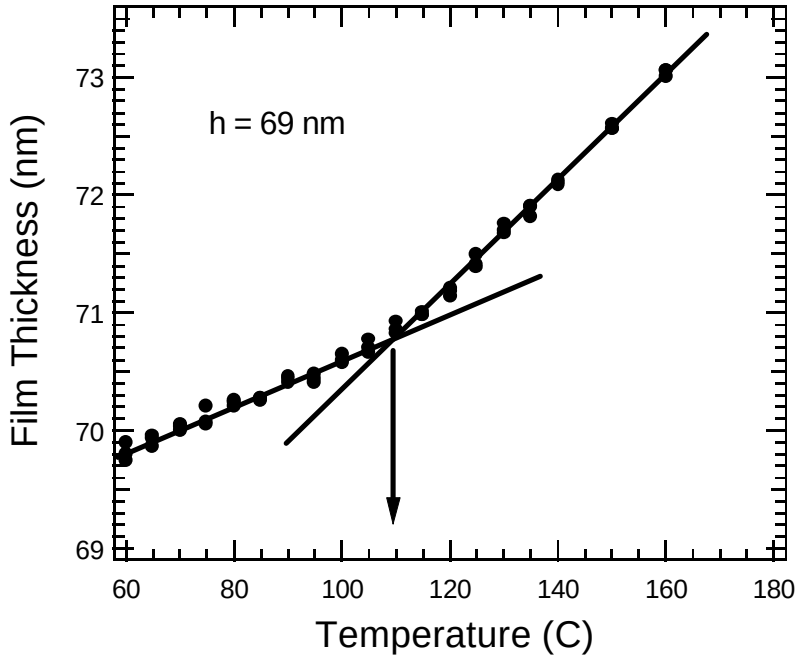

Figure 5-1b: Typical film thickness versus temperature for PS590k/5wt% layered silicate clay film thicknesses. The glass transition temperature (T_g) is identified as the temperature at which the two straight lines intersect.

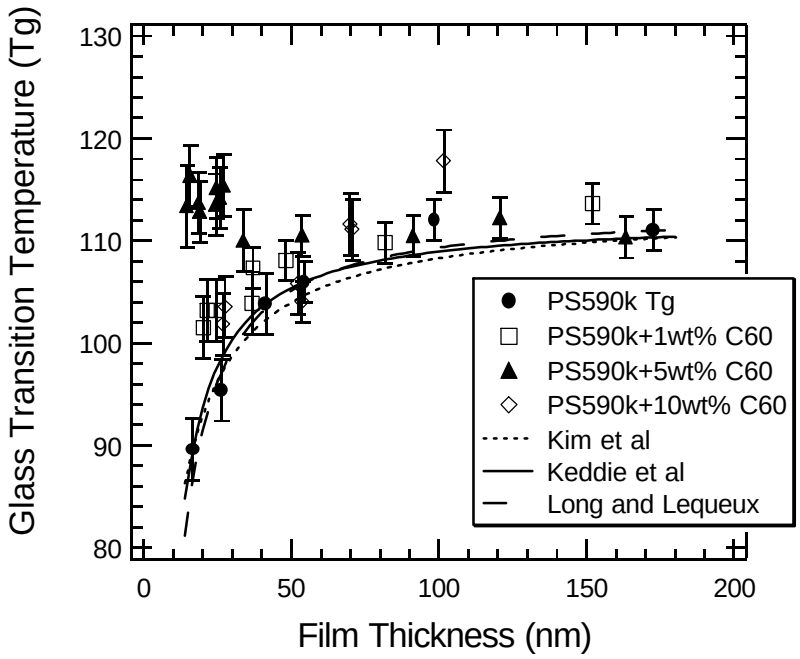

Figure 5-2a: Film thickness dependence of T_g for thin films PS590k/C_{60} nanocomposites

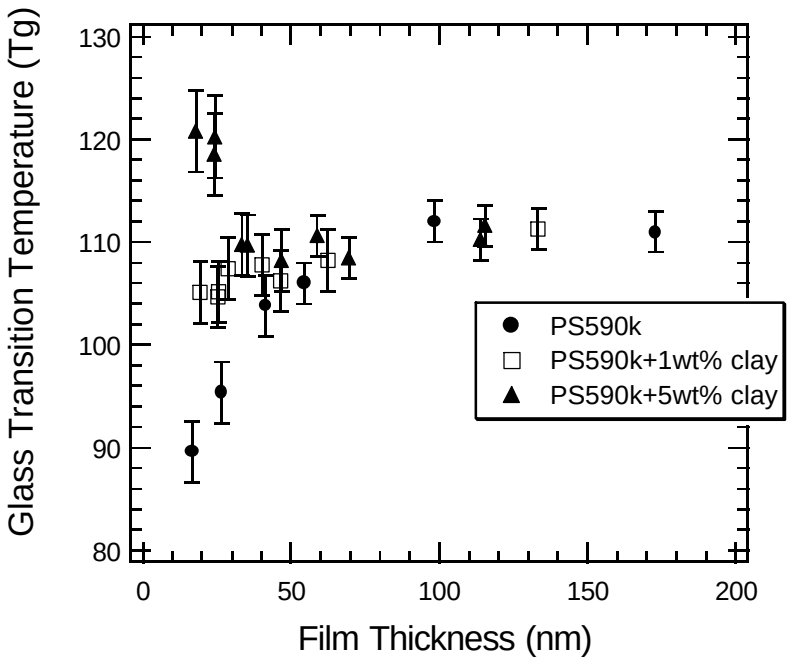

Figure 5-2b: Film thickness dependence of T_g for PS590k/layered silicate clay nanocomposites thin films

The extent of the reduction of the T_g in PS-LSi(1%) films is similar to that exhibited by the PS/f-SWNT system **[10]**.

The T_g's of PS/C_{60} fullerene nanocomposite thin films are plotted in Figure 5.2b. The T_g of PS/1wt% C_{60} decreased with decreasing film thickness when the film is sufficiently thin (for h less than approximately 45 nm), similar to the behavior of the PS-LSi(1%) and PS/f-SWNT nanocomposite thin films **[10]**. Within experimental error, the magnitude of T_g depression in each of the three systems for the thinnest film is $\Delta T_g \sim$ 6°C.

The T_g of PS/C_{60}(5 wt%) nanocomposite films increased with decreasing film thickness as did the T_g of the PS-LSi(5 wt%) films. However the magnitude of increase is slightly smaller for the PS/C_{60}(5 wt%) nanocomposite thin films. These data indicate the strong influence of particles of nano-scale dimensions on the T_g of thin polymer films.

While several models have been proposed to explain the film thickness dependence of T_g in polymers; there is no general consensus regarding the origin of this phenomenon. Keddie et al., who first reported this phenomenon, proposed an empirical equation to describe the depression of T_g with decreasing h in polymer thin films **[13, 14]**.

$$T_g(h) = T_g(\infty)\,[1-(A/h)^{\delta}] \qquad (5.1)$$

In this equation, $T_g(\ )$ is the glass transition temperature of the bulk, A is a length scale and δ specifies the rate at which the T_g decreases with decreasing h. This model is based on the notion that a liquid-like layer exists in the vicinity of the free surface, and this liquid-like layer exerts increasing influence on the T_g with decreasing h leading to the depression. It is known that the configurational freedom of chains at a free surface is larger than those in the bulk (lower segmental packing density) **[35,55,56,58-60]**. In this regard, the notion of higher mobility surface segments is not entirely unreasonable. The curves drawn through the PS data in Figure 5.2a were computed with equation 5.1 using values of A = 8.0 nm and δ = 1.55 ± 0.2 for the fitting parameters. These values are comparable to those used Kawana and Jones (A = 8.0 nm and δ = 1.1) to describe PS data **[25]**. For the nanocomposite thin films, values of A = 4.9 nm and δ = 1.52 ± 0.2 were used to describe PS-C_{60} (1%) fullerene data and A = 5.0 nm and δ = 1.72 ± 0.3 were used to describe the PS-LSi(1%) data. The fits are illustrated in Figures 5.3a and 5.3b, respectively. The difference between the data of the nanocomposites is statistically insignificant.

Kim et al. proposed a model based on the notion that the film is composed of many layers each with a different T_g **[26,27]**. The layer at the free surface would possess the lowest T_g, and as the distance from the free surface increases the T_g increases. Independent measurements suggest the existence of a surface T_g in thin polymer films and in this regard the basis for this model may not be unreasonable **[32,60]**.

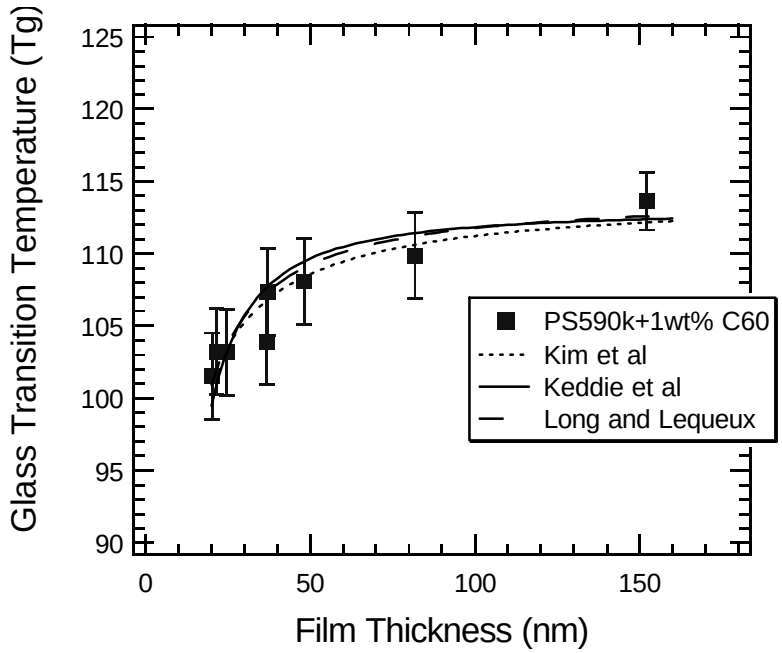

Figure 5-3a: The glass transition temperatures versus film thickness are plotted for PS590k/1wt% C_{60}. The solid lines were computed using equation 5.1; the broken lines were computed using equation 5.2; the dashed lines were computed using equation 5.3.

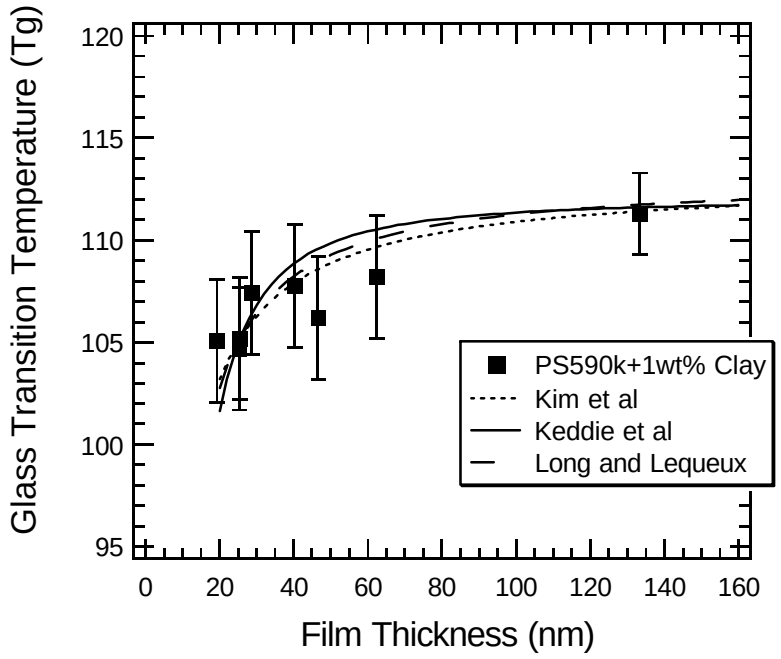

Figure 5-3b: The glass transition temperatures versus film thickness are plotted for PS590k/1wt% layered silicate clay. The solid lines were computed using equation 5.1; the broken lines were computed using equation 5.2; the dashed lines were computed using equation 5.3.

Equations 5.2 is the prediction for the film thickness dependence of T_g for systems in which T_g decreases with decreasing h

$$T_g(h) = T_g(\infty)h/(h + \xi) \qquad (5.2)$$

In this equation ξ is a length scale measuring the extent to which T_g decreases with h. Fitting parameters ξ = 4.3 nm, ξ = 2.5 nm and ξ = 1.9 nm were found to adequately describe our pure PS, PS/1 wt % C_{60} and PS/1 wt % clay data, respectively (Figures 5.3a and 5.3b). While both models described thus far provided a reasonable description of the data, another model has also been proposed.

Long and Lequeux proposed a phenomenological model to estimate the T_g of polymer thin films **[23]**. This model based on dynamic heterogeneity, wherein the dynamics within the sample are characterized by fast and slow domains. With decreasing temperature, the fraction of slow domains increases, and the onset of T_g coincides with the percolation of the slow domains. Because the percolation threshold is higher in 3-D than in 2-D, the glass transition occurs at a lower temperature in 2-D. Since thin films can be described as quasi 2-D, the decreasing of T_g with decreasing h may be rationalized in terms of this picture. The following equation was proposed:

$$T_g(h) = T_{g,bulk}\left[1 - b\left(\frac{a}{h}\right)^b\right] \qquad (5.3)$$

In this equation, β is a measure of the size of the slow domains and is of order unity, as suggested by the author. *a* is a monomer size and *1/b* is a critical exponent for percolation in three dimensional, *b » 1.1*. We used *a* = 0.6 nm, *b* = 1.1 and β = 9 to describe our data for the PS/SiOx/Si system. The values of *a* = 0.6 nm, *b* = 1.1 and β = 4.3 best describes PS/LSi(1%) data, and *a* = 0.6 nm, *b* = 1.1 and β = 5.4 describes PS/C_{60}(1%) data. The smaller values of β used to describe PS/clay and PS/C_{60} nanocomposites indicate that the average cluster size of the slow domain is larger in the nanocomposites than those of pure PS. The percolation threshold of the slow domains of nanocomposites occurs at higher temperatures than those of pure PS resulting in a smaller depression of T_g with decreasing h. We speculate that this is the result of confinement of polymer segments and their interactions with the large surface area of the nanoparticles

The results from the foregoing analysis indicate that interactions between the nanoparticles and the chain segments increase the effective fraction of slow domains in the sample, leading to an enhancement of the effective T_g in the thinnest films compared to that of PS. These results, by implication, indicate that if the fraction of nanoparticles in the sample increases, the T_g of the thinnest films should increase in relation to that of pure polystyrene if the nanoparticles are dispersed within the polymer films. This is indeed observed. In fact, as discussed above, T_g increases with decreasing h for h<45 nm in films composed of 5 % C60 or 5 % LSi. This enhancement of T_g can be rationalized in terms of the aforementioned dynamic heterogeneity model. If the fraction of slow domains in the sample increases, then eventually a point should be reached where the T_g

of the thin film occurs above that of polystyrene. The enhancement of T_g is predicted by the following equation **[23]**,

$$\frac{T_g(h) - T_g(\infty)}{T_g(\infty)} \approx l\left(\frac{a}{h}\right)^b \qquad (5.4)$$

where λ is a function of the size of the slow domains and $T_g(\infty)$ is bulk T_g.

The corresponding prediction based on the multiple T_g model **[26,27]** is

$$T_g(h) = T_g(\infty)h(2k+h)/(h + \xi)^2 \qquad (5.5)$$

In this equation, ξ measures the extent to which T_g decreases with h, and k indicates the degree of interaction between the polymer and the substrate. Data representing the film thickness dependencies of T_g for the PS-C_{60}(5%) and PS-LSi(5%) samples were fit with equation 5.5 using fitting parameters, k = 1.5 nm and ξ = 0.81 nm for the C_{60} system and k = 2.0 nm and ξ = 0.53 nm for layered silicate system. As shown in Figures 5.4a and 5.4b, these parameters were adequately described the data. By contrast values of k = 0.8 nm (ξ = 0.66 nm), k = 1.5 nm (ξ = 0.68 nm) and k = 1.37 nm (ξ = 0.72 nm) were used to describe the data for the PMMA/SiO_xSi, PVP/SiO_xSi and TMPC/SiO_xSi systems, respectively **[11,26,27]**.

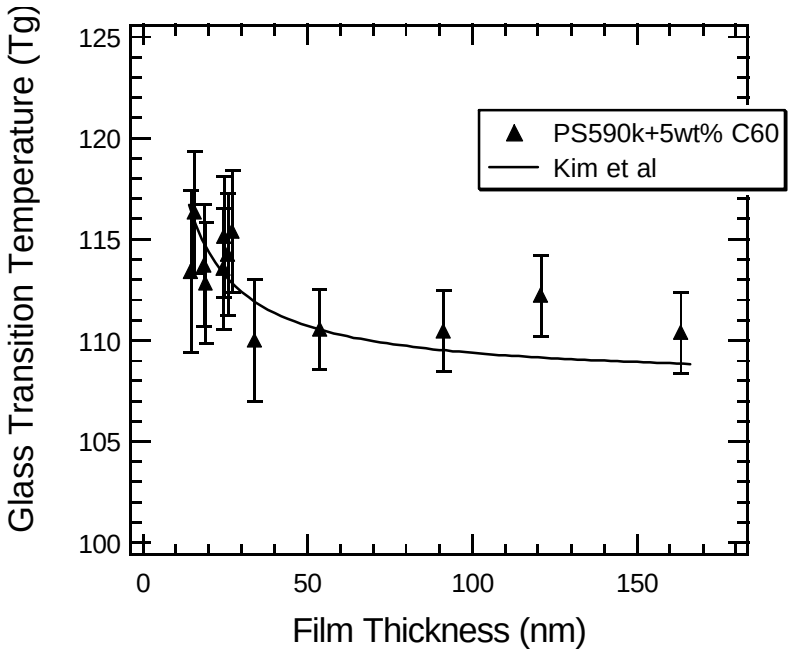

Figure 5-4a: The glass transition temperatures versus film thickness are plotted for PS590k/5wt% C60. The solid lines were calculated using equation 5.5.

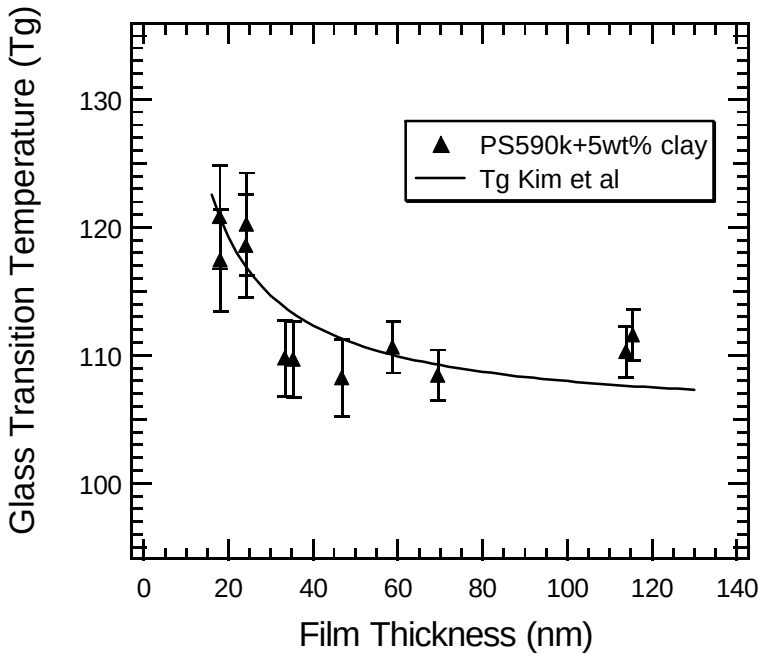

Figure 5-4b: The glass transition temperatures versus film thickness are plotted for S590k/5wt% layered silicate clay. The solid lines were calculated using equation 5.5.

Regardless of the values of the fitting parameters, it is clear that trends in the data of the PS-based nanocomposite systems are similar to the behavior of homopolymer/SiO_x/Si systems in which the polymer segments exhibit strong interactions with the substrate.

In light of the aforementioned, the following comments regarding the T_g of thin films are worthwhile considering. If the configurational entropy of chains that compose the film exceeds that of the bulk, then the T_g of the film would be lower than that of the bulk. Indeed it is well documented that the configurational freedom of chains at free surfaces exceeds those in the bulk. McCoy and Curro showed that if the density of the thin film is lowered than that of the bulk, then the T_g of the film is lowered, $\Delta T_g < 0$; otherwise, $\Delta T_g > 0$ **[24]**. The model of McCoy and Curro, however, considered an idealized case where a strip of polymer is removed from the bulk. The density of this strip was compared with that of the bulk and found to be lower. In this regard, their analysis is limited. Nevertheless, the essential point is the configurational entropy determines the sign of ΔT_g.

In the case of a hard surface, the configurational freedom of the chains is lower due to the interactions **[55-58]**. Therefore for a film confined at both interfaces, one would expect the T_g of this system to be higher than the bulk analogue. Generally, the configurational freedom of the entire film determines the sign of ΔT_g. Hence, if the interactions between the film and the substrate are strong (eg H-bonding) then the observation that $\Delta T_g > 0$ in such homopolymer films is not unreasonable.

The situation involving miscible blends in which the overall specific volume increases beyond that of a rule of mixtures is an exception. In the miscible PS-TMPC

system, the T_g of the mixture decreases for h < 45 nm throughout most of the composition range (PS volume factions greater that about 10%) **[11,12]**. This effect evidently outweighs any interactions between TMPC and substrate might contribute to an increase in T_g. This is particularly noteworthy since PS resides preferentially at the free surface and TMPC at the substrate, and the T_g of TMPC is much larger that that of PS (220°C compared to 100°C). These experiments have further implications. Blends containing PS with molecular weights of 900,000 g/mol and 4000 g/mol, with T_gs of 100°C and 65°C, respectively with TMPC were examined **[12]**. The magnitude of the T_g depression in the mixture was comparable to that of PS. If the liquid–like layer, or a surface T_g for that matter, were responsible to the depression, then the depression observed in the mixture with the lower molecular weight PS component would be lowered. This was not observed. These results point to the picture of the configurational freedom of chains in the interior of the film as the cause. Essentially, we speculate that in thin films the interior segments organize themselves in a manner somewhat different from the bulk. Evidently, while equations 5.1, 5.2 and 5.3 describe the data well, the interpretation of the results in light of their basis of the equations can be misleading.

The dynamic heterogeneity model, based on the notion of slow and fast domains, provides a consistent prediction of our data. Interactions between the polymer segments and hard surfaces increase the fraction of slow domains in the sample. Since the polymer segment-nanoparticles interactions decrease the configurational freedom of the chain segments, the effective T_g of the film is expected to increase relative to that of PS, for h < 45 nm.

These results show that the magnitude and sign of the thickness dependence of the T_g of polymer thin film can be manipulated by incorporating nanoparticles. The effect is apparent regardless of strength of interactions between the polymer segments and the nanoparticles. The important point is that there must exist some level of intermixing between the polymer and the nanoparticles. There might be a critical nanoparticle concentration above which the nanoparticles aggregate, leading to a diminishing effect. Preliminary measurements of the T_g dependence on film thickness of PS/C_{60}(10 wt %) nanocomposites show $\Delta T_g < 0$ rather than the expected $\Delta T_g > 0$. We speculate that at this high concentration, the nanoparticles aggregate internally forming a network as well as migrate to the substrate, as shown by the work of Barnes et al. and Chen et al. **[46,61]**. Under these conditions the relative PS-substrate interactions would have the opposite effect. Again, the interfacial interactions and the configurational entropy of the interior of the film contribute to the overall T_g of the film.

5.4 CONCLUSIONS

We showed that incorporating 1-5 wt. % of particles of nano-scale dimensions into PS has a profound effect on the film thickness dependence of the glass transition temperature. The T_gs of the nanocomposite films containing 1% C_{60} and 1% LSi decreased with film thickness for h < 45 nm. While the magnitude of the decrease is comparable for both systems (and in fact comparable to the decrease exhibited by thin film nanocomposites of polystyrenes with 0.75 wt.% functionalized single walled carbon nanotubes), the decrease exhibited by *polystyrene* thin films is more significant. With the addition of 5%, the T_g increased with decreasing h for h < 45 nm. The presence of the

nanoparticles, regardless of the strength of the interactions with the polymer segments, evidently has the effect of reducing the configurational freedom of the chains, which leads to an enhancement of the T_g of the film compared to pure PS.

5.5 REFERENCES

(1) Rotello, V. "*Nanoparticles: Building Blocks for Nanotechnology*" Kluver Academic/Plenum Publishers: New York, **2004**.

(2) Giannelis, E. P. *Appl. Organomet. Chem.* **1998**, 12, 675.

(3) Saito, R.; Dresselhaus, G.; Dresselhaus, M. S. "*Physical Properties of Carbon Nanotube*" Imperial College Press: London **1998**.

(4) Giannelis, E. P.; Krishnamoorti, R.; Manias, E. *Adv. Polym. Sci.* **1999**, 138:107-147.

(5) Schoder, C. *Fullerene Science and Technology* **2001**, 9, 281.

(6) Dai, L.; Mau, A. W. H. *Advanced Materials* **2001**, 13, 899.

(7) Binder, K. *Adv. Polymer Sci.* **1994**, 112, 181.

(8) Masson, J. L.; Green, P. F. *Phys. Rev. E.* **2002**, 65, 031806

(9) Limary, R.; Green, P. F.; Shull, K. *Eur. Phys. J. E.* 2002, 8, 103.

(10) Pham, J. Q.; Mitchell, C. A.; Bahr, J. L.; Tour, J. M.; Krishanamoorti, R.; Green, P. F. *J. Poly. Sci. Part B: Poly. Phys.* **2003**, 41, 3339.

(11) Pham, J. Q.; Green, P. F. *J. Chem. Phys.* **2002**, 116, 5801.

(12) Pham J. Q.; Green, P.F. *Macromolecules* **2003**, 36, 1665.

(13) Keddie, J. L.; Jones, R. A.; Cory, R. A. *Faraday Discuss.* **1994**, 98, 219

(14) Keddie, J. L.; Jones, R. A.; Cory, R. A. *Europhys. Lett.* **1994**, 27. 59.

(15) van Zanten, J. H.; Wallace, W. E.; Wu, W. *Phys. Rev. E* **1996**, 53, R 2053.

(16) Efremow, M. Y.; Warren, J. T.; Olson, E. A.; Zhang, M.; Kwan, A. T.; Allen, L. H. *Macromolecules* **2002**, 35, 1481.

(17) Forrest, J. A.; Dalnoki-Veress, K.; Stevens, J. R.; Dutcher, J. R. *Phys. Rev. Lett.* **1996**, 77, 2002.

(18) Forrest, J. A.; Dalnoki-Veress, K. *Advances in Colloid and Interface Science* **2001**, 94, 167.

(19) Forrest, J. A.; Mattsson, J. *Phys. Rev. E* **2000**, 61, R53; Mattsson, J.; Forrest, J. A.; Borjesson, L. *Phys. Rev. E* **2000**, 62, 5187.

(20) Fukao, K.; Miyamoto, Y. *Europhys. Lett.* **1999**, 46, 649.

(21) Grohens, Y.;Hamon, L.;Soldera, A.;Holl, Y. *Eur. Phys. J. E.* **2002**, 8, 217.

(22) Torres, J. A.; Nealy, P. F.; de Pablo, J. J. *Phys. Rev. Lett.* **2000**, 85, 3221.

(23) Long, D.; Lequeux, F. *Eur. Phys. J. E.* 2001, 4, 371; Long, D.; Sotta, P. *Los Alamos National Lab., Preprint Archive: Condense Matter* **2003**, 1-33. Berriot, J.; Montes, H.; Lequeux, F.; Long, D.; Sotta, P. *Europhys. Lett.* **2003**, 64, 50.

(24) McCoy, J. D.; Curro, J. G. *J. Chem. Phys.* 2002, 116, 9154.

(25) Kawana, S.; Jones, R. A. *Phys. Rev. E* **2001**, 63, 21501.

(26) Kim, J. H.; Jang, J.; Zin, W-C. *Langmuir* **2001**, 17, 2703

(27) Kim, J. H.; Jang, J.; Zin, W-C. *Langmuir* **2000**, 16, 4064.

(28) Kim, J. H.; Jang, J.; Lee, D-Y.; Zin, W-C. *Macromolecules* **2002**, 35, 311.

(29) Grohens, Y.; Brogly, M.; Labbe, C.; David, M. –O.; Schultz, J. *Langmuir* **1998**, 14, 2929.

(30) Tsui, O. K. C.; Zhang, H. F. *Macromolecules* **2001**, 34, 9139.

(31) Fryer, S. D.; Nealey, F. P.; de Pablo, J. J. *Macromolecules* **2000**, 33, 6439.

(32) Fryer, S. D.; Peters, D. R.; Kim, J. E.; Tomaszewski, E. J.; de Pablo, J. J.; Nealey, F. P.; White, C. C.; Wu, W-L. *Macromolecules* **2001**, 34, 5627.

(33) Tate, S. R.; Fryer, S. D.; Pasqualini, S.; Montague, F. M.; de Pablo, J. J.; Nealey, F. P. *J. Chem. Phys.* **2001**, 115, 9982.

(34) Doruker, P.; Mattice, L. W. *Macromolecules* **1999**, 32, 194.

(35) de Gennes, P. G. *Euro. Phys. J. E.* **2000**, 2, 201.

(36) Lin, E. K.; Kolb, R.; Satija, S.; Wu, W. *Macromolecules* **1999**, 32, 3753.

(37) Green, P. F.;Limary, R. *Adv. Colloid Interface Sci.* **2001**, 94, 53.

(38) Russell,T.P. *Current Opinion in Colloid and Interface Science* **1996**, 1, 107.

(39) Fasolka, M. J.;Mayes, A. M. *Ann. Rev. Mater. Res.* 2001, 31, 323.

(40) Knoll, A.; Horvat, A.; Lyakhova, K. S.; Krausch, G.; Sevink, J. A.; Zvelindovsky, A. V.; Magerle, R. *Phys. Rev. Lett.* **2002**, 89, 035501.

(41) Despotopoulou, M. M.; Frank, C. W.; Miller, R. D.; Rabolt, J. F. *Macromolecules* **1996**, 29, 5797.

(42) Reiter, G. *J. Poly. Sci. Part b: Poly. Phys.* **2003**, 41, 1869; Reiter, G. *Phys. Rev. Lett.* **1992**, 68, 75.

(43) Wei, C.; Shrivastava, D.; Choi, K. *Nano Letters* **2002**, 2, 647.

(44) Limary, R.; Swinnea, S.; Green, P. F. *Macromolecules* **2000**, 33, 5227.

(45) Ren, J.; Silva, A. S.; Krishanomoorti, R. *Macromolecules* **2002**, 33, 3739.

(46) Barnes, K. A.; Karim, A.; Douglas, J. F.; Nakatani, A. I.; Gruell, H.; Amis, E. J. *Macromolecules* **2000**, 33, 4177.

(47) Sharma, S.; Rafailovich, M. H.; Peiffer, D.; Sokolov, J. *Nano Letters* **2001**, 1, 511.

(48) Ferreiro, V.; Douglas, J. F.; Warren, J.; Karim, A. *Physical Review E* **2002**, 65, 051606.

(49) Zax, D. B.; Yang, D. K.; Santos, R. A.; Hegemann H.; Giannelis, E. P.; Manias, E. *J. Chem. Phys.* **2000**, 112:2945-2951.

(50) Vaia, R. A.; Giannelis, E. P. *Macromolecules* **1997**, 30, 7990.

(51) Ginzburg, V. V.; Balazs, A. C. *Macromolecules* **1999**, 32, 5681.

(52) Hackett, E.; Manias, E.; Giannelis, E. P. *J. Chem. Phys.* **1998**, 108, 7401.

(53) Ishida, H.; Li, Y. *Polymer* **2003**, 44, 6571.

(54) Kim, J.; Lee, S-S. *J. Poly. Sci.: Part B, Poly. Phys.* **2004**, 42, 246.

(55) Mansfield, K. F.; Theodorou, D. N. *Macromolecules* **1991**, 24, 6283.

(56) Baschnagel, J.; Binder, K. *Macromolecules* **1995**, 28, 6808..

(57) Bitsanis, I.; Hadziioannous, G. *J. Chem. Phys.* **1990**, 92, 3827.

(58) Binder, K.;Baschnagel, J.;Bennemann, C.;Paul, W. *J. Phys. Condens. Matter* **1999**, 11, A47.

(59) Wallace, W. E., Fischer, D. A., Efimenko, K.; Wu, W.-L.; Genzer, J., *Macromolecules* **2001**, 34, 5081.

(60) Tanaka, K.; Takahara; A.; Kajiyama, T. *Macromolecules* **1998**, 31, 863.

(61) Chen, G.; Ma, G. *Applied Physics Lett.* **1998**, 72, 3294.

Chapter 6: Pressure, Temperature and Thickness Dependence of CO_2-Induced Devitrification of Polymer Films

Preprint with permission from:

Pham, J. Q.; Sirard, S. M.; Johnston, K. P.; Green, P. F. *Phys. Rev. Lett.* **2003**, 91, 175503-1 – 175503-4.

The glass transition temperature is known to increase with decreasing film thickness, h, for sufficiently thin poly(methylmethacrylate) (PMMA) films supported by silicon oxide substrates. We show that this system undergoes a CO_2 pressure induced devitrification transition, P_g, which is film thickness dependent, $P_g(h)=\Delta P_g + P_g^{bulk}$. P_g^{bulk} is the bulk glass transition and ΔP_g can be positive or negative depending on T and P. The phenomenon of retrograde vitrification, wherein the polymer exhibits a rubbery-to-glassy-to-rubbery transition upon changing temperature isobarically, is also shown to occur in this system, and it is film thickness dependent.

6.1 INTRODUCTION

Thin films play an important role in various chemical, biological and microelectronic processes, with applications ranging from coatings, lubricants and membranes to active material components in various organic electronic and sensor technologies. Entropic effects (confinement), enthalpic, polymer-"wall" (substrate and free surface) interactions, and various interfacial processes associated with long-range van der Waals interactions are responsible for a range of phenomena in thin films, not observed in the bulk **[1-15]**. Prominent among these effects is a film thickness dependence of the vitrification temperature, shown to exist in sufficiently thin polymer films **[1,2,4-6]**.

The effects of near-critical CO_2 on the glass transition of thin polymer films are of interest in this chapter of the dissertation. CO_2 has also been shown to influence the phase behavior of polymer-polymer mixtures **[16]**. Liquid and supercritical carbon dioxide (CO_2) are attractive, non-toxic, alternatives to organic solvents in many polymer processes such as foaming, impregnation, coating, "green" lithographic processes and synthesis **[17-19]**. Moreover, because of its negligible surface tension, supercritical CO_2 is effective at drying aqueous-based photoresist films without collapsing the high-aspect ratio features with dimensions below 150 nm, a problem associated with the use of organic solvents **[18]**. With this in mind, it is noteworthy that the effect of CO_2 on the glass transition of thin polymer films, a central issue associated with these processes, has received little attention **[10]**.

In thin polymer films, the vitrification transition is known to differ from the bulk transition, T_g^{bulk}, $\Delta T_g = T_g(h) - T_g^{bulk}$, where ΔT_g may be positive or negative, depending on the polymer and the substrate. For freely standing films, on the other hand, $\Delta T_g < 0$ **[4]**. Generally, $\Delta T_g > 0$ when monomer-substrate interactions are comparatively strong, such as hydrogen bonding between monomer segmental groups and the substrate. Interactions between poly vinyl pyridine, poly(methylmethacrylate) (PMMA) and tetramethyl bisphenol polycarbonate, and oxidized silicon wafer are examples **[2,5,13]**. In the absence of specific monomer-substrate interactions, as is the case for PS/SiO_x/Si, $\Delta T_g < 0$ **[2,5,6]**. These examples illustrate that ΔT_g is not an intrinsic property of the polymer.

The origins of the film thickness dependence of T_g are still a matter of debate. Simulations suggest that the monomer packing densities determine the sign of ΔT_g **[1]**. Other explanations such as the existence of multiple glass transition temperature **[6]** or "liquidlike" surface layers **[2]** provide the basis for alternative explanations. The influence of dynamic heterogeneity on vitrification of the system has also been considered as a potential explanation **[20]**.

Most of the experimental work on this topic has concentrated on pure homopolymer systems and, more importantly, temperature is the only variable used to control vitrification. In light of the limited experimental information, it is not surprising that predictions based on each of the proposals mentioned heretofore are consistent with much of the experimental data. Experiments that reveal more systematic information about the vitrification transition, including conditions under which it could be induced

would be helpful toward the development of a better understanding of the phenomenon. Recently, we showed evidence of a CO_2-induced devitrification transition in PMMA thin films ($h > 85$ nm), suggesting that pressure provides an additional "lever" which can be used to systematically control the vitrification transition in polymer thin films **[10]**.

In this chapter of the dissertation we show evidence of a film thickness dependence of the CO_2 pressure-induced devitrification transition of ultra-thin PMMA films supported by SiO_x/Si substrates, $P_g(h) = \Delta P_g + P_g^{bulk}$, where P_g^{bulk} is the bulk transition. The magnitude and sign of ΔP_g can be controlled independently by T and P. This observation has implications regarding the additional role of diluent interactions on the devitrification of thin films. Moreover, a retrograde *vitrification envelope* is shown to exist in this system. The polymer undergoes a transition from rubbery-to-glassy-to-rubbery upon changing temperature isobarically. The maximum pressure associated with the envelope shifts to lower pressures when h becomes sufficiently small.

6.2 EXPERIMENTAL SECTION

PMMA (M_w = 227 kg/mol; M_w/M_n = 1.04), purchased from Polysciences Inc., was dissolved in toluene and spin cast onto cleaned silicon (100) wafers (Wafer World Inc). The silicon substrate had a native SiO_x layer thickness of ~ 1.5 nm, as determined by spectroscopic ellipsometry. The films ranged in thickness between 10 and 200 nm. All samples were annealed at 170°C under vacuum for over 24 hours to remove residual solvent and to establish the same thermal history.

Measurements were performed using a variable angle spectroscopic ellipsometer (J.A. Woollam Co.). High-pressure ellipsometry cells were used to measure the CO_2-induced glass transitions of PMMA at different film thicknesses at two temperatures: 35°C and 75°C. In addition, P_g's were measured for samples of thicknesses h = 15 nm and h=80 nm at additional temperatures of 25°C, 50°C, and 100°C. The design of the cells and the experimental setup may be found elsewhere **[9,10]**. For thick films (h > 30 nm), the measurements were made using an angle of incidence of 70 degrees from the vertical, while an angle of 76 degrees was used for thinner films. Once a sample was loaded in the cell, at least one hour was allowed for thermal equilibration. The temperature was controlled with an accuracy of ± 0.2°C. After reaching thermal equilibrium, ellipsometric angles, y and D, were measured for different CO_2 (Air Products; > 99.9999 % purity) pressures for both sorption and desorption. The pressure was controlled with an accuracy of ± 0.2 bars. Each sample was equilibrated at each pressure for 10-20 minutes.

Studies of the solubility/dilation of CO_2 in bulk conditioned polymers indicate that at pressures, P, below the P_g(h), sorption and desorption isotherms exhibit negative curvature as a function of P. Furthermore, a hysteresis is observed for $P < P_g$ between the initial sorption isotherms for the unconditioned glassy polymer and the subsequent desorption/sorption isotherms on the conditioned polymer. In contrast, for $P > P_g$, the isotherms are reversible and exhibit positive curvature **[12,21,22]**. The pressure at which the change in curvature occurs is identified as the P_g (i.e., sufficient CO_2 is absorbed by

the polymer to induce a devitrification transition). In conditioned samples, subsequent sorption and desorption runs give the same transition.

We measured the ellipsometric angle, y, as a function of CO_2 pressure at different wavelengths (from 400 nm to 700 nm) for both sorption and desorption isotherms. Since y is related to the film thickness, it also exhibits a change in curvature, denoting the onset of P_g. We find that the P_g's determined for the thickest films compare favorably to the related bulk values, demonstrating that the P_g for the thin films can be determined by spectroscopic ellipsometry without explicitly fitting the ellipsometric angles to a model. Furthermore, a hysteresis is also observed between the initial sorption isotherms and the subsequent sorption and desorption isotherms at $P < P_g$, supporting the observation that a glass transition is present. All data presented in this paper were determined by using y's from initial desorption isotherms. Typical y versus CO_2 pressure desorption isotherms for film thickness of h = 26 nm and h = 50 nm are shown in Figures 6-1a and 6-1b. The trends in the data in each figure clearly reveal distinct glassy and rubbery regimes. Before concluding the experimental section it is important to note that an anomalous dilation is exhibited by the films at pressures higher than the P_g's **[10]**. This anomalous dilation behavior is associated with the compressibility of the solvent, whereas the measured P_g is evidently not correlated with the solvent compressibility **[15]**.

6.3 RESULTS AND DISCUSSION

Three important observations are apparent from the data in Figure 6-2. (1) The P_g's at 35°C and 75°C decrease with decreasing film thickness, $\Delta P_g < 0$, for h less than ~ 50 nm,

indicating that lower pressures are required to induce devitrification in thinner films. These P_g's are independent of film thickness at large h. (2) A larger pressure is required to induce the devitrification transition at 35^0C than at the higher temperature of 75^0C. (3) The change in ΔP_g with decreasing h is larger at 75^0C than at 35^0C, [$\Delta P_g(75^0C) > \Delta P_g(35^0C)$].

We begin by discussing the film thickness dependence of P_g. The decrease of the devitrification transition with decreasing h is, at first glance, surprising based on the dependence of the transition on film thickness for the pure (solvent-less) PMMA/SiO_x/Si case. In the solvent-less case, the interactions (hydrogen bonding) of the *atactic* PMMA with the SiO_x layer is implicated for the increase in the transition over the bulk. The effect of the enhanced interactions is to increase the local monomer-monomer density in the vicinity of the substrate **[1,5,7,8,14]**. An associated effect is that the mobility of chain segments in the vicinity of the substrate is reduced. Therefore one might assume that the devitrification transition would occur at higher pressures with decreasing h. In the case of CO_2-PMMA/SiO_x/Si, CO_2 interacts with the carbonyl groups of PMMA, plasticizing the system **[19,23]**. This alone would have the effect of changing the effective PMMA/SiO_x interactions, and hence, the configurational freedom on the chains in the vicinity of the substrate. In fact, CO_2 also interacts with the hydroxyl groups on the substrate **[19,23-25]**. Therefore it is reasonable to argue that the interactions of PMMA with the surface silanol groups will be screened in the presence of CO_2.

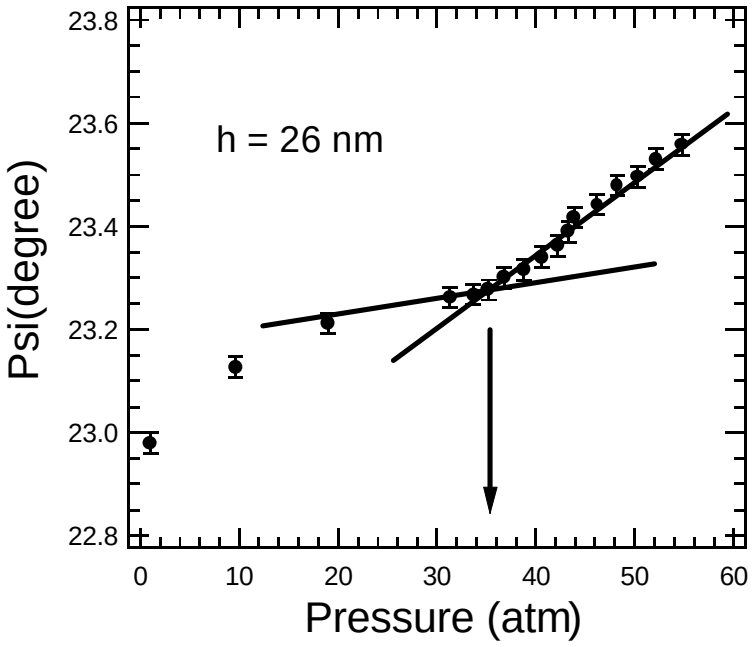

Figure 6-1a: Typical ellipsometric angle (y) versus CO_2 pressure plots are shown here for PMMA film thicknesses of 26 nm at 75°C. The CO_2 induced glass transition, P_g, is identified as the pressure at which the curvature of the desorption isotherm changes.

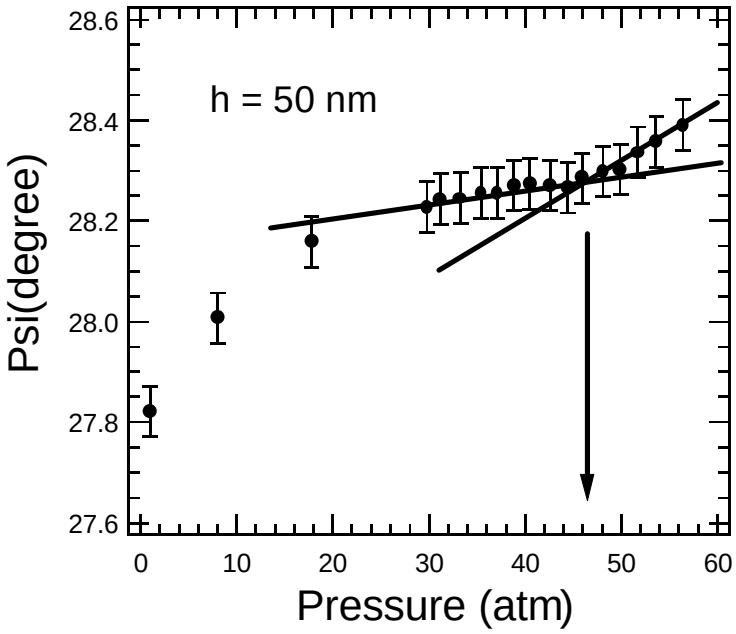

Figure 6-1b: Typical ellipsometric angle (y) versus CO_2 pressure plots are shown here for PMMA film thicknesses of 50 nm at 75°C. The CO_2 induced glass transition, P_g, is identified as the pressure at which the curvature of the desorption isotherm changes.

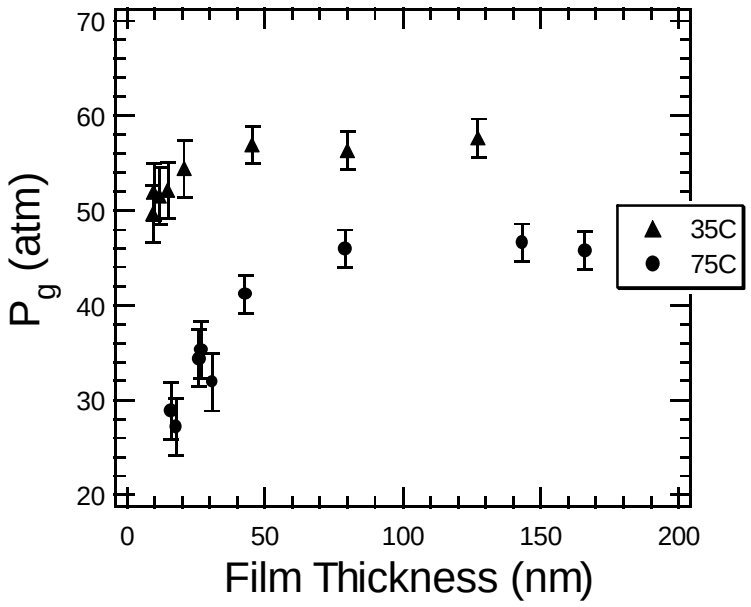

Figure 6-2: P_g is shown here as a function of h at 35°C and 75°C.

One natural consequence of this would be the mediation of the influence of the "interacting" substrate on the segmental packing density and hence the mobility of chain segments. A third effect is the high concentration of CO_2 at the surface (adsorption) of the film **[9-11,26]**. This has the effect of providing more configurational freedom to chain segments near the free surface. These effects, collectively, induce the devitrification transition to occur at lower pressures with decreasing film thickness. While interactions between the chain segments and the external interfaces are fundamentally associated with the thickness dependent virtification transitions, it should also be evident that the collective dynamics and segmental distributions throughout the entire film would be affected.

The reason that the $P_g(h)$ versus h isotherms shift to higher pressures as the temperature decreases from 75°C to 35°C is associated with the fact that a greater solubility of CO_2 in the PMMA is required to counterbalance the decrease in thermal motion. The data at large h are consistent with independent measurements performed on bulk samples **[27]**. The difference in the film thickness effects on the glass transition at the two temperatures $\Delta P_g(75^0C) > \Delta P_g(35^0C)$ is due in part to the distribution of CO_2 between the surfaces and the interior of the film. At 35^0C the solubilities of CO_2 are much higher than at 75^0C over the pressure ranges studied. Thus the gradient in CO_2 composition from the interior of the film to the free surface may be expected to be smaller at 35^0C than at 75^0C consistent with a smaller ΔP_g at 35 ^{o}C.

A retrograde vitrification phenomenon as shown in Fig. 6-3, wherein at constant pressure the system exhibits rubbery-glassy transitions at two different temperatures, is observed in this system. The vitrification envelope is shown here for the bulk and for thin h = 80 nm and h = 15 nm films. The behavior of the h = 80 nm films is nearly the same as the bulk, consistent with the thickness dependence of the P_g shown in Fig. 6-2. It is noteworthy that the envelope shifts to lower pressures, by ~ 10-20 bars, for the thinnest film. Retrograde vitrification is associated with the increasing CO_2 solubility in the polymer with decreasing temperature. At high temperatures and low pressures, the rubbery state is associated with the availability of sufficient thermal energy and mobility of chain segments. As the temperature is reduced isobarically, vitrification occurs for the typical reasons associated with the time-scale of the dynamics versus the time-scale of observation (loss of ergodicity). However, as the temperature is reduced further, the solubility of CO_2 increases appreciably, resulting in the plasticization of the film at lower T, i.e. devitrification. In this regard, the explanation of the phenomenon in thin films is the same as that for the bulk. However, the envelope shifts to lower pressures for thin films. This shift is associated with reasons provided earlier, the decreasing devitrifcation transition with decreasing h. We note the existence of a cross-over at high T and low P, which is not unexpected. At ~20 atmospheres and T~100°C, a cross-over occurs, where the vitrification transition occurs at the same temperature and pressure for thin films and bulk. At pressures lower than ~20 atmospheres, vitrification increases with decreasing film thickness. This occurs in the regime where the CO_2 solubility is very low. Indeed, one should eventually arrive at a cross-over transition where the behavior of the solvent-less case is recovered.

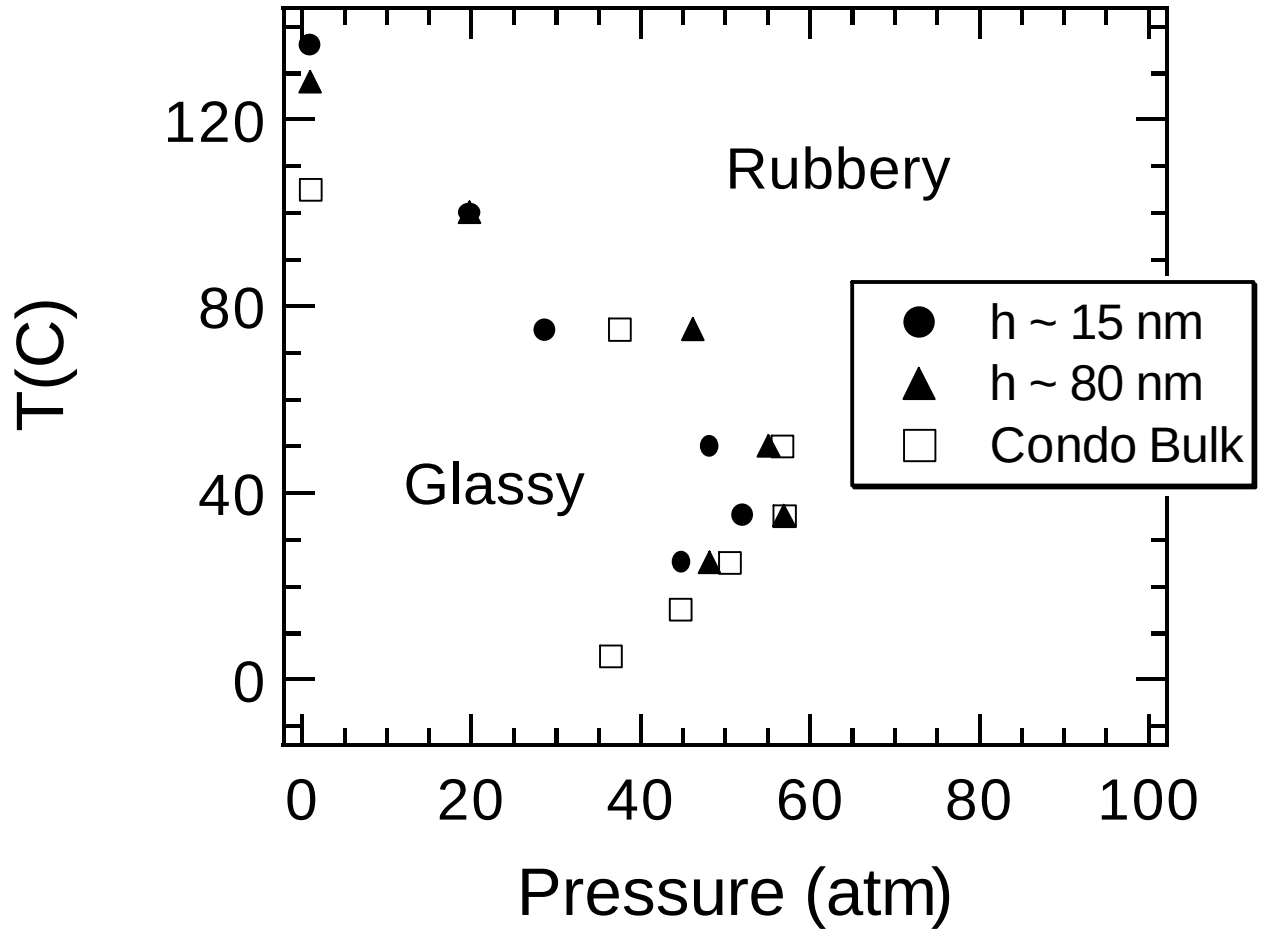

Figure 6-3: Temperature versus pressure plots are shown here for bulk PMMA (from ref. 27) and for films of h ~15 nm and h ~ 80 nm.

6.4 CONCLUSIONS

We have shown that the vitrification transition in PMMA thin films could be controlled by changing the conditions of temperature and CO_2 pressure. A novel crossover pressure is presented in which the sign of ΔP_g changes due to the interactions among polymer, solvent and substrate at the interfaces. Furthermore, the phenomenon of retrograde vitrification occurs in the CO_2/PMMA/SiO_x/Si system, wherein upon decreasing temperature, isobarically, PMMA undergoes a rubbery-to-glassy transition and upon a further decrease, a glassy-to-rubbery transition occurs. This phenomenon is associated with the interplay between the increasing thermal energy of the system with increasing temperature and the increasing CO_2 solubility in the system with decreasing temperature. The vitrification envelope shifts to lower pressures by 10-20 atm when the films are sufficiently thin. The results presented here not only have important implications regarding CO_2-based semiconductor processing and gas separation membranes in polymer based systems, but they provide an important basis for the further development of theories of the glass transition in thin polymeric films.

6.5 REFERENCES

(1) McCoy, J. D.; Curro, J. G. *J. Chem. Phys.* **2002**, 116, 9154.

(2) Keddie, J. L.; Jones, R. A.; Cory, R. A. *Europhys. Lett.* **1994**, 27. 59.

(3) Binder, K. *Adv. Polym. Sci.* **1994**, 112, 181

(4) Forrest, J. A.; Dalnoki-Veress, K. *Adv. Colloid and Interface Sci.* **2001**, 94, 167.

(5) Torres, J. A.; Nealy, P. F.; de Pablo, J. J. *Phys. Rev. Lett.* **2000**, 85, 3221.

(6) Kim, J. H.; Jang, J.; Zin, W-C. *Langmuir* **2001**, 17, 2703; Kim, J. H.; Jang, J.; Zin, W-C. *Langmuir* **2000**, 16, 4064.

(7) Mansfield, K. F.; Theodorou, D. N. *Macromolecules* **1991**, 24, 6283.

(8) Baschnagel, J.; Binder, K. *Macromolecules* **1995**, 28, 6808; Bitsanis, I; Hadziioannous, G. *J. Chem. Phys.* **1990**, 92, 3827

(9) Sirard, S. M.; Green, P. F.; Johnston, K. P. *J. Phys. Chem. B* **2001**, 105, 766.

(10) Sirard, S. M.; Zeigler, K. J.; Sanchez, I. C.; Green, P. F.; Johnston, K. P. *Macromolecules* **2002**, 35, 1928.

(11) Sirard, S. M.; Gupta, R. R.; Russell, T. P.; Watkins, J. J.; Green, P. F.; Johnston, K. P. *Macromolecules* **2003**, 36, 3365.

(12) Kamiya, Y.; Mizoguchi, K.; Naito, Y. *J. Polym. Sci., Polym. Phys.* **1986**, 24, 535.

(13) Pham, J. Q.; Green, P. F. *Macromolecules* **2003**, 36, 1665.

(14) van der Lee, A. *Langmuir* **2001**, 17, 7664

(15) Wu, W.; Majkrzak, C. F.; Satija, S. K.; Ankner, J. F.; Orts, W. J.; Satkowski, M.; Smith, S. D. *Polymer* **1992**, 33, 5081.

(16) Watkins, J. J.; Brown, G. D.; Ramachandra Rao, V. S.; Pollard, M. A.; Russell, T. P. *Macromolecules* **1999**, 32, 7737.

(17) Wells, S. L.; DeSimone, J. *Angewandte Chemie* **2001**, 40, 518.

(18) Weibel, G. L.; Ober, C. K. *Microelectronic Engineering* **2003**, 65, 145; Namatsu, H. *J. Vac. Sci. Technol. B* **2000**, 18, 3308.

(19) Kazarian, S. G.; Vincent, M. F.; Bright, F. V.; Liotta, C. L.; Eckert, C. A. *J. Am. Chem. Soc.* **1996**, 118, 1729.

(20) Long, D., Lequeux, F. *Eur. Phys. J. E.* 2001, 4, 371.

(21) Koros, W. J.; Paul, D. R. *J. Polym. Sci.; Polym. Phys. Ed.* **1978**, 16, 1947.

(22) Wissinger, R. G.; Paulaitis, M. E. J. *Polym. Sci. Part B: Polym. Phys.* **1987**, 25, 2497.

(23) Tripp, C. P.; Combes, J. R. *Langmuir* **1998**, 14, 7384.

(24) Strubinger, J. R.; Pratcher, J.F. *Anal. Chem.* **1989**, 61, 951; Strubinger, J.R.; Song, H.; Pratcher, J.F. *Anal. Chem.* **1989**, 63, 98.

(25) Jia, M.; McCarthy, T.J. *Langmuir* **2002**, 18, 683.

(26) Findenegg G. H. "*Fundamentals of Adsorption*", edited by Meyer, A.L. and Belfort, G. (Engineering Foundation, New York, 1984) p.207

(27) Condo, P. D.; Paul, D. R.; Johnston, K. P. *Macromolecules* **1994**, 27, 365; Condo, P. D.; Johnston, K. P. *Macromolecules* **1992**, 25, 6730.

Chapter 7: Retrograde Vitrification in CO_2/Polystyrene Thin Films

Preprint with permission from:

Pham, J. Q.; Johnston, K. P.; Green, P. F. *J. Phys. Chem. B* **2004**, 108, 3457-3461.

The devitrification of polystyrene, PS, thin films, supported by oxidized silicon (SiO_x/Si) wafers was examined under various conditions of CO_2 pressure and temperature using *in situ* spectroscopic ellipsometry. PS films in the thickness range of 15 nm <h< 200 nm were studied at temperatures from 25°C to 75°C. The CO_2 pressures, P_g, at which devitrification of the PS films occurred decreased with decreasing film thickness for $h \leq 50$ nm, at each temperature, indicating the effect of excess CO_2 in the free surface and substrate regions. For thicker films, P_g remained constant. The largest drop of the transition pressure in this thickness range (15 nm < h < 50 nm) occurred at 75°C. The phenomenon of retrograde vitrification is shown to occur in this system, wherein with decreasing temperature isobarically, a PS film would first undergo the expected rubbery-to-glassy transition and at yet lower T the film would subsequently exhibit a glassy-to-rubbery (devitrification) transition. Retrograde vitrification is characterized by a vitrification envelope below a maximum pressure (~ 60 atm.) on a P versus T plot. This phenomenon is absent in bulk PS.

7.1 INTRODUCTION

Bulk polymer/liquid (or supercritical) CO_2 systems are known to exhibit atypical vitrification effects under various conditions of temperature and CO_2 pressure **[1-6]**. Condo et al. showed that bulk polymethylmethacrylate (PMMA) and polyethylmethacrylate (PEMA) undergo retrograde vitrification, wherein upon decreasing temperature isobarically the polymers exhibit a rubbery-to-glassy (vitrification) transition and at lower temperatures exhibit a glassy-to-rubbery, devitrification, transition **[1-3]**. On a temperature versus CO_2 pressure plot, the boundaries of the glassy region can be defined by a vitrification envelope. Devitrification in these systems is associated with the increasing solubility of CO_2 with decreasing temperature in the polymer at constant pressure. Clearly, these transitions result from the delicate interplay between thermal energy and the temperature and pressure dependence of the solubility of CO_2 in polymers.

The effects of CO_2 on polymer thin films is an important area of research because liquid and supercritical carbon dioxide are attractive alternatives to organic solvents in many polymer processes such as foaming, impregnation, separations, coating and synthesis as well as in the formation, development, and cleaning of photoresist films **[7-17]**. CO_2 is non-toxic and non-flammable and its solvent strength can be tuned markedly with pressure and temperature. Moreover, supercritical CO_2 with small amounts of surfactant and water has been successfully used to remove etched and ashed residues from deep trenches and vias of low k dielectric porous methylsilsesquioxane (MSQ) without damaging the features **[18]**. Because of its low surface tension, liquid and

supercritical CO_2 have been successfully used to dry aqueous based photoresist films without collapsing the high-aspect ratio features with spacings below 150 nm **[13-15]**.

Recently, Pham et al. investigated the CO_2 induced devitrification of PMMA thin films supported by SiO_x/Si substrates **[19]**. In ambient environments in the absence of CO_2, the vitrification temperature of PMMA (vacuum/PMMA/SiO_x/Si) increased with decreasing film thickness for sufficiently thin films **[22-24]**. In contrast, over the same thickness range at sufficiently high pressures in CO_2 environments, PMMA (in the CO_2/PMMA/SiO_x/Si) experienced devitrification, and the CO_2 pressure, P_g, at which devitrification occurs decreases with decreasing film thickness **[19]**. This study showed that depending on pressure and temperature, the shift of the transition in thin films relative to that in the bulk could be positive or negative. A vitrification envelope characterizes the phenomenon in thin film PMMA, as it does in bulk PMMA **[19-21]**. However, the vitrification envelope shifts to lower pressures when the film becomes sufficiently thin. It is noteworthy that whereas the retrograde vitrification phenomenon is observed in bulk PMMA and PEMA it is not observed in polystyrene (PS) **[1-3]**.

The properties of the bulk PS/CO_2 system are different in that only the vitrification transition occurs with decreasing T, isobarically. This vitrification temperature (T_g) decreases with increasing pressure and eventually becomes relatively constant above pressures of 70 atm **[2]**. There is no evidence of a devitrification transition at lower T under isobaric conditions. In this chapter of the dissertation, we show that unlike the situation with bulk PS the phenomenon of retrograde vitrification occurs in the CO_2/PS/SiOx/Si thin film system.

7.2 EXPERIMENTAL SECTION

Sample Preparation.

PS (Mw 590 kg/mol; M_w/M_n = 1.06), purchased from Pressure Chemical was dissolved in toluene and spin cast onto a cleaned silicon (100) substrate (Wafer World Inc). The substrate cleaning procedure can be found elsewhere **[20,21]**. The silicon substrate had a native SiOx thickness of ~ 1.5 nm, as determined by ellipsometry. Uniform film thicknesses ranging from 10 nm to 200 nm were prepared by adjusting solution concentrations and spin rates. All samples were annealed at 130ºC, which is above the vitrification temperature of PS, for 3 hours to remove residual solvent and establish the same thermal history.

Vitrification Temperature (T_g) of PS Thin Film.

After samples were annealed, thermal measurements were performed using a custom-built heating stage and variable angle spectroscopic ellipsometer (J.A Wollam Co.). Spectroscopic ellipsometric angles y and D were measured at temperature intervals of 5-10ºC. These ellipsometric angles were fitted for film thickness using a Cauchy model. The temperature where the ellipsometric angles and film thickness indicated a change in slope was identified as the glass transition temperature of the sample. A description of the detailed experimental setup and an explanation of T_g determination can be found elsewhere **[22-26]**.

CO_2-induced devitrification measurements.

Custom-built high-pressure ellipsometry cells were used to measure the CO_2-induced devitrification (plasticization) of PS at different thicknesses and at four different temperatures: 25ºC, 35ºC, 50ºC and 75ºC. The design of the cells and the experimental setup can be found elsewhere **[20-21]**. For thick films (h > 30 nm), the measurements were made using an angle of incidence of 70 degrees from the vertical, and an angle of 76 degrees was used for thinner films. Once a sample was placed in the cell, at least one hour was allowed for thermal equilibration. The temperature was controlled within an accuracy of ± 0.2ºC. After the sample reached thermal equilibrium, ellipsometry angles, y and D were measured for different CO_2 (Matheson 99.9999% purity) pressures for both sorption and desorption. Each sample was equilibrated at each pressure for 10-20 minutes. The pressure was controlled with an accuracy of ± 0.2 bar.

Solubility studies of CO_2 in bulk conditioned polymers indicate that at pressures below the devitrification pressure, P_g, the sorption and desorption isotherms exhibit negative curvature (concave down), whereas for $P > P_g$, the isotherms exhibit positive curvature **[27,28]**. In fact both thin and bulk polymer films exhibit this behavior **[20-21]**. In other words, P_g is identified with a change in the concavity of the film thickness versus CO_2 pressure curve. Many researchers have suggested that at low pressures CO_2 sorption in polymers is described by a dual mode mechanism (dissolution described by Henry's law and adsorption into microvoids) signified by a non-linear, concave down sorption isotherm while at pressures higher than the P_g, linear sorption behavior is observed **[27-28]**.

Several approaches can be employed to determine the CO_2-induced P_g of polymer thin films. The first approach relies on using ellipsometry to measure the swelling and the refractive index isotherms of the films. This method requires fitting the ellipsometric parameters y and D to a model to obtain the film thickness and refractive index. This method works well for films of thickness h > 60nm, yielding values that are equivalent to that obtained using independent techniques. However, for thinner films large statistical uncertainties associated with correlations between fitting parameters arise. An alternative, yet simple and effective, method that does not require fitting the data to a model and accurately determines P_g is to measure the ellipsometric angle, y, versus CO_2 pressure at different wavelengths (from 400 nm to 700 nm) for both sorption and desorption isotherms. Because changes in y reflect changes in film thickness, y also exhibits a change in curvature at P_g (One potential drawback to this approach is that y may be affected by the birefringence of the cell windows. We examined both uncorrected y's and y's corrected to account for window birefringence, and within experimental error they gave the same P_g. Thus, the birefringence has an insignificant effect on y, which is consistent with the small out-of-plane window corrections that were determined when the ellipsometer was calibrated). Indeed this method is reliable because P_g's determined from the curvature in y yield identical values to those obtained from film thickness and refractive index data over a range of thicknesses

Figures 7-1a, 7-1b and 7-1c show y versus P data for initial desorption isotherms for PS films of different thicknesses. These figures show two distinct regions characterized by different curvature.

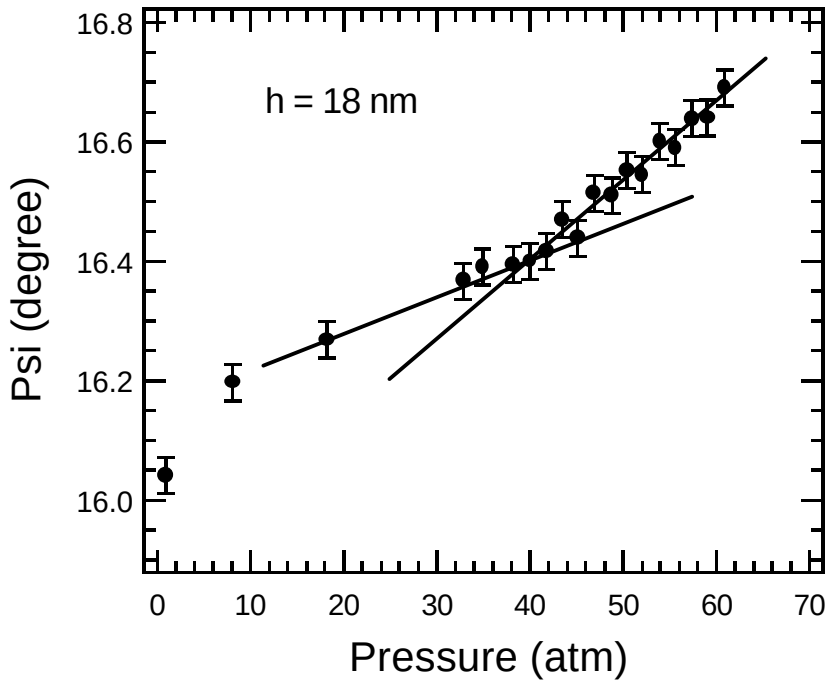

Figure 7-1a: Typical ellipsometric angle (y) versus CO_2 pressure desorption isotherm of PS (Mw = 590k) film at 18 nm. Two straight lines were used to identify the point where the curvatures changed. The glass transition pressure (P_g) is identified as the pressure at which the change in the curvature occurs in the desorption isotherm.

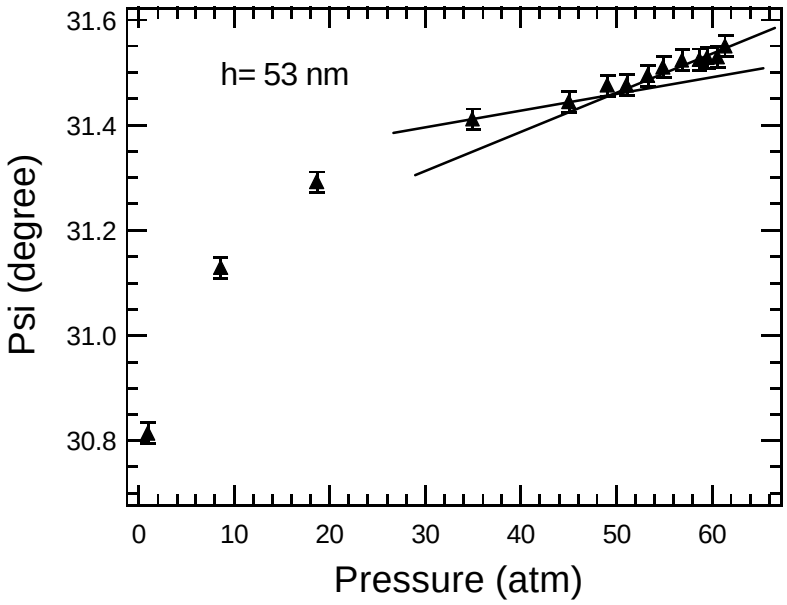

Figure 7-1b: Typical ellipsometric angle (y) versus CO_2 pressure desorption isotherm of PS (Mw = 590k) film at 53 nm. Two straight lines were used to identify the point where the curvatures changed. The glass transition pressure (P_g) is identified as the pressure at which the change in the curvature occurs in the desorption isotherm.

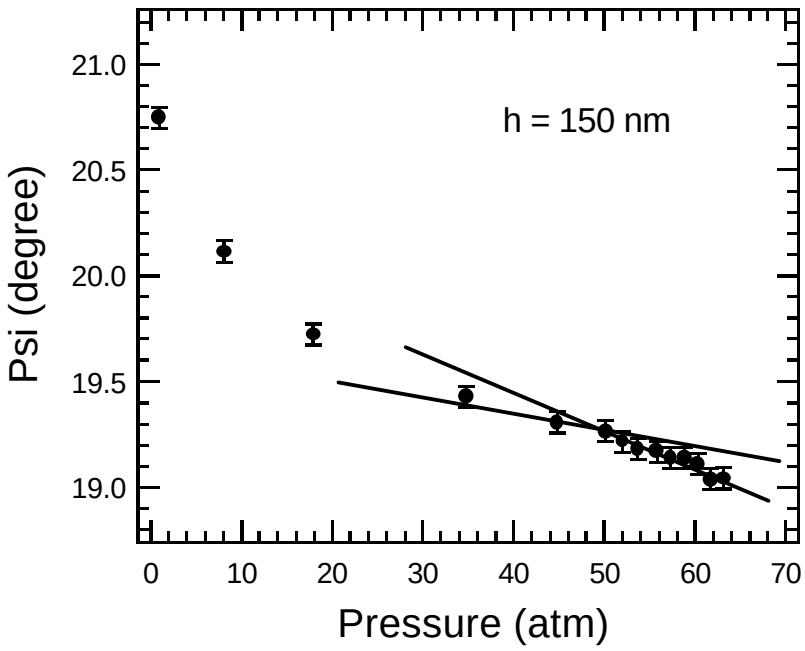

Figure 7-1c: Typical ellipsometric angle (y) versus CO_2 pressure desorption isotherm of PS (Mw = 590k) film at 150 nm. Two straight lines were used to identify the point where the curvatures changed. The glass transition pressure (P_g) is identified as the pressure at which the change in the curvature occurs in the desorption isotherm.

The CO_2 pressure where the change in curvature occurs is identified as the devitrification pressure, P_g. We constructed two straight lines on each figure to identify the pressure where the change in the curvature occurs (P_g). Further details of this procedure may be found in reference 19. A wide range of wavelengths, 427.4 nm, 459.2 nm, 469.7 nm, 535.6 nm, 606.2 nm, 621.7 nm, and 707.7 nm were used to determine the P_g. All of these wavelengths gave similar P_g values, and the reported values are the average of the seven wavelengths given above.

7.3 RESULTS AND DISCUSSION

Measurements of the thickness dependence of the glass transition of PS thin film in vacuum (vacuum/PS/SiO_x/Si) were performed on a PS sample of molecular weight 590 kg/mol. The results, plotted in Figure 7-2, are consistent with measurements performed by other groups, revealing that the glass transition temperature (T_g) decreases with a decrease in film thickness, $\Delta T_g/\Delta h < 0$; ($\Delta T_g = T_g(h) - T_{g,bulk}$) **[24-26,29-33]**. The thickness dependencies of CO_2-induced devitrification transition pressures, P_g, of PS thin films at temperatures of 25ºC, 35ºC, 50ºC and 75ºC are illustrated in Figure 7-3. P_g decreases with decreasing film thickness for the isotherms ($\Delta P_g/\Delta h < 0$), indicating that lower CO_2 pressures are required to plasticize thinner films.

In an effort to establish a context to understand the significance of the properties of CO_2-based thin polymer film systems, we begin by briefly reviewing possible reasons for the thickness dependence of T_g of polymer films under normal (ambient) environments when h is sufficiently small.

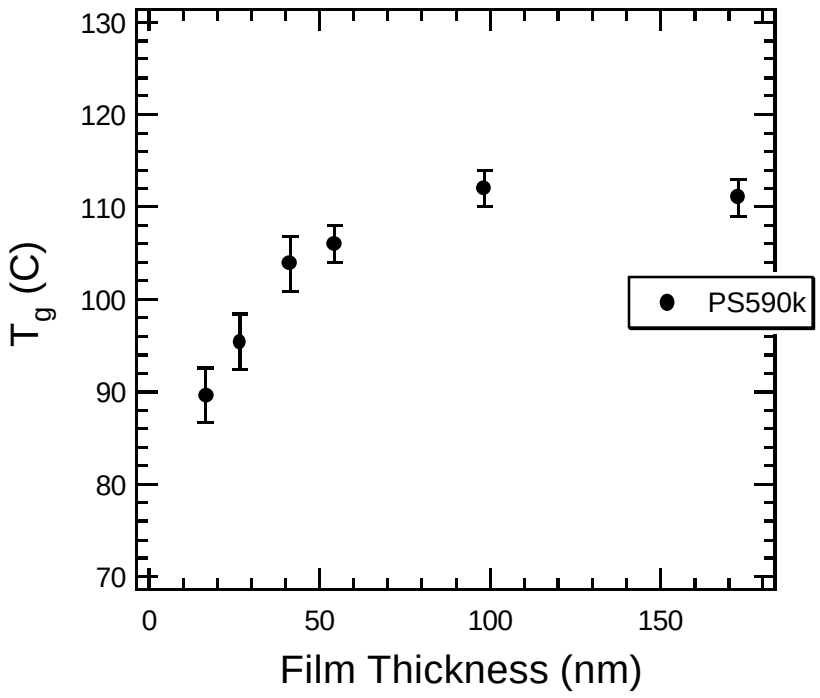

Figure 7-2: T_g versus film thickness dependence is shown here for PS (Mw = 590k) films.

The temperatures, T_g, that homopolymers that exhibit specific interactions, such as hydrogen bonding, with a substrate undergo vitrification increase with decreasing film thickness, $\Delta T_g/\Delta h > 0$. Examples include PMMA, poly(vinyl pyridine) (PVP) and tetramethylbisphenol polycarbonate (TMPC) films supported by oxidized silicon wafers [22-24,31,32]. However, for systems such as $PS/SiO_x/Si$, for which such specific interactions of the nature described above between the polymer and substrate are absent, as well as for freely standing films, T_g decreases with decreasing h, $\Delta T_g/\Delta h < 0$ **[24-26,29,30,32,33]**.

Several models have been proposed to explain the film thickness dependence of the glass transition, though to date there is no universally accepted explanation. An empirical model proposed by Keddie et al. suggests the existence of a "liquid-like" layer at the free surface of the sample that exerts an increasing influence on the effective glass transition of the film as the film thickness decreases to explain the behavior of the $PS/SiO_x/Si$ system **[24]**. An alternative proposal is based on the notion of multiple T_g's **[25,26]**. Specifically the sample is imagined to be divided into layers, and the T_g of each layer, starting from the free surface, increases toward the substrate. This model, with appropriate fitting parameters, is capable of describing the T_g changes that occur in a variety of systems. Long and Lequeux proposed a phenomenological model based on the notion that the material is composed of fast and slow domains (dynamic heterogeneity) **[34]**. The onset of the glass transition is determined by the percolation of slow domains during sample cooling. The thin film can be viewed as a quasi-2D sample, and because the percolation threshold in 3D is larger than in 2D, thin films should vitrify

at lower temperatures than the bulk. The T_g-h dependence of samples in which $\Delta T_g > 0$, however, can be reconciled by the fact that the effect of a substrate that strongly "interacts' with the polymer segments is to induce percolation into the film. A more recent series of simulations by McCoy and Curro show that the value of ΔT_g can be predicted by comparing the average density of the film with that of the identical material in the bulk **[35]**. In systems in which there exist specific interactions between the polymer and substrate, the average segmental density in the vicinity of the substrate is larger than that of the interior of the film **[36-39]**. It is also true that at the free surface the segmental packing density is somewhat diminished compared to that in the interior. If the average density of the film is smaller than that of the bulk, then $\Delta T_g < 0$; otherwise, ΔT_g is greater than zero. McCoy and Curro showed that many experimental observations are consistent with this notion.

We now discuss the temperature dependence of $P_g(\infty)$ for the thickest films. These data are shown in Figure 7-3. The glass transition isotherms shift to higher pressures (with the associated increase in CO_2 fraction) as the temperature decreases from 75ºC to 35ºC. In other words, more CO_2 is required to devitrify the film at the lower temperature (at constant P), in part, because of the lower thermal energy in the system. The relative locations of the isotherms at large h for different temperatures are consistent with the well documented bulk behavior. When the temperature is further decreased from 35ºC to 25ºC, however, the isotherm shifts to lower pressures, indicating that a lower CO_2 content is associated with the transition, P_g. This decrease in the transition pressure is not observed in the bulk. The consequences of this effect are discussed later.

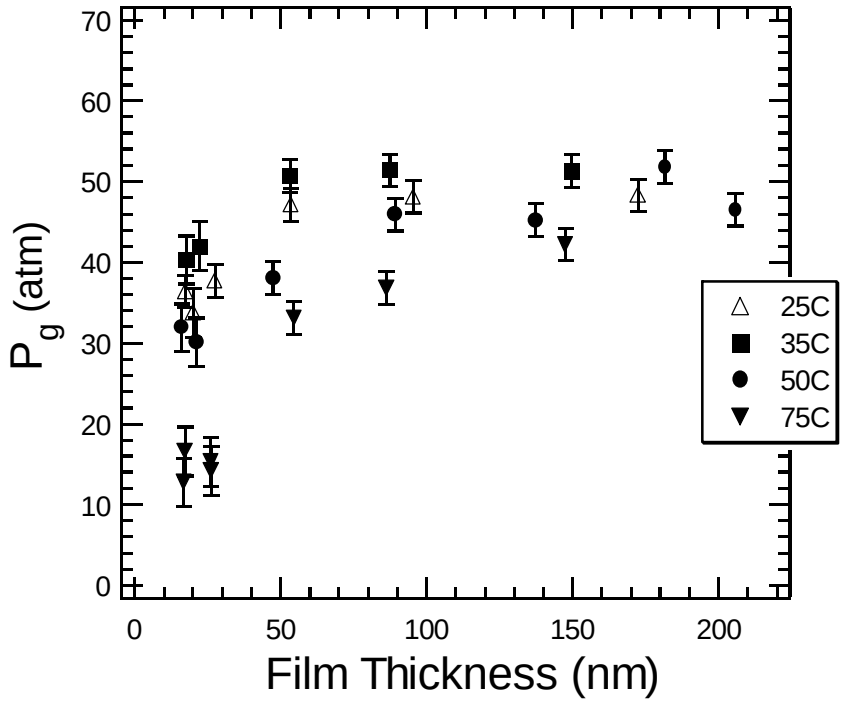

Figure 7-3: The devitrification pressure (P_g) versus h isotherms are shown here for PS (Mw = 590k) films at: 25°C, 35°C, 50°C and 75°C.

The data in Figure 7-3 also show that when the films become sufficiently thin, h less than ~ 50 nm, P_g decreases appreciably with decreasing film thickness. The depression, ΔP_g, should be related to the relative amount of CO_2 in the films at a given temperature. In other words, if the average amount of CO_2 in the film increases with decreasing film thickness at constant T, then P_g should decrease. These experimental observations would have to be reconciled in terms of the influence of the interfaces (free surface and substrate) on the overall CO_2 content of the films. The configurational freedom of chains at the free surface and the polymer/substrate interface relative to the interior of the film is an important consideration. The segmental density at a free surface is lower than that in the interior. Near a hard or interacting substrate, the segmental packing density is known to be slightly higher **[36-41]**. With this in mind, it is important to note that the CO_2 plasticization of polymer thin films is controlled by the overall CO_2 solubility in the entire film, which includes CO_2 at the free surface and substrate regions (interfaces) and in the interior of the film. To this end, experiments show that CO_2 adsorbs and forms a wetting layer on various hard, impenetrable surfaces **[19,20,42-48]**. The adsorption of excess CO_2 at the free surface has the effect of increasing the configurational freedom (lower packing segmental density) of chain segments in that region. CO_2 also interacts favorably with the hydroxyl groups on the SiO_x/Si substrate, with the effect of screening the segmental interactions of the polymer with the substrate **[19,20, 42-44]**. Moreover, neutron reflectivity measurements by Sirard et al. indicate that there exists an enhancement of CO_2 sorption in the PDMS/SiO_x/Si thin film system due evidently to the larger influence of the excess CO_2 at the boundaries, leading to larger swelling of PDMS thin films than in bulk PDMS **[20,48]**. We attempted to model an

adsorbed CO_2 layer at the substrate and/or an adsorbed layer at the free surface with a swollen PS layer for films thicker than ~ 60 nm. However, this model proved to be unreliable, producing correlations and large statistical uncertainties in the fitting parameters. In any event, in the case of soft material interfaces, such a layer would be infinitesimally small and not measurable with ellipsometry. The effects would be manifested primarily in very thin films where the overall percent swelling is larger than their thicker analogues. It is noteworthy that our results are consistent with neutron reflectivity experiments of $PS(CO_2)/SiO_x/Si$ thin film systems that indicate excess sorption of CO_2 in thin films compared to that in the bulk. This effect extends to approximately $h = 10\ R_g$ **[49-51]**. Clearly, with decreasing film thickness the influence of the interfaces on the overall CO_2 content in films becomes more significant. The behavior of the CO_2-$PS/SiO_x/Si$ system, with $\Delta P_g/\Delta h<0$, is consistent with the aforementioned, the effective increase of CO_2 in the system with decreasing h.

There is an apparent temperature dependence of the magnitude of the depression of ΔP_g between 50 nm and 15 nm. We denote this depression as $(\Delta P_g)_{max}$ for convenience. At 75ºC, the maximum depression is $(\Delta P_g)_{max} \approx 27$ atm; at 50^0C $(\Delta P_g)_{max} \approx$ 12 atm; at 35ºC $(\Delta P_g)_{max} \approx 9$ atm; and finally at 25ºC, $(\Delta P_g)_{max} \approx 16$ atm. The smallest value of $(\Delta P_g)_{max}$ occurred at 35ºC, the temperature where the compressibility of CO_2 is largest. A similar temperature dependence in the trend of the $(\Delta P_g)_{max}$ was also observed in the $PMMA/CO_2$ thin film system **[19]**. The magnitude of $(\Delta P_g)_{max}$ should be related to the amount of CO_2 in thinner films relative to the amount in thick films at each temperature, as suggested earlier. To this end, the data indicate that the smallest value of

$(\Delta P_g)_{max}$ was observed at the temperature where the CO_2 compressibility is largest, 35°C. The difference in the CO_2 fraction between the interfaces and that of the interior is evidently smaller at this temperature than at other temperatures. The largest value of $(\Delta P_g)_{max}$ is observed at 75°C, the highest temperature, where the bulk CO_2 solubility is smallest.

Further implications of the film thickness and temperature dependencies of P_g in this system are now discussed. The data are now considered on a temperature versus pressure plot in Figure 7-4 for films with initial thicknesses of ~ 17 nm and ~ 90 nm and for the bulk. The thin films exhibit a vitrification envelope, retrograde vitrification. The envelope is not present in bulk polystyrene, as shown by Condo and Wissinger **[1-4]**. As mentioned earlier, retrograde vitrification is, in part, characterized by a glassy to rubbery transition with a decrease in temperature at constant pressure. The increase in CO_2 solubility overcomes the ordinary loss of thermal energy upon cooling. The existence of the envelope in thin films reflects the fact that thin films are plasticized at lower pressures than bulk films, as illustrated in Figure 7-3. The maximum pressure of the vitrification envelope shifts inward with decreasing film thickness. For temperatures above that which denotes the maximum pressure of the envelope, the thinner films vitrify at lower temperatures than thick films. Below this maximum pressure, the films undergo devitrification, whereas the bulk does not. Thinner films experience devitrification at higher temperatures (Figure 7-3) than thicker films. When the film becomes sufficiently thick (bulk) devitrification does not occur.

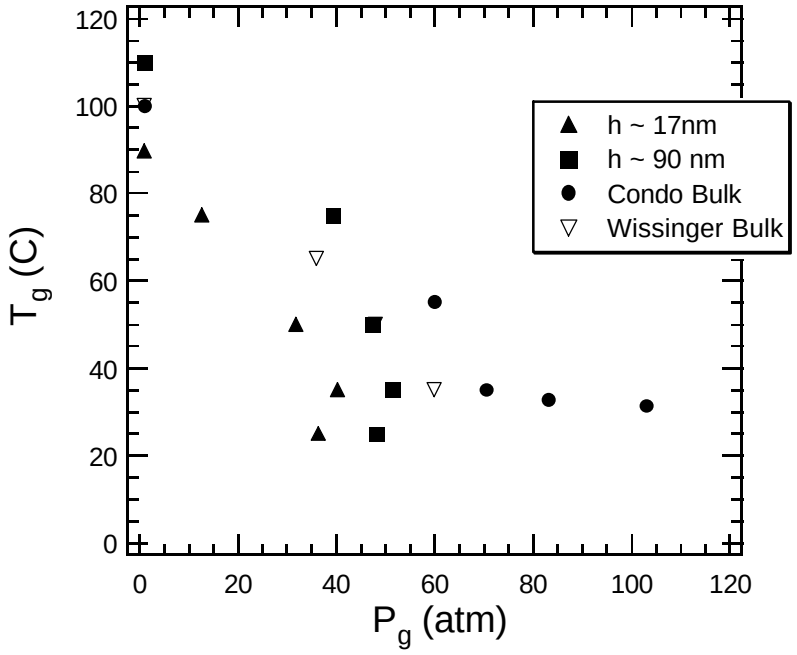

Figure 7-4: Tg versus Pg for PS films with thickness h~ 90 nm and with h ~ 17 nm are shown here. The data for bulk PS, shown in the figure as well, were extracted from references 2 and 4.

This would be consistent with the notion that the effective amount of CO_2 in the films increases with decreasing film thickness at a given temperature.

Finally, as a self-consistent check, it is worthwhile to examine differences between bulk and thin films by considering CO_2 activities because the activities include effects of temperature and pressure. In light of this we consider the difference between the transition temperature, T_g, under normal ambient conditions and T_{g-CO_2}, the transition temperature in the presence of CO_2, plotted as a function of CO_2 activity. $T_g - T_{g-CO_2}$ versus CO_2 activity is plotted in Figure 7-5, where the difference between bulk and thin films is evident; the data for thin films collapse onto a line that is distinct from the line that characterized the behavior of the bulk samples. These data indicate that for a given value of CO_2 activity, the difference between the normal T_g and the T_g in the presence of CO_2 is much larger in thin films than in the bulk and this difference increases with increasing CO_2 activity. Indeed, the effects of CO_2 are more significant on thin film PS than in the bulk. The excess CO_2 in the film at the free surface and substrate regions may be expected to cause this larger T_g depression for a given CO_2 activity.

7.4 CONCLUSIONS

We have examined the thickness dependence of the CO_2 induced devitrification of PS thin films using in-situ spectroscopic ellipsometry. The devitrification pressure (P_g) decreased with decreasing film thickness ($\Delta P_g < 0$), implying that lower CO_2 pressures are required to plasticize thinner films.

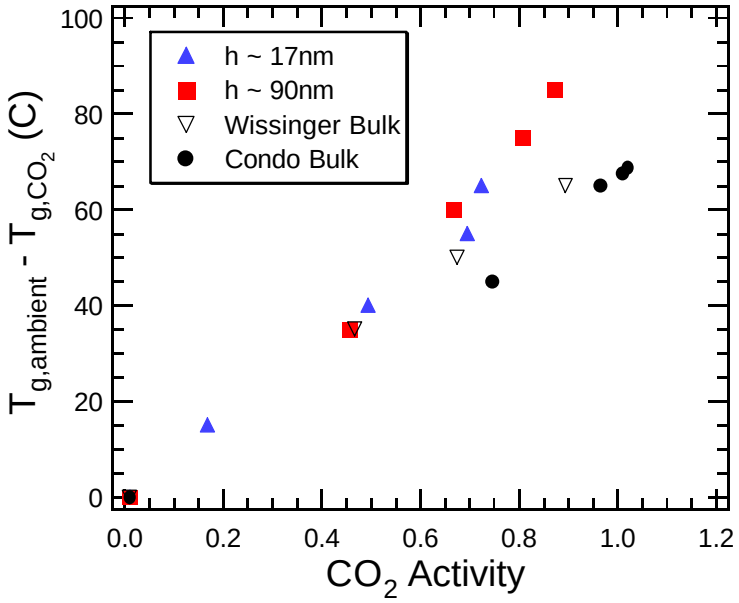

Figure 7-5: Shown here is the ($T_{g,ambient} - T_{g,CO2}$) versus CO_2 activity for PS film with h ~ 90 nm and with h ~ 17 nm. The bulk PS shown here were extracted from references 2 and 4.

The film thickness dependence of P_g ($\Delta P_g < 0$) is similar to that of T_g for systems under ambient conditions, ($\Delta T_g < 0$). At a given temperature, the smaller pressures (or CO_2 activities) required to devitrify thin films versus bulk films indicate enhanced plasticization by excess CO_2 in the free surface and substrate regions. We also showed evidence of retrograde vitrification in the thin film PS system, whereas it does not occur in bulk PS. Devitrification is associated with the increasing CO_2 solubility with decreasing temperature, which overcomes the normal loss in segmental motion upon cooling. The fact that the retrograde devitrification occurs in the thin films is associated with the fact that lower CO_2 pressures are required to devitrify thin PS films than bulk PS. As the film thickness decreases and the excess solubility of CO_2 in the free surface and substrate regions becomes increasingly important, the large increases in CO_2 solubility with decreasing temperature become sufficient to induce retrograde devitrification.

7.5 REFERENCES

(1) Condo, P. D.; Paul, D. R.; Johnston, K. P. *Macromolecules* **1994**, 27, 365.

(2) Condo, P. D.; Johnston, K. P. *Macromolecules* **1992**, 25, 6730.

(3) Condo, P. D.; Johnston, K. P. *J. Polym. Sci. Part B: Polym. Phys.* **1994**, 32, 523.

(4) Wissinger, R. G.; Paulaitis, M. E. *J. Polym. Sci. Part B: Polym. Phys.* **1987**, 25, 2497.

(5) Wang, W-C. W.; Kramer, E. J.; Sachse, W. H. *J. Polym. Sci., Polym. Phys. Ed.* **1982**, 20, 1371.

(6) Chiou, J. S.; Barlow, J. W.; Paul, D. R. *J. Appl. Polym. Sci.* **1985**, 30, 2633.

(7) Stafford, C. M.; Russell, T. P.; McCarthy, T. J. *Polymer Preprints* **1999**, 40, 551.

(8) Stafford, C. M.; Russell, T. P.; McCarthy, T. J. *Macromolecules* **1999**, 32, 7610.

(9) Kazarian, S. G. *Polymer Science, Ser. C* **2000**, 42, 78.

(10) Kazarian, S. G;Vincent, M. F.;Bright, F. V.;Liotta, C. L.; Eckert, C. A. *J. Am. Chem. Soc.* **1996**, 118, 1729.

(11) DeSimone, J. M.; Maury, E. E.; Menceloglu, Y. Z.; McClain, J. B.; Romack, T. J.; Combes, J. R. *Science* **1994**, 265, 356.

(12) Wells, S. L.; DeSimone, J. *Angewandte Chemie* **2001**, 40, 518.

(13) Goldfarb, D. L.; de Pablo, J. J.; Nealy, P. F.; Simons, J. P.; Moreau, W. M.; Angelopoulos M. *J. Vac. Sci. Technol. B* **2000**, 18, 3313.

(14) Namatsu, H. *J. Vac. Sci. Technol. B* **2000**, 18, 3308.

(15) Weibel, G. L.; Ober, C. K. *Microelectronic Engineering* **2003**, 65, 145.

(16) Wind, J. D.; Sirard, S. M.; Paul, D. R.; Green, P. F.; Johnston, K. P.; Koros, W. J. Macromolecules **2003**, 36, 6442.

(17) Wind, J. D.; Sirard, S. M.; Paul, D. R.; Green, P. F.; Johnston, K. P.; Koros, W. J. *Macromolecules* **2003**, 36, 6433.

(18) Zhang, X.; Pham, J. Q.; Martinez, H. J.; Wolf, J.; Green, P. F.; Johnston, K. P. *J. Vac. Sci. Technol. B* **2003**, 21, 2590.

(19) Pham, J. Q.; Sirard, S. M.; Johnston, K. P.; Green, P. F. *Phys. Rev. Lett.* **2003**, 91, 175503.

(20) Sirard, S. M.; Green, P. F.; Johnston, K. P. *J. Phys. Chem. B* **2001**, 105, 766.

(21) Sirard, S. M.; Zeigler, K. J.; Sanchez, I. C.; Green, P. F.; Johnston, K. P. *Macromolecules* **2002**, 35, 1928.

(22) Pham, J. Q.; Green, P. F. *J. Chem. Phys.* **2002**, 16, 5801.

(23) Pham, J. Q.; Green, P. F. *Macromolecules* **2003**, 36, 1665.

(24) Keddie, J. L.; Jones, R. A.; Cory, R. A. *Europhys. Lett.* **1994**, 27. 59.

(25) Kim, J. H.; Jang, J.; Zin, W-C. *Langmuir* **2001**, 17, 2703.

(26) Kim, J. H.; Jang, J.; Zin, W-C. *Langmuir* **2000**, 16, 4064.

(27) Kamiya, Y.; Mizoguchi, K.; Naito, Y. *J. Polym. Sci., Polym. Phys.* **1986**, 24, 535.

(28) Koros, W. J.; Paul, D. R. *J. Polym. Sci.; Polym. Phys. Ed.* **1978**, 16, 1947.

(29) Kawana, S.; Jones, R. A. *Phys. Rev. E* **2001**, 63, 21501.

(30) Fukao, K.; Miyamoto, Y. *Europhys. Lett.* **1999**, 46, 649.

(31) van Zanten, J. H.; Wallace, W. E.; Wu, W. *Phys. Rev. E* **1996**, 53, R 2053.

(32) Torres, J. A.; Nealy, P. F.; de Pablo, J. J. *Phys. Rev. Lett.* **2000**, 85, 3221.

(33) Forrest, J. A.; Dalnoki-Veress, K. *Adv. Colloid and Interface Sci.* **2001**, 94, 167.

(34) Long, D., Lequeux, F. *Eur. Phys. J. E.* **2001**, 4, 371.

(35) McCoy, J. D.; Curro, J. G. *J. Chem. Phys.* **2002**, 116, 9154.

(36) Mansfield, K. F.; Theodorou, D. N. *Macromolecules* **1991**, 24, 6283.

(37) Baschnagel, J.; Binder, K. *Macromolecules* **1995**, 28, 6808.

(38) Bitsanis, I; Hadziioannous, G. *J. Chem. Phys.* **1990**, 92, 3827.

(39) Wu, W.; Majkrzak, C. F.; Satija, S. K.; Ankner, J. F.; Orts, W. J.; Satkowski, M.; Smith, S. D. *Polymer Communication 1992,* 33, 5081.

(40) Binder, K. *Adv. Polym. Sci.* **1994**, 112, 181.

(41) Green, P. F.; Limary, R. *Adv. Colloid Interface Sci.* **2001**, 94, 53.

(42) Tripp, C. P.; Combes, J. R. *Langmuir* **1998**, 14, 7384.

(43) Strubinger, J. R.;Pratcher, J. F. *Anal. Chem.* **1989**, 61, 951.

(44) Strubinger, J. R.;Song, H.;Pratcher, J. F. *Anal. Chem.* **1989**, 63, 98.

(45) Jia, X.;McCarthy, T. J. *Langmuir* **2002**, 18, 683.

(46) Findenegg, G. H. "*Fundamental of Adsorption*"; Myers, A. L.; Belfort, G., Eds.; Engineering Foundation: New York, **1984**.

(47) Miura, K.; Otake, K.; Kurosawa, S.; Sako, T.; Sugeta, T.; Nakane, T.; Sato, K.; Tsuji, T.; Hiaki, T.; Hongo, M. *Fluid Phase Equilib.* **1998**, 144, 181.

(48) Sirard, S. M.; Gupta, R. R.; Russell, T. P.; Watkins, J. J.; Green, P. F.; Johnston, K. P. *Macromolecules* **2003**, 36, 3365.

(49) Koga, T.; Seo, Y-S.; Hu, X.; Zhang, Y.; Rafailovich, M. H.; Sokolov, J. C.; Chu, B.; Satija, S. K. *Europhys. Lett.* **2002**, 60, 559.

(50) Koga, T.; Seo, Y-S.; Zhang, Y.; Shin, K.; Kusano, K.; Nishikawa, K.; Rafailovich, M. H.; Sokolov, J. C.; Chu, B.; Peiffer, D.; Occhiogrosso, R.; Satija, S. K. *Phys. Rev. Lett.* **2002**, 89, 125506.

(51) Koga, T.; Seo, Y-S.; Zhang, Y.; K.; Rafailovich, M. H.; Sokolov, J. C.; Chu, B.; Satija, S. K. *Macromolecules* **2003**, 36, 5236.

Chapter 8: Conclusions and Recommendations for Future Work

The research in this dissertation revealed that the glass transition of polymer thin films is influenced by many factors such as confinement effects, polymer segment-segment interactions as well as polymer interactions with the substrate and free surface. In this final chapter, key findings as well as the significance of the research involving the glass transition temperature of polymer based thin film systems are summarized. Recommendations for future work are also proposed.

8.1 CONCLUSIONS

8.1.1 The glass transition temperature of polymer thin film blends

The influence of film thickness, composition and molecular weight on the effective T_g of TMPC/PS miscible blends on SiO_x/Si substrates were examined using spectroscopic ellipsometry. These studies revealed that while the T_g of pure TMPC increased with decreasing film thickness, the T_g of TMPC/PS blends decreased with decreasing film thickness for films thinner than ~ 50 nm. The depression of the T_g remained relatively constant regardless the molecular weight of the PS. The primary influence of the low molecular weight PS component is to decrease $T_g(h=\infty)$, which is expected for miscible blends. The variation of T_g with blend composition was also examined and the deviation from linear additivity was smaller in thin films than in the bulk, reflecting the influence of confinement on the entropic (free volume) contribution to the T_g of the thin film system.

The results of these investigations provide basis for understanding the glass transition temperature of polymer thin films. An interpretation of the above results in light of current theory and simulations indicated that the entropic, "chain packing", effects and enthalpic effects associated with the interactions between dissimilar chain segments and the external interfaces (free surface and substrate) determine the T_g of blend thin films. Moreover, since many properties of polymer thin films are dependent on their glass transition temperatures, understanding factors that influence the glass transition temperature of polymer thin films not only the enhance polymer thin films fabrication but also improve the performance of many polymer thin film applications.

8.1.2 The glass transition temperature of polymer-inorganic nanocomposite thin films

The film thickness dependencies of the glass transition temperatures of polystyrene based nanocomposite thin films containing small concentrations, 1-5 wt. %, of layered silicate clays, C_{60} fullerenes, and carbon nanotubes on SiOx/Si substrates were investigated using spectroscopic ellipsometry. The T_g's of PS/functionalized-SWNT(0.75wt%), PS/LSi(1wt%) and PS/C_{60}(1wt%) nanocompsite thin films decreased with decreasing film thickness for film less than approximately 45 nm. This thickness dependence is similar to that of pure PS, except that in PS the depression is more pronounced. On the other hand, the T_gs of PS/LSi(5wt%) and PS/C_{60}(5wt%) increased with decreasing film thickness when the film is sufficiently thin. Experimental results of higher concentrations of C_{60} did not show the improvement of T_g because C_{60} is known to

segregate to the substrate as well as crystallize in these PS-C_{60}/SiO_x/Si systems reducing the effective surface area.

The results of these studies showed that regardless of the strength of nanoparticles-polymer interactions, the addition of nanoparticles into polymer thin film matrix have a profound effect on the glass transition temperature of polymer thin films. Both the magnitude and sign of T_g depression can be manipulated by incorporating nanoparticles into the polymer thin films. These results provide insight into the glass transition of polymer thin films by reaffirming the influence of both the confinement effects and the interfacial interactions on the glass transition temperature of polymer thin films. Furthermore, understanding the influence of nanoparticles on the glass transition of polymer thin films offers new pathways to "tailor" properties such as mechanical, thermal, and electrical of polymer thin films and achieve properties not possible with the homopolymer.

8.1.3 CO_2-induced devitrification (plasticization) of polymer thin films

In-situ spectroscopic ellipsometry was shown to be an effective technique to measure the CO_2-induced devitrification (plasticization) of polymer thin films. The devitrification pressure (P_g) was found to decrease with decreasing film thickness for both PS and PMMA thin films meaning that it takes less CO_2 pressure to plasticize thinner films. Upon decreasing temperature isobarically, some polymers exhibit a rubbery-to-glassy transition at high temperatures and at lower temperatures exhibit a glassy-to-rubbery devitrification. This retrograde vitrification phenomenon was observed in both PMMA and PS thin films. The retrograde vitrification envelop of both polymer

thin films shift to lower pressures relative to that of their bulk values suggesting that it takes less pressure to plasticize thinner films. This phenomenon is associated with the interplay between the increasing thermal energy of the system with increasing temperature and the increasing CO_2 solubility in the system with decreasing temperature.

These results indicated that the devitrification (plasticization) transition of polymer thin films could be manipulated by changing the temperature and CO_2 pressure. Since the CO_2 plasticization plays a critical role in many polymer and microelectronic processes, understanding CO_2-induced devitrification enhances the processing of polymer thin films in CO_2 environments. The retrograde devitrification observed in thin films allows thermally labile polymer based thin film systems to be processed at much lower temperatures. Furthermore, due to CO_2 interactions with polymer and external interfaces, the results of glass transition of polymer thin films in CO_2 environments also provide additional insights into understanding the effects of polymer external surfaces interactions on the glass transition of polymer thin films.

8.2 RECOMMENDATIONS FOR FUTURE WORK

In chapter 4 and 6, CO_2-induced glass transition temperature were investigated for homopolymers thin films. It has been shown that the plasticization pressure decreased with decreasing film thickness for both PMMA and PS thin films **[1,2]**. In addition, retrograde vitrification phenomenon was also observed in PMMA and PS thin films **[1,2]**. This was attributed to the excess adsorption of CO_2 at the free surface and at the substrate. Incorporation of nanoparticles into polymer thin film host increases the available surface area for CO_2 to adsorb; hence the sorption and swelling of CO_2 in the

film would increase with decreasing film thickness and the magnitude of plastization pressure depression is expected to increase. This research would enable one to gain insights into the influence of hard surfaces on the plasticization and sorption of CO_2 into polymer nanocomposite thin films.

In the TMPC/PS blend system, one can tailor the effects of free surface and substrate **[3,4]**. Compressed CO_2 is known to mediate the interaction between the polymer and the substrate **[1,2,5,6]**. Measuring sorption, swelling, and CO_2-induced plasticization of TMPC/PS blend thin films may provide additional evidence of the compressed CO_2 modifications the effects of free surface and substrate.

Spectroscopic ellipsometry has been shown to be a great technique to measure the T_g of homopolymers, blends and polymer-nanocomposite thin films **[3,4,7]**. Weakly interacting nanoparticles have been incorporated into polymers and the influence of nanoparticles on the T_g of homopolymers has been examined **[7]**. It is expected the enhancement of T_g become more exaggerated if the polymer host has a strong interactions (hydrogen bonds) with the nanoparticles. Spectroscopic ellipsometry should be a great tool to investigate the effects of interactive nanoparticles on the T_g of polymer thin films.

8.3 REFERENCES

(1) Pham, J. Q.; Sirard, S. M.; Johnston, K. P.; Green, P. F. *Phys. Rev. Lett.* **2003**, 91, 175503.

(2) Pham, J. Q.; Johnston, K. P.; Green, P. F. *J. Phys. Chem. B* **2004**, 108, 3457.

(3) Pham, J. Q.; Green, P. F. *J. Chem. Phys.* **2002**, 116, 5801.

(4) Pham, J. Q.; Green, P. F. *Macromolecules* **2003**, 36, 1665.

(5) Sirard, S. M.; Green, P. F.; Johnston, K. P. *J. Phys. Chem. B* **2001**, 105, 766.

(6) Sirard, S. M.; Zeigler, K. J.; Sanchez, I. C.; Green, P. F.; Johnston, K. P. *Macromolecules* **2002**, 35, 1928.

(7) Pham, J. Q.; Mitchell, C. A.; Bahr, J. L.; Tour, J. M.; Krishanamoorti, R.; Green, P. F. *J. Poly. Sci. Part B: Poly. Phys.* **2003**, 41, 3339.

Bibliography

(1) Frank, C. W.; Rao, V.; Despotopoulou, M. M.; Pease, R. F.; Hinsberg, W. D.; Miller, R. D.; Rabolt, J. F. *Science* **1996**, 273, 912.

(2) Dimitrakopoulos, C. D.; Mascaro, D. J. *IBM Journal of Research and Development* **2001**, 45, 11.

(3) Ziemelis, K. *Nature* **1998**, 393, 619.

(4) Ibn-Elhaj, M.; Schadt, M. *Nature* **2001**, 410, 796.

(5) Ashok, B.; Muthukumar, M.; Russell, T. P. *J. Chem. Phys.* **2001**, 115, 1559.

(6) Black, C. T.; Guarini, W.; Milkove, R.; Baker, S. M.; Russell, T. P.; Tuominen, M. T. *Applied Phys. Lett.* **2001**, 79, 409.

(7) Keddie, J. L.; Jones, R. A.; Cory, R. A. *Europhys. Lett.* **1994**, 27. 59.

(8) Torres, J. A.; Nealy, P. F.; de Pablo, J. J. *Phys. Rev. Lett.* **2000**, 85, 3221.

(9) Kawana, S.; Jones, R. A. *Phys. Rev. E* **2001**, 63, 21501.

(10) Pham, J. Q.; Green, P. F. *J. Chem. Phys.* **2002**, 116, 5801.

(11) van Zanten, J. H.; Wallace, W. E.; Wu, W. *Phys. Rev. E* **1996**, 53, R 2053.

(12) Forrest, J. A.; Dalnoki-Veress, K. *Advances in Colloid and Interface Science* **2001**, 94, 167.

(13) Binder, K. *Adv. Poly. Sci.* **1999**, 138, 1.

(14) Green, P. F.; Limary, R. *Adv. Colloid and Interfacial Science* **2001**, 94, 53.

(15) Lin, E. K.; Wu, W.; Satija, S. K. *Macromolecules* **1997**, 30, 7224.

(16) Lin, E. K.; Kolb, R.; Satija, S.; Wu, W. *Macromolecules* **1999**, 32, 3753.

(17) Zheng, X.; Rafailovich, M. H.; Sokolov, J.; Strzhemecheny, Y.; Schwarz, S. A.; Sauer, B. B.; Rubinstein, M. *Phys. Rev. Lett.* **1997**, 79, 241.

(18) Reiter, G. *Phys. Rev. Lett.* **1992**, 68, 75.

(19) Rudin, A. "*The Elements of Polymer Science and Engineering*" Academic Press, San Diego, **1998**.

(20) Richards, R. W.; Jones, R. A. L. "*Polymers at Surfaces and Interfaces*" Cambridge University Press, Cambridge U.K. **1999**.

(21) Gibbs, J. H.; DiMazio, E. A. *J. Chem. Phys.* **1958**, 28, 373.

(22) Adam, G.; Gibbs, J. H. *J. Chem. Phys.* **1965**, 43, 139.

(23) Angell, C. A. *J. Phys. Chem. Solid* **1988**, 49, 863.

(24) Cohen, M. H.; Turnbull, D. J. *J. Chem. Phys.* **1959**, 31, 1164.

(25) Desimone, J. M. *Science* **2002**, 297, 799.

(26) Cooper, A. I. *J. Mater. Chem.* **2000**, 10, 207.

(27) DeSimone, J. M.; Maury, E. E.; Menceloglu, Y. Z.; McClain, J. B.; Romack, T. J.; Combes, J. R. *Science* **1994**, 265, 356.

(28) Teja, A. S.; Eckert, C. A. *Ind. Eng. Chem. Res.* **2000**, 39, 4442.

(29) Perrut, M. *Ind. Eng. Chem. Res.* **2000**, 39, 4531.

(30) Kazarian, S. G. *Polymer Science, Ser. C* **2000**, 42, 78.

(31) Weibel, G. L.; Ober, C. K. *Microelectronic Eng.* **2003**, 65, 145.

(32) Wells, S. L.; DeSimone, J. *Angewandte Chemie* **2001**, 40, 518.

(33) Namatsu, H. *J. Vac. Sci. Technol. B* **2000**, 18, 3308.

(34) Goldfarb, D. L.; de Pablo, J. J.; Nealy, P. F.; Simons, J. P.; Moreau, W. M.; Angelopoulos M. *J. Vac. Sci. Technol. B* **2000**, 18, 3313.

(35) Zhang, X.; Pham, J. Q.; Martinez, H. J.; Wolf, J.; Green, P. F.; Johnston, K. P. *J. Vac. Sci. Technol. B* **2003**, 21, 2590.

(36) Zhang, X.; Pham, J. Q.; Ryza, N.;Green, P. F.; Johnston, K. P. *J. Vac. Sci. Technol. B* **2004**, 22, 818.

(37) Sihvonen, M.; Jarvenpaa, E.; Hietaniemi, V.; Huopalahti, R. *Trends in Food Science & Technology* **1999**, 10, 217.

(38) Long, D. P.; Blackburn, J. M.; Watkins, J. J. *Advanced Materials* **2000**, 12, 913.

(39) Ye, X.; Wai, C. M. *J. Chem. Edu.* **2003**, 80, 198.

(40) Stafford, C. M.; Russell, T. P.; McCarthy, T. J. *Macromolecules* **1999**, 32, 7610.

(41) Zhang, Y.; Gangwani, K. K.; Lemert, R. M. J. *Supercritical Fluids* **1997**, 11, 115.

(42) Condo, P. D.; Paul, D. R.; Johnston, K. P. *Macromolecules* **1994**, 27, 365.

(43) Condo, P. D.; Johnston, K. P. J. *Polym. Sci. Part B: Polym. Phys.* **1994**, 32, 523.

(44) Wissinger, R. G.; Paulaitis, M. E. *J. Polym. Sci. Part B: Polym. Phys.* **1987**, 25, 2497.

(45) Wang, W-C. W.; Kramer, E. J.; Sachse, W. H. *J. Polym. Sci., Polym. Phys. Ed.* **1982**, 20, 1371.

(46) Chiou, J. S.; Barlow, J. W.; Paul, D. R. *J. Appl. Polym. Sci.* **1985**, 30, 2633.

(47) Sirard, S. M.; Green, P. F.; Johnston, K. P. *J. Phys. Chem. B* **2001**, 105, 766.

(48) Sirard, S. M.; Zeigler, K. J.; Sanchez, I. C.; Green, P. F.; Johnston, K. P. *Macromolecules* **2002**, 35, 1928.

(49) Koga, T.; Seo, Y-S.; Zhang, Y.; Shin, K.; Kusano, K.; Nishikawa, K.; Rafailovich, M. H.; Sokolov, J. C.; Chu, B.; Peiffer, D.; Occhiogrosso, R.; Satija, S. K. *Phys. Rev. Lett.* **2002**, 89, 125506.

(50) Pham, J. Q.; Sirard, S. M.; Johnston, K. P.; Green, P. F. *Phys. Rev. Lett.* **2003**, 91, 175503.

(51) Pham, J. Q.; Johnston, K. P.; Green, P. F. *J. Phys. Chem. B* **2004**, 108, 3457.

(52) Gupta, R. R.; Lavery, K. A.; Francis, T. J.; Webster, J. R.; Smith, G. S.; Russell, T. P.; Watkins, J. J. *Macromolecules* **2003**, 36, 346.

(53) Liao, X.; Wang, J.; Li, G.; He, J. *J. Poly. Sci. Part B: Poly. Phys.* **2004**, 42, 280.

(54) Kato, S.; Tsujita, Y.; Yoshimizu, H.; Kinoshita, T.; Higgins, J. S. *Polymer* **1997**, 38, 2807.

(55) Meli, L.; Pham, J. Q.; Johnston, K. P.; Green, P. F. *Accepted to Physical Review E*.

(56) Watkins, J. J.; Brown, G. D.; RamachandraRao, V. S.; Pollard, M. A.; Russell, T. P. *Macromolecules* **1999**, 32, 7737.

(57) Vogt, B. D.; Brown, G. D.; RamachandraRao, V. S.; Watkins, J. J. *Macromolecules* **1999**, 32, 7907.

(58) Vedam, K. *Thin Solid Films* **1998**, 313.

(59) Kressler,J.; Higashida, N.; Inoue, T.; Heckmann, W.; Seitz, F. *Macromolecules* **1993**, 26, 2090.

(60) Malmsten, M. J. *Colloid Interface Sci.* **1994**, 166, 333.

(61) Nee, S.-M. F. *Appl. Opt.* **1988**, 27, 2819.

(62) Azzam, R. M.; Bashara, N. M. *Ellipsometry and Polarized Light*; North-Holland Publishing Co.: Elsevier, **1997**.

(63) Tompkins, H. G.; McGahan, W. A. *Spectroscopic Ellipsometry and Reflectometry*; John Wiley & Sons, Inc.: New York, **1999**.

(64) Styrkas, D.; Doran, S. J.; Gilchrist, V.; Keddie, J. L.; Lu, J. R.; Murphy, E.; Sackin, R.; Su, T-J.; Tzitzinou, A. *Polymer Surfaces and Interfaces III*, edited by Richards, R. W.; Peace, S. K. John Wiley & Sons Ltd. **1999**.

(65) Keddie, J. L.; Jones, R. A.; Cory, R. A. *Faraday Discuss.* **1994**, 98, 219.

(66) Orts, W. J.; van Zanten, J. H.; Wu, W.; Satija, S. K. *Phys. Rev. Lett.* **1993**, 71, 867

(67) Wu, W.; van Zanten, J. H.; Orts, W. J. *Macromolecules* **1995**, 28, 771.

(68) Tseng, K.C., Turro, N.J. and Durning, C.J. *Phys. Rev. E.* **2000**, E61, 1800.

(69) Wallace, W.E.; van Zanten, J. H.; Wu, W. *Phys. Rev. E* **1995**, 52, R3329.

(70) Frank, B.; Gast, A. P.; Russell, T. P.; Brown, H. R.; Hawker, C. *Macromolecules* **1996**, 29, 6531.

(71) Forrest, J. A.; Dalnoki-Veress, K.; Stevens, J. R.; Dutcher, J. R. *Phys. Rev. Lett.* **1996**, 77, 2002.

(72) Wallace, W.E., Fischer, D.A., Efimenko, K., Wu, Wen-Li and Genzer, J., *Macromolecules* **2001**, 34, 5081.

(73) Forrest, J. A.; Mattsson, J. *Phys. Rev. E* **2000**, 61, R53.

(74) Mattsson, J.; Forrest, J. A.; Borjesson, L. *Phys. Rev. E* **2000**, 62, 5187.

(75) de Gennes, P. G. *Euro. Phys. J. E* **2000**, 2, 201.

(76) Xie, L.; DeMaggio, G. B.; Frieze, W. E.; DeVries, J.; Gidley, D. W.; Hristov, H. A.; Yee, A. F. *Phys. Rev. Lett.* **1995**, 74, 4947.

(77) Kim, J. H.; Jang, J.; Zin, W. *Langmuir* **2001**, 17, 2703.

(78) DeMaggio, G. B.; Frieze, W. E.; Gidley, D. W.; Hristov, H. A.; Yee, A. F. *Phys. Rev. Lett.* **1997**, 78, 1524.

(79) Grohens, Y.; Brogly, M.; Labbe, C.; David, M. –O.; Schultz, J. *Langmuir* **1998**, 14, 2929.

(80) Fukao, K.; Miyamoto, Y. *Europhys. Lett.* **1999**, 46, 649.

(81) Kerle, T.; Klein, J.; Binder, K. *Phys. Rev. Lett.* **1996**, 77, 1318.

(82) Kerle, T.; Klein, J.; Binder, K. *Euro. Phys. J. E.* **1999**, 7, 401.

(83) Muller-Buschbaum, P.; Gutmann, J. S.; Stamm, M. *Macromolecules* **2000**, 33, 4886.

(84) Mansfield, K. F.; Theodorou, D. N. *Macromolecules* **1991**, 24, 6283.

(85) Baschnagel, J.; Binder, K. *Macromolecules* **1995**, 28, 6808.

(86) Ferry, J. D. *Viscoelastic Properties of Polymers*, Academic Press, New York, **1980**.

(87) Di Marzio, E. A. *Polymer* **1990**, 31, 2954.

(88) Gordon, M.; Taylor, J. S. *J. Appl. Chem., USSR* **1952**, 2, 493.

(89) Schnieder, H. A.; DiMarzio, E. A. *Polymer* **1992**, 33, 3453.

(90) Brekner, M. –J.; Schneider, H. A.; Cantow, H. –J. *Polymer* **1988**, 78, 78.

(91) Fernandez, A. C.; Barlow, J. W.; Paul, D. R. *Polymer* **1986**, 27, 1788.

(92) Kim, C. K.; Paul, D. R. *Polymer* **1992**, 33, 1630.

(93) Gou, W.; Higgins, J. S. *Polymer* **1990**, 31, 699.

(94) Kim, E.; Krausch, G.; Kramer, E. J.; Osby, J. O. *Macromolecules* **1994**, 27, 5927.

(95) Kim, E.; Kramer, E. J.; Osby, J. O. *Macromolecules* **1995**, 28, 1979.

(96) Kim, E.; Kramer, E. J.; Osby, J. O.; Walsh, D. J. *J. Poly. Science part B: Poly. Phys.* **1995**, 33, 467.

(97) Lui, J.; Jean, Y. C.; Yang, H. *Macromolecules* **1995**, 28, 5774.

(98) Long, D., Lequeux, F. *Eur. Phys. J. E.* 2001, 4, 371.

(99) Kim, J. H.; Jang, J.; Lee, D-Y.; Zin, W-C. *Macromolecules* **2002**, 35, 311.

(100) Keddie, J. L.; Jones, R. A.; Cory, R. A. *Faraday Discuss.* **1994**, 98, 219.

(101) Efremow, M. Y.; Warren, J. T.; Olson, E. A.; Zhang, M.; Kwan, A. T.; Allen, L. H. *Macromolecules* **2002**, 35, 1481.

(102) Jain, T. S.; de Pablo, J. J. *Macromolecules* **2002**, 35, 2167.

(103) Kim, J. H.; Jang, J.; Zin, W-C. *Langmuir* **2000**, 16, 4064.

(104) Kleidciter, G.; Prucker, O.; Bock, H.; Frank, C.; Lechner, M.; Knoll, W. *Macromol. Symp.* **1999**, 145, 95.

(105) Tsui, O. K. C.; Zhang, H. F. *Macromolecules* **2001**, 34, 9139.

(106) Fryer, S. D.; Nealey, F. P.; de Pablo, J. J. *Macromolecules* **2000**, 33, 6439.

(107) Fryer, S. D.; Peters, D. R.; Kim, J. E.; Tomaszewski, E. J.; de Pablo, J. J.; Nealey, F. P.; White, C. C.; Wu, W-L. *Macromolecules* **2001**, 34, 5627.

(108) Tate, S. R.; Fryer, S. D.; Pasqualini, S.; Montague, F. M.; de Pablo, J. J.; Nealey, F. P. *J. Chem. Phys.* **2001**, 115, 9982.

(109) Doruker, P.; Mattice, L. W. *Macromolecules* **1999**, 32, 194.

(110) Soles, C. L.; Douglas, F. J.; Wu, W. –l.; Dimeo, R. M. *Phys. Rev. Lett.* **2002**, 88, 037401-1.

(111) Kajiyama, T.; Tanaka, K.; Takahara, A. *Macromolecules* **1995**, 28, 3482.

(112) Tanaka, K.; Taura, A.; Ge, S-R.; Takahara, A.; Kajiyama, T. *Macromolecules* **1996**, 29, 3040.

(113) Tanaka, K.; Takahara, A.; Kajiyama, T. *Macromolecules* **1997**, 30, 6626.

(114) Kajiyama, T.; Tanaka, K.; Takahara, A. *Macromolecules* **1997**, 30, 280.

(115) Kajiyama, T.; Tanaka, K.; Satomi, N.; Takahara, A. *Macromolecules* **1998**, 31, 5150.

(116) Tanaka, K.; Jiang, X.; Nakamura, K.; Takahara, A.; Kajiyama, T.; Ishizone, T.; Hirao, A.; Nakaham; S. *Macromolecules* **1998**, 31, 5150.

(117) Tanaka, K.; Takahara; A.; Kajiyama, T. *Macromolecules* **1998**, 31, 863.

(118) Xie, F.; Zhang, H. F.; Lee, F. K.; Du, B.; Tsui, O. K.; Yokoe, Y.; Tanaka, K.; Takahara, A.; Kajiyama, T.; He, T. *Macromolecules* **2002**, 35, 1491.

(119) DiMarzio, E. A.; Gibbs, J. H., *J. Polym. Sci.* **1959**, 40, 121.

(120) DiMarzio, E. A.; Gibbs, J. H. *J. Polym. Sci.* **1963**, A1, 1417.

(121) McCoy, J. D.; Curro, J. D. *J. Chem. Phys.* **2002**, 116, 9154.

(122) Binder, K. *Adv. Polym. Sci.* **1994**, 112, 181.

(123) Bitsanis, I; Hadziioannous, G. *J. Chem. Phys.* **1990**, 92, 3827.

(124) Sirard, S. M.; Gupta, R. R.; Russell, T. P.; Watkins, J. J.; Green, P. F.; Johnston, K. P. *Macromolecules* **2003**, 36, 3365.

(125) Kamiya, Y.; Mizoguchi, K.; Naito, Y. *J. Polym. Sci., Polym. Phys.* **1986**, 24, 535.

(126) Pham, J. Q.; Green, P. F. *Macromolecules* **2003**, 36, 1665.

(127) van der Lee, A., *Langmuir* **2001**, 17, 7664.

(128) Wu, W.; Majkrzak, C. F.; Satija, S. K.; Ankner, J. F.; Orts, W. J.; Satkowski, M.; Smith, S. D. *Polymer* **1992**, 33, 5081.

(129) Kazarian, S. G.; Vincent, M. F.; Bright, F. V.; Liotta, C. L.; Eckert, C. A. *J. Am. Chem. Soc.* **1996**, 118, 1729.

(130) Koros, W. J.; Paul, D. R. *J. Polym. Sci.; Polym. Phys. Ed.* **1978**, 16, 1947.

(131) Tripp, C. P.; Combes, J. R. *Langmuir* **1998**, 14, 7384.

(132) Strubinger, J. R.; Pratcher, J.F. *Anal. Chem.* **1989**, 61, 951

(133) Strubinger, J. R.; Song, H.; Pratcher, J. F. *Anal. Chem.* **1989**, 63, 98.

(134) Jia, M.; McCarthy, T.J. *Langmuir* **2002**, 18, 683.

(135) Findenegg G. H. "*Fundamentals of Adsorption*", edited by Meyer, A.L. and Belfort, G. (Engineering Foundation, New York, 1984) p.207.

(136) Condo, P. D.; Johnston, K. P. *Macromolecules* **1992**, 25, 6730.

(137) Saito, R., Dresselhaus, G., Dresselhaus, M. S., "*Physical Properties of Nanotubes*", Imperial College Press, London **1998**.

(138) Russell, T. P. *Current Opinion in Colloid and Interface Science* **1996**, 1, 107.

(139) Fasolka, M. J.; Mayes, A. M. *Ann. Rev. Mater. Res.* **2001**, 31, 323.

(140) Masson, J. L.; Green, P. F. *Phys. Rev. E.* **2002**, 65, 031806.

(141) Limary, R.; Green, P. F.; Shull, K. *Eur. Phys. J. E.* **2002**, 8, 103.

(142) Binder, K; Baschnagel, J.; Bennemann, C.; Paul, W. *J. Phys. Condense Matter* **1999**, 11, A47.

(143) Grohens, Y.; Hamon, L.; Soldera, A.; Holl, Y. *Eur. Phys. J. E.* **2002**, 8, 217.

(144) Zax DB, Yang DK, Santos RA, Hegemann H, Giannelis EP, Manias E, *J. Chem. Phys.* **2000**, 112:2945-2951.

(145) Giannelis, E. P.; Krishnamoorti R.; Manias E. *Adv. Polym. Sci.* **1999**, 138:107-147.

(146) Krishnamoorti R.; Silva, A. S.; Mitchell, C. A. *J. Chem. Phys.* **2001**, 108:7175.

(147) Mitchell, C. A.; Bahr, J. L.; Arepalli, S.; Tour, J. M. Tour; Krishanamoorti, R. *Macromolecules* **2002**, 35, 8825 – 8830.

(148) Bahr, J. L.; Tour, J. M. *Journal of Materials Chemistry* **2002**, 12, 1952-1958.

(149) Bahr, J. L.; Tour, J. M. *Chemistry of Materials* **2001**, 13, 3823.

(150) Bahr, J. L.; Yang, J. P.; Kosynkin, D. V.; Bronikowski, M. J.; Smalley, R. E.; Tour, J. M. *J. Am. Chem. Soc.* **2001**, 123, 6536-6542.

(151) Lodge, T. P.; McLeish, T. C. B. *Macromolecules* **2002**, 33, 5278.

(152) Stafford, C. M.; Russell, T. P.; McCarthy, T. J. *Polymer Preprints* **1999**, 40, 551.

(153) Wind, J. D.; Sirard, S. M.; Paul, D. R.; Green, P. F.; Johnston, K. P.; Koros, W. J. *Macromolecules* **2003**, 36, 6442.

(154) Wind, J. D.; Sirard, S. M.; Paul, D. R.; Green, P. F.; Johnston, K. P.; Koros, W. J. *Macromolecules* **2003**, 36, 6433.

(155) Miura, K.; Otake, K.; Kurosawa, S.; Sako, T.; Sugeta, T.; Nakane, T.; Sato, K.; Tsuji, T.; Hiaki, T.; Hongo, M. *Fluid Phase Equilib.* **1998**, 144, 181.

(156) Koga, T.; Seo, Y-S.; Hu, X.; Zhang, Y.; Rafailovich, M. H.; Sokolov, J. C.; Chu, B.; Satija, S. K. *Europhys. Lett.* **2002**, 60, 559.

(157) Koga, T.; Seo, Y-S.; Zhang, Y.; K.; Rafailovich, M. H.; Sokolov, J. C.; Chu, B.; Satija, S. K. *Macromolecules* **2003**, 36, 5236.

(158) Rotello, V. "*Nanoparticles: Building Blocks for Nanotechnology*" Kluver Academic/Plenum Publishers: New York, **2004**.

(159) Giannelis, E. P. *Appl. Organomet. Chem.* **1998**, 12, 675.

(160) Schoder, C. *Fullerene Science and Technology* **2001**, 9, 281.

(161) Dai, L.; Mau, A. W. H. *Advanced Materials* **2001**, 13, 899.

(162) Pham, J. Q.; Mitchell, C. A.; Bahr, J. L.; Tour, J. M.; Krishanamoorti, R.; Green, P. F. *J. Poly. Sci. Part B: Poly. Phys.* **2003**, 41, 3339.

(163) Sotta, P. *Los Alamos National Lab., Preprint Archive: Condense Matter* **2003**, 1-33.

(164) Berriot, J.; Montes, H.; Lequeux, F.; Long, D.; Sotta, P. *Europhys. Lett.* **2003**, 64, 50.

(165) Knoll, A.; Horvat, A.; Lyakhova, K. S.; Krausch, G.; Sevink, J. A.; Zvelindovsky, A. V.; Magerle, R. *Phys. Rev. Lett.* **2002**, 89, 035501.

(166) Despotopoulou, M. M.; Frank, C. W.; Miller, R. D.; Rabolt, J. F. *Macromolecules* **1996**, 29, 5797.

(167) Reiter, G. *J. Poly. Sci. Part b: Poly. Phys.* **2003**, 41, 1869.

(168) Chenyu, W.; Shrivastava, D.; Choi, K. *Nano Letters* **2002**, 2, 647.

(169) Limary, R.; Swinnea, S.; Green, P. F. *Macromolecules* **2000**, 33, 5227.

(170) Ren, J.; Silva, A. S.; Krishanomoorti, R. *Macromolecules* **2002**, 33, 3739.

(171) Barnes, K. A.; Karim, A.; Douglas, J. F.; Nakatani, A. I.; Gruell, H.; Amis, E. J. *Macromolecules* **2000**, 33, 4177.

(172) Sharma, S.; Rafailovich, M. H.; Peiffer, D.; Sokolov, J. *Nano Letters* **2001**, 1, 511.

(173) Ferreiro, V.; Douglas, J. F.; Warren, J.; Karim, A. *Phys. Rev. E* **2002**, 65, 051606.

(174) Vaia, R. A.; Giannelis, E. P. *Macromolecules* **1997**, 30, 7990.

(175) Ginzburg, V. V.; Balazs, A. C. *Macromolecules* **1999**, 32, 5681.

(176) Hackett, E.; Manias, E.; Giannelis, E. P. *J. Chem. Phys.* **1998**, 108, 7401.

(177) Ishida, H.; Li, Y. *Polymer* **2003**, 44, 6571.

(178) Kim, J.; Lee, S-S. *J. Poly. Sci.: Part B, Poly. Phys.* **2004**, 42, 246.

(179) Chen, G.; Ma, G. *Applied Physics Lett.* **1998**, 72, 3294.

Vita

Joseph Quan Anh Pham was born on April 27th, 1975 in Saigon, Vietnam to Tu Viet Pham and Men Thi Bui. In October 1990, his family left Vietnam and settled in Fort Worth, Texas. After graduating from Paschal High School in May 1994, he entered the University of Texas at Austin and received a Bachelor Degree in Chemical Engineering in December 1998. In January 1999, he enrolled in the graduate program Materials Science and Engineering at The University of Texas at Austin and completed the Master of Science degree in Materials Science and Engineering in August 2002. While a graduate student, he worked as a teaching assistant and received The University of Texas Continuing Fellowship.

Permanent address:

715 South Emma Drive

Arlington Texas 76002

This dissertation was typed by the author.